NOTE TO USERS

This reproduction is the best copy available.

UMI®

DISTRIBUTION AND GEOCHEMISTRY OF SHELLS OF EXTANT MOLLUSCS OF THE HUDSON ESTUARY, NEW YORK

by

ELIZABETH RUDOLPH

A dissertation submitted to the Graduate Faculty in Earth and Environmental Sciences in partial fulfillment of the degree of Doctor of Philosophy, The City University of New York

2004

ProQuest Information and Learning Company
300 North Zeeb Road
P.O. Box 1346
Ann Arbor, MI 48106-1346

This manuscript has been read and accepted for the Graduate Faculty in Earth and Environmental Sciences in satisfaction of the dissertation requirement for the degree of Doctor of Philosophy.

1/27/04
Date

Chair of Examining Committee

1/27/04
Date

Executive Officer, EES

Jeffrey C. Steiner

John A. Chamberlain

Frederick C. Shaw

Supervisory Committee

THE CITY UNIVERSITY OF NEW YORK

Abstract

DISTRIBUTION AND GEOCHEMISTRY OF SHELLS OF EXTANT MOLLUSCS OF THE HUDSON ESTUARY, NEW YORK

By

Elizabeth Rudolph

Adviser: Dr. Jeffrey C. Steiner

Estuarine bivalves constitute excellent potential markers of metal-influx stemming from upstream industrialization since they tend to be immobile but otherwise extremely reactive to environmental stresses. To date there is meager information regarding the concentration of metals in mollusc shells from estuarine environments (Dodd, 1965; Borbas et al, 1991; Babukutty and Chacko, 1992; Zamarreno et al, 1996), although significant advances have been made with regard to the metal content of soft tissues in organisms residing in estuarine environments (Leung et al, 2002; Wang, 1999; Bordin et al, 1996; and others). The purpose of this study is to characterize the benthic species within the lower reaches of the Hudson Estuary examining in particular: (1) Evidence for a changing benthic community since the 1970s research. (2) Evidence for systematic variation in the trace metal content of mollusc shells as a function of salinity and channel characteristics. (3) Evidence for systematic distortion of the unit cell structure of mollusc shells related to trace metal content. The benthic community structure has modified over the past 20 years with a marked shift in the *Macoma balthica* range from Manhattan to Piermont with the heaviest population near the upper west side of Manhattan. This finding does not appear to be salinity controlled. *Mya arenaria* and *Mytilopsis leucophaeta* have each suffered a population decline that may result from either poor water or sediment quality or stresses from competition. This research

publishes the first recorded occurrence of *Rangea cuneata* in the Croton-on-Hudson area and north. Trace metal variation and the resultant influence on shell structure, in *Macoma balthica* shells are arguably indicators of the health of the estuarine environment. The variation is a result of a dynamic combination of differential metal sequestering due to salinity variation and local metal availability.

ACKNOWLEDGEMENT

This process would not have been possible without the selfless contribution and generosity of Dr. Jeffrey C. Steiner who supervised the entire project and provided expertise on shaping geochemical investigations, devising protocols, and providing guidance in the evaluation of bivalve shell aragonite. I am also indebted to Dr. Frederick C. Shaw who resurrected the Hudson reexamination, provided resources for bivalve and water parameter data collection and welcomed me aboard. Dr. John A. Chamberlain critically reviewed this document and provided invaluable suggestions. Well before my decision to undertake a doctoral degree, Dr. Chamberlain guided me throughout my undergraduate academic career. Jennifer Donlan assisted in the much needed but ever-tedious sample preparation and shared in my mollusc excitement. Karin Block, Marc Cesaire, and Lucy Williams provided lab support and encouragement and many laughs. Dee Breger provided her usual expertise at the SEM at Lamont Doherty Earth Observatory. And thanks to Teresa Bandosz, CCNY chemistry department, for the lead calibrations and the Oregon State University Radiation Laboratory for generously donating the neutron activation analyses. A special acknowledgement is owed to my family and friends in appreciation for their unending support throughout this long endeavor.

TABLE OF CONTENTS

LIST OF TABLES

LIST OF ILLUSTRATIONS

CHAPTER 1: INTRODUCTION

Ever since the 1987 amendment to the Clean Water Act that created the National Estuary Program (NEP) large urban estuaries, including the Hudson River Estuary have gained attention. The main purpose of the NEP is the design, implementation and evaluation of a monitoring program geared toward assessing, protecting and improving water quality for aquatic biota in large estuarine systems. The Hudson Estuary resides in part in a large urbanized metropolitan city, New York City. In such a region there are countless processes than can affect the living environment of local biota, from aerosol particle input to highway runoff and septic system leakages. It is necessary, therefore to identify temporal and spatial distribution of benthic infaunal organisms, primarily bivalves, and to categorize the current community structure, as it is a function of the conditions of the environment. Infaunal organisms are useful indicators of environmental conditions since they are immobile yet reactive to environmental stresses. A survey conducted in the mid-1970s, (Shaw 1975, 1978) prior to the establishment of the NEP will provide a baseline for comparison. In addition to community structure determination, geochemical information derived from shell material will provide insight as to how organisms cope with heavy metals and other pollutants in their environment. The sum total of information gathered will define the condition of the benthic habitat.

To date there is meager information regarding the concentration of metals in mollusc shells from estuarine environments (Mg and Sr by Dodd (1965), trace metals by Babukutty and Chacko (1992), Sr/Ca ratio by Palacios et al, (1994), and Pb by Pitts & Wallace (1994)), although significant advances have been made with regard to the metal

content of soft tissues in organisms residing in estuarine environments (Cd by Leung et al (2002), Cd and Mn by Yang & Sanudo-Wilhelmy (1998), trace metals by Bordin et al (1996), K and Rb by Deitz & Byrne (1990) and many others). Previous studies have suggested that trace metal uptake is determined primarily by metal bioavailability (Leung, 2002; Babukutty and Chacko, 1992) or in some instances as a species-specific response mechanism controlled by metallothionien production (Leung et al, 2002; Bordin et al, 1997). In general, all divalent cations that are broadly similar in ionic size have the ability to substitute directly for calcium ion in the aragonite structure during shell generation processes in the mantle. Observations of trace metal content in organic aragonite have shown that strontium, sodium, and magnesium are the three primary calcium-replacing cations (Speer, 1983). Alternatively, metals can simply be adsorbed preferentially onto shell surface through direct contact with seawater creating an interlayer complex (Thomas & Young, 1998). The metal content of mollusc tissue typically exceeds that of shells, though this is not well established except for manganese, lead and cobalt (Babukutty & Chacko, 1992). Thomas and Young (1998) contend that metal concentrations in tissue fluctuate as a function of season, age, size and depuration rates, while equivalent shell levels remain relatively constant.

The literature contains a wide range of highly specialized research efforts, none of which establishes the relationship between shell geochemistry of bivalves in large polluted urban estuaries. The purpose of this study is to characterize the benthic species within the lower reaches of the Hudson estuary examining in particular:

1. Evidence for a changing benthic community over the 20 years since the Shaw study (Shaw, 1975, 1978 and unpublished[1]) of the same portion of the Hudson estuary.

2. Evidence for systematic variation in the trace metal content of mollusc shells as a function of salinity and perhaps other channel characteristics.

3. Evidence for systematic distortion of the unit cell structure of mollusc shells related to trace metal content.

Each phase of this investigation will produce results that can be directly correlated with trace metal concentration within the Hudson benthos. The metal content of shells and the manner in which it is distributed within the shell structure, therefore, constitutes a potentially valuable means of searching for shifts in the dissolved and sediment adsorbed metals in the estuarine environment. The response of benthic organisms to metal contamination is apparent in the assemblage and distribution modifications over time and in the variation in shell chemistry from site to site.

This study presents data that suggests that (1) iron, silicon, magnesium, sodium, aluminum, potassium, certain transition metals and REE concentrate in sufficient quantities to be used as marker elements for this purpose, (2) metal concentration variation may in part be attributed to magnesite, strontianite, witherite, or other carbonate substitution for aragonite, (3) though the Hudson sediments are not pristine, mollusc

[1] Fred Shaw has permitted the use of his benthic measurements in this study; these are annotated in Appendix 5.

assemblages and species distributions are substantial and are primarily salinity dependent, and (4) bivalves that are more sensitive to pollution, *Mulinia lateralis* and *Mytilopsis leucophaeta*, show reduced populations as compared to the 1970s distributions while the more tolerant, *Macoma balthica*, has expanded but moved its distribution center north.

In the tidally influenced, turbulent bottom Hudson estuary, sediment redistribution is rapid and constant, and water is constantly moving. Infaunal bivalve species that spend their entire 5-7 year lifetime in the same location, may record the most complete record of chemistry variation in the estuarine environment. The complete absence or severe reduction in population of expected bivalves may further suggest that the environment is too polluted to support infaunal life forms. Therefore, the bivalve shell may hold the key to understanding the health of the estuarine environment.

CHAPTER 2: BACKGROUND

A. The Hudson Estuary

The Hudson River is a complex environment, ranging in characteristics from its fresh water northern source, Lake Tear of the Clouds in the upper Adirondacks, to its tidal estuary terminus 507 km south in Upper New York Bay (Figure 1).

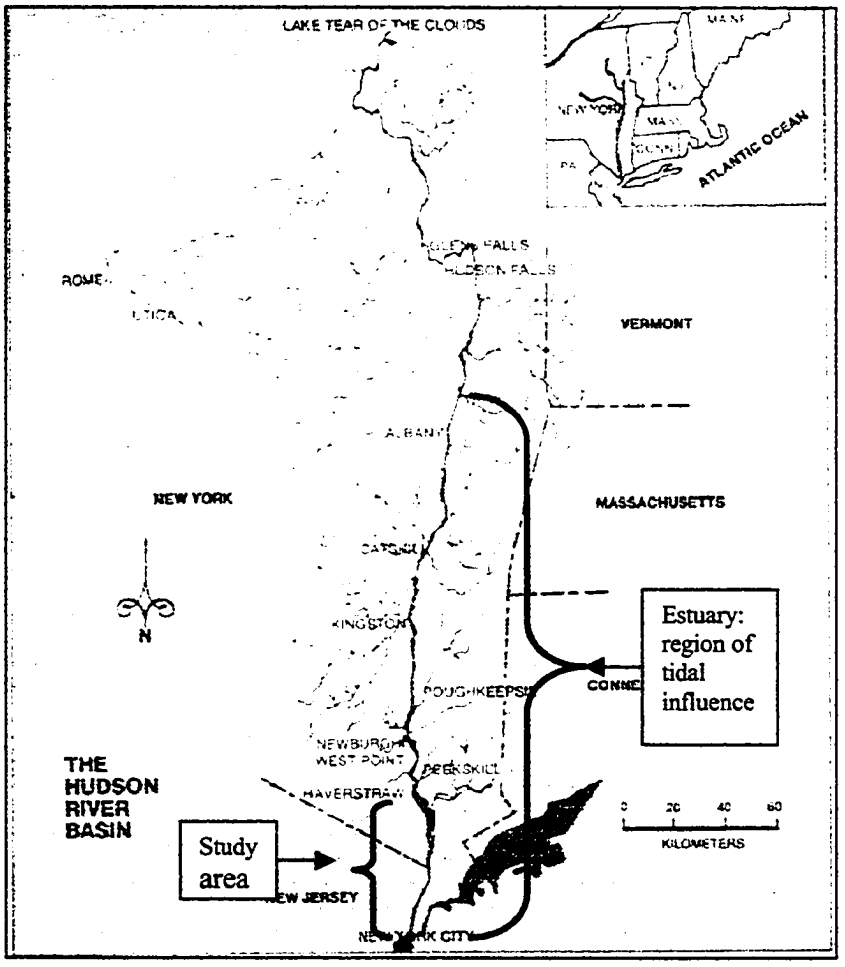

Figure 1. *The Hudson River Estuary. Estuarine portion marked. Study area also noted. From: An Atlas of Biological Resources of The Hudson Estuary, Boyce Thompson Institute for Plant Research, 1977.*

Within these contrasting environments are localized tidal marshes, man-made beaches and other restricted eco-zones. The Hudson Estuary is considered a fiord, a deep and narrow indentation that results in the case of the Hudson, from the encroachment of the sea in a U-shaped valley created by the Pleistocene glaciation. The lower 243 kilometers of the Hudson incorporating the Battery to Federal Dam, Troy, NY are influenced by tidal fluctuations that generate a salinity gradient from several parts per thousand to near normal ocean salinity.

The Hudson River Estuary (watershed/basin) began its valley formation in the Cretaceous with uplift, followed by erosion in the Tertiary and much later molded by the ebb and flow of the Wisconsin ice sheet, some 18,000 years ago. Where mountains form a lateral restriction, the ice carved a deeper channel, resulting in the maximum depth at West Point, NY, just north of this study area with shallower depths toward the mouth (Cooper et al, 1988) (See Figure 2). Hydrologically, the Hudson can be divided into four reaches over the estuarine interval from the Battery 243 kilometers north to Troy, New York that broadly correlate with estuarine salinities (Ristich & Fortier, 1977). The present study area includes the southern two reaches (Figure 3). The southernmost reach extends from the Battery to Yonkers, almost completely within the polyhaline salinity zone defined by salinities between 18 to 30 ppt (Venice salinity zonation scheme, 1959). The region north of the Bronx comprises the mesohaline zone salinities at less than 18 ppt. Along the entire length of Reach 1, the navigation channel depth varies from 12 to 21 meters (the actual depth outside of the channel is somewhat shallower) and is located along the eastern margin of the estuary. The Tappan Zee/Haverstraw complex, Reach 2,

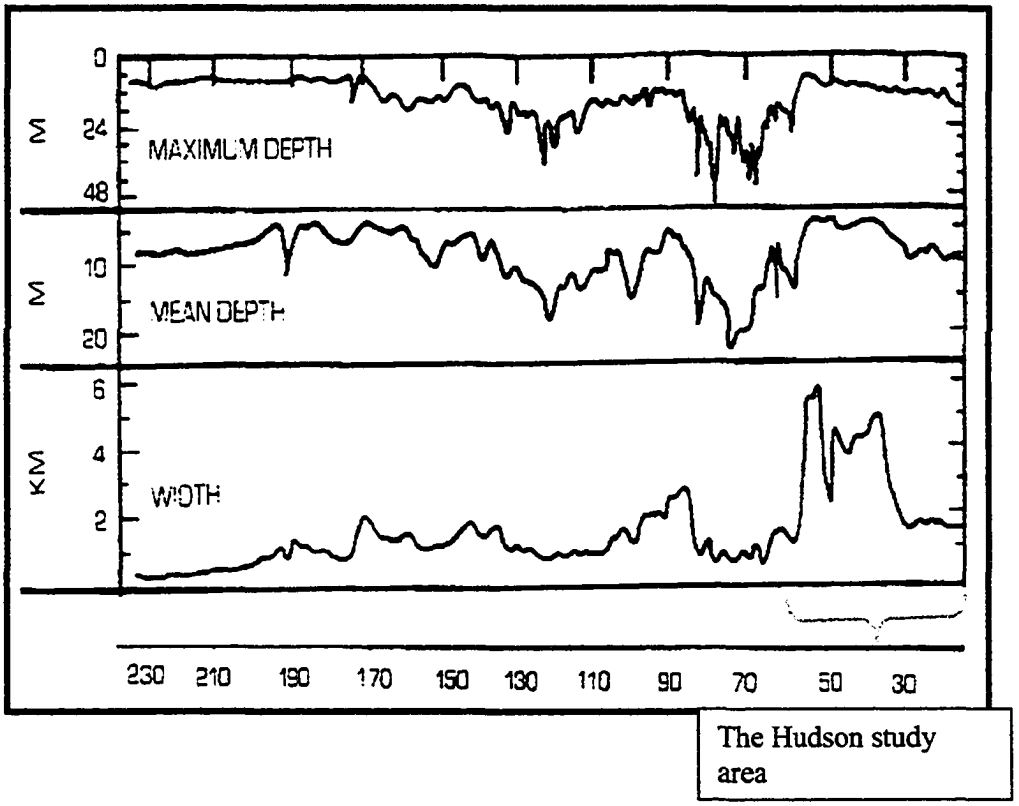

Figure 2. *Depth and width variation in lower Hudson. Distance in kilometers from the Battery. From Cooper et al, 1988.*

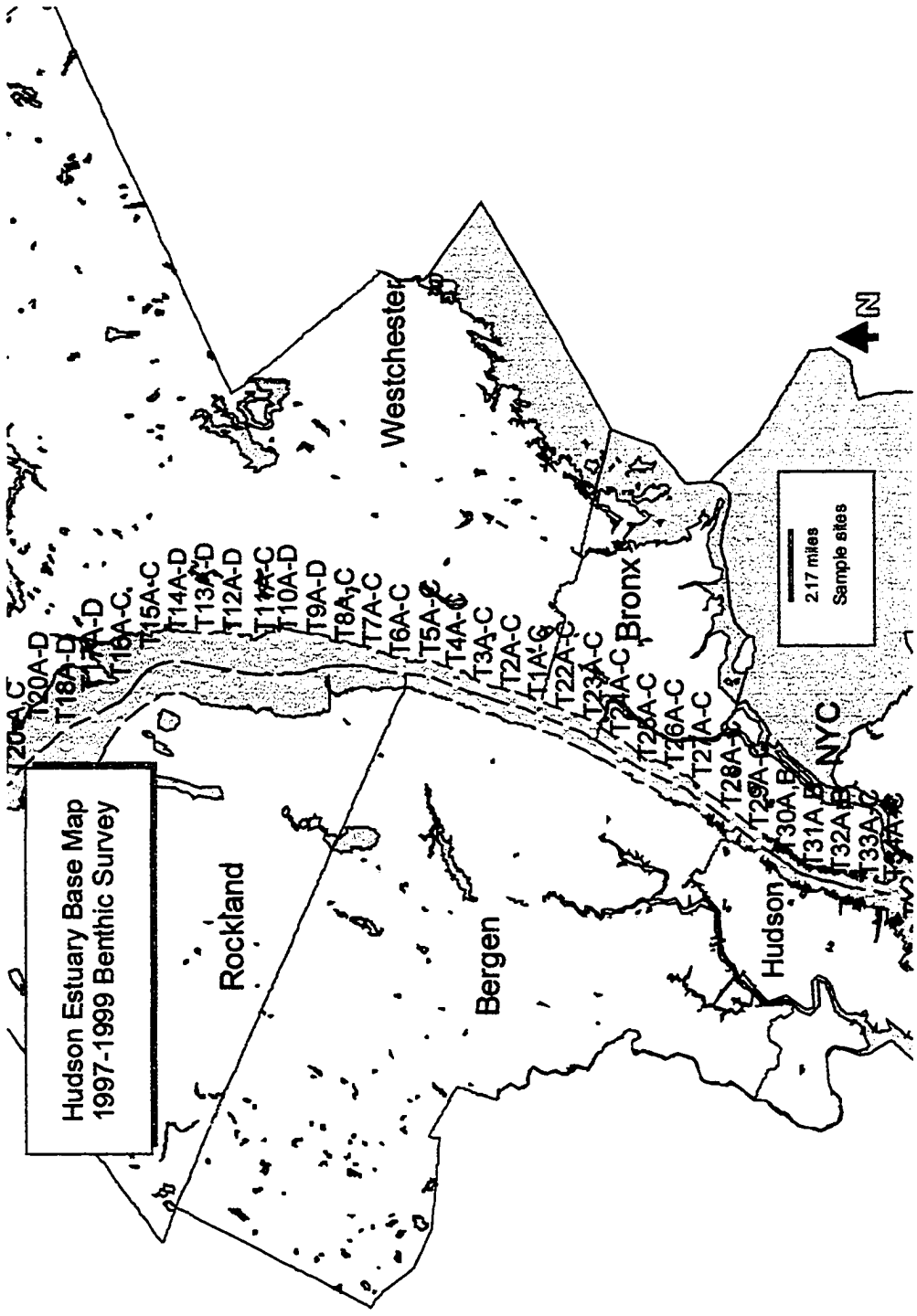

Figure 3. *Base map for 1997 – 1999 Hudson Estuary benthic sampling. Transect spacing approximately 2 kilometers (1 nautical mile).*

comprises the remainder of the mesohaline salinity zone defined by salinities between 5 and 18 ppm, extending from Yonkers to Haverstraw/Croton-on-Hudson. Haverstraw-Croton is the approximate location of the northernmost sample site in this study. Two additional reaches lie above Reach 2; Reach 3 extends from Haverstraw through the Hudson Highlands and Reach 4 ends at Troy, Poughkeepsie, the northern extent of brackish waters. North of Haverstraw-Croton, the salinity is defined as mesohaline to oligohaline defined by a salinity range of less than 10 ppt.

The salt-water front, that region that separates the saline from fresh water, oscillates over a distance of approximately 50 miles, between Chelsea Pump station (Poughkeepsie) and Hastings, New York depending upon the season (Figure 4). Fresh water input and tides are the major controls on the location of the front (Giese & Bar, 1988); the spring rains and melt-water push the salt front south as the stream progresses. The present study includes field seasons in the summer-1997, a small re-sampling in the fall of 1998 and a final season, summer of 1999. Over this 3-year interval, the salt front extended over a very narrow range from 60 to 70 miles up river in the summers of 1997 and 1998, and was even further upstream in 1999. It resided at approximately 70 to 80 km upstream, just south of Poughkeepsie in 1999 as a result of severe drought conditions.

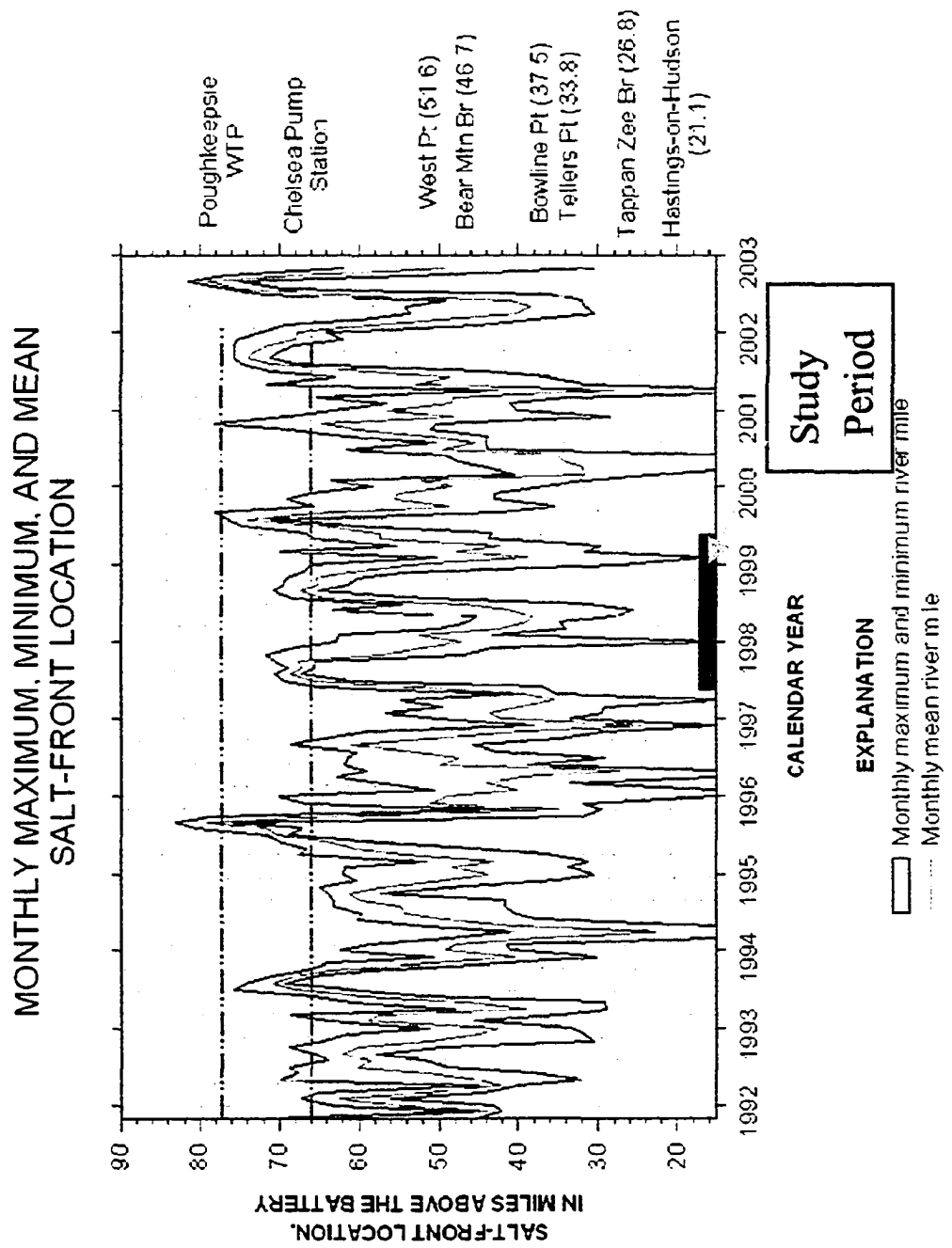

Figure 4. *Hudson salt front data 1992 through 2002. Blue line and arrows indicate present study interval and approximate locations of salt front during sampling.*
From: http://ny.usgs.gov/htdocs/dialer_plots/saltfront.html

The dynamic created by salinity front-migration resulting from tidal effects and watershed contribution interactions produces a marked two-layered salinity based structure (Weiss, et al 1978) particularly in the summer months. During the remainder of the year the Hudson is considered partially mixed. The gradient stimulates both lateral and vertical turbulence and influences the distribution of bottom sediments and resident organisms at least while in larval stage (Ristich & Fortier, 1977). Salinity flux, anthropogenic pollutant influx from air deposition, urban and agricultural runoff, leaching and wastewater discharge from sewage treatment plants, and ground water transport of contaminants from septic systems may have vastly modified the original ecologic assemblages (Carriker, 1985). For the last several decades, opportunistic estuarine bivalves have become widely established in the Hudson (Shaw, 1974, 1975, 1978). Most of these organisms can tolerate a fair amount of salinity fluctuations and anthropogenic disturbance. Over the research interval and beyond diversity has not changed, but numbers of individuals have increased dramatically as will be discussed in detail in Chapter 4.

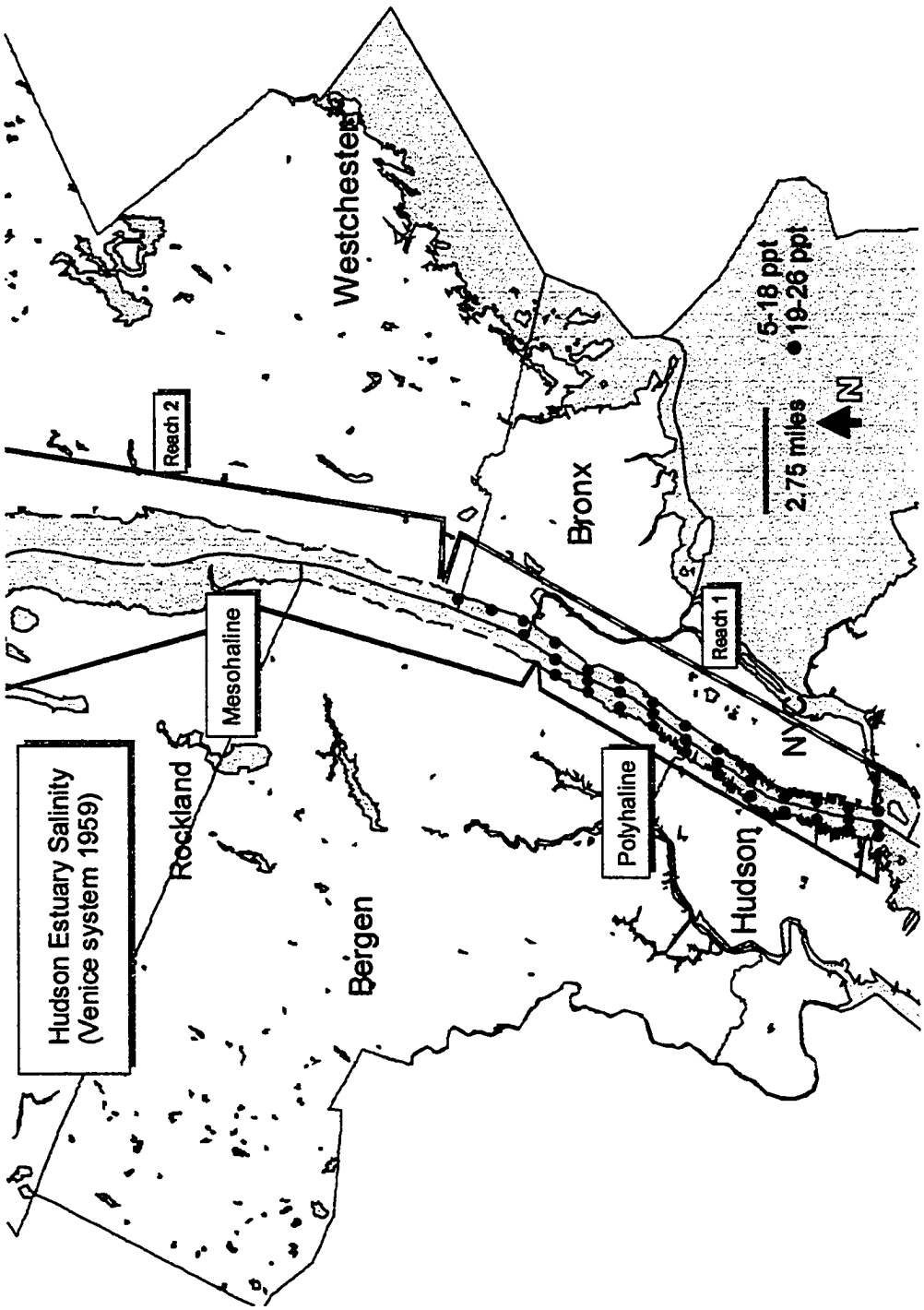

Figure 5: *Hudson estuary salinity base map.*

B. Estuarine Pelecypods

Order Bivalvia of the phylum Mollusca, contains organisms defined by a carbonate bivalve exoskeleton that is generally elongate and with bilateral symmetry. The exoskeleton lacks segmentation. The soft parts include a digestive tract but no body cavity and microstructure of soft tissue reveals an acoelomate condition (possessing three cell layers) (Moore, Lalicker, Fischer 1952). (See Figure 6 for general morphology and distinguishing features). Bivalves posses a meaty foot-like structure used for burrowing that protrudes from the anterior ventral end of the bivalve shell. The general circulatory, respiratory, and digestive systems are simple for bivalves and the organism lacks a distinct head. However, the gills are relatively complex for such a simple organization. Gills are of three-four organization types, the most complex of which exhibits complicated folds and feathering. The mantle envelopes the internal organs and has the function of secreting calcium carbonate used in shell production. (Moore, Lalicker, Fischer 1952) The ions used in shell production are extracted from seawater and carried to the mantle via the circulatory system.

1. Aragonite formation

Bioprocesses contribute to the generation of most sedimentary rocks, significantly impacting the physical and chemical modification of the biosphere through time (Lowenstam, 1981). Calcium minerals constitute two-thirds of all bio-minerals (Lowenstam, 1981). About twenty-five percent of the calcium minerals are colloidal deposits, rather than fully structured minerals. Biomineralization is a process that is widely considered to be either primarily biologically induced or biologically controlled. Biologically induced growth, primarily involves a matrix mediated growth step leading to the construction of a

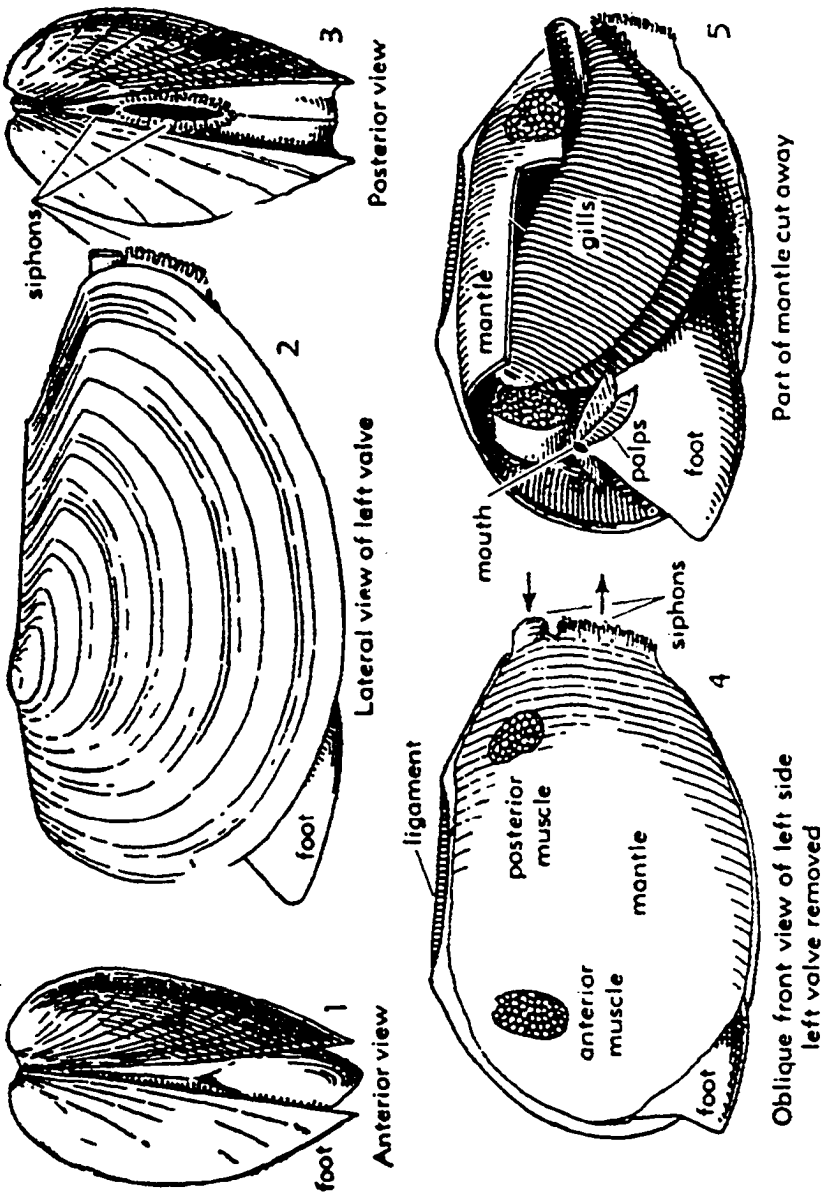

Figure 6. *Design of pelecypod (clam) illustrating bilateral symmetry in anterior and posterior view and location of gills and shell generating mantle. (From Moore Lalicker, 1952)*

framework upon which subsequent and continued deposition take place.

In contrast, biologically controlled growth is takes place without matrix building and is accomplished extra-cellularly, likened to pure precipitation from solution. Induced mineralization is deemed more primitive, and is carried out by bacteria and blue-green algae. Shell aragonite production is clearly influenced and to some degree controlled by the presence of organic compounds that form adsorption layers on already precipitated carbonate layers (Teng et al, 1998). The presence of aspartic acid near the surface of precipitation reduces the symmetry of the mineral being produced by shifting the direction of crystal growth. This type of mineral generation is completely controlled by environmental chemistry. Skeletal growth always proceeds as a biologically controlled mechanism. The skeletal substance may adopt structures ranging from entirely crystalline to various types of amorphous growth (Bottjer & Hickman, 1981). Crystalline structures contain individual crystals held together within an organic matrix, (see Solem, 1974; Krampitz, in Lowenstam, 1989) or at least in part a complex aggregates of interlocking crystals framed with amorphous microcrystalline material.

Molluscs create shells through secretion of a calcium carbonate from a mantle derived supersaturated solution; crystallization occurs outside the mantle. Aragonite, the orthorhombic form, is the predominant carbonate precipitated by most extant molluscs with the exception of oysters.

2. Lifestyles of Estuarine Molluscs

Bivalves exhibit three general lifestyles from various forms of epifaunal strategies to infaunal boring and burrowing and occupy three ecological niches. Molluscs of the Hudson Estuary are primarily of the infaunal burrowing type, except for the mussels and mid-estuary oysters which both attach to the hard bottom surfaces. Shells are specially

designed accommodate the living environments. For example, rock boring clams have long, narrow, ventrally sharp shells that operate like a drill as the organism rotates its shell over the rocky substrate. Many epifaunal bivalves tend to have shells designed for 'floating' on the substrate, possessing large surface area and hull design. Others attach by means of a byssus (mussels) or cement themselves to hard objects (oysters). Estuarine molluscs of the Hudson are predominantly burrowers in mesohaline soft-bottom localities and of the sessile, bysally-attached variety in the navigation channel sites in the polyhaline zone and further north in the upper mesohaline. Diversity is uniformly low with a marked decrease up estuary where fresh-water intolerant species are absent (Carriker, 1985). Epibenthic organisms that prefer higher salinities are certainly absent. Infaunal organisms adapt better to regions of fluctuating salinity because they are protected from direct contact with water. As a result, virtually all of the infaunal Hudson molluscs exhibit a broad salinity tolerance so that mud-bottom locales are densely populated. Apart from resident location within the benthos, clams also have two feeding modes, filter- and deposit-feeding. Sessile, bysally attached bivalves are active filter feeders. It has been demonstrated that the filter-feeding invader species, the Zebra mussel (*Dreissena polymorpha*) in the upper Hudson Estuary successfully out competes local molluscs because of superior filtering capabilities and a rapid reproduction rate. In fact, many observers argue that the water of the upper Hudson has been 'purified' by the filtering of this invader (Roditi & Caraco, 1996). Burrowers are also active filter feeders, but one species in particular, *Macoma balthica*, also has the ability to forage the bottom sediments with its inhalent siphon when suspended nutrients are scarce. Organisms with this type of feeding strategy may prove valuable in evaluating the general health of an

estuary since chemical analyses of the shell and tissue will reflect both dissolved and adsorbed contaminants.

3. Hudson Estuary Bivalve Species

The primary bivalve species of the Hudson Estuary are small by diversity standards but great as far as population (numbers of individuals) (see Figure 7).

Figure 7. *Molluscs of the Hudson Estuary* ***Mesohaline organisms****: a)Mya arenaria, b) Macoma balthica, g) Rangia cuneata h) Crassostrea virginica;* ***Polyhaline organisms****: c) Mulinia lateralis, d)Mytilus edulis , e) Yoldia limatula., f) Razor clam, Gastropoda: i) Nassarius sp., j) Crepidula s.*

Mytilus edulis is a mussel that resides in the lowermost regions of the estuary closest to normal ocean salinity. Adult *Mytilus edulis* attain a size of at least 70 mm. The shell is dark blue to black and elongate. Growth lines (growth interruption lines) are evident and may be used for age determination supported by release and recovery experiments of marked specimens and size frequency studies. This mussel lives for an average of 6 years, but average age may be dramatically reduced as a result of competition.

Mulinia lateralis, little or dwarf surf clam is similar to *Spissula solidissima* the larger surf clam. *Mulinia* grows to a maximum size of 19 mm and adopts a somewhat triangular shape with a thin, delicate shell. The hinge has a very distinct triangular cup-like chondrophore and backslope that is flattened.

Macoma balthica is a bivalve that reaches a maximum size of 25 mm in diameter with an almost circular shell and centered umbone. The surface is grayish to tan where the periostracum is attached, usually toward the ventral region. Growth lines are evident as are larger yearly bands with apparent summer versus winter partitions. This mollusc lives on average 5 to 10 years. It typically burrows several centimeters into mud to sandy mud to sand bottoms and is prevalent in estuaries and inter-tidal flats. *Macoma balthica* has a high tolerance for salinity variation and occurs in environments ranging from 18 to 40 psu or parts per mil, though it prefers mesohaline conditions, 3 – 10 parts per mil (Ristich & Fortier, 1977). In actual fact, *Macoma balthica* was recovered in lower mesohaline regions of higher salinity, 10-16.5 parts per mil. Of all the estuarine species it is the only active suspension and obligate deposit feeder. Suspension feeding occurs as the inhalent and exhalent siphons are projected into the water column. As suspended

nutrients diminish, *Macoma balthica* uses the inhalent siphon to 'vacuum' the estuary bottom and process nutrients in the sediment. The diet of *Macoma balthica* consists of phytoplankton, diatoms, and organic matter in detritus, including bacteria.

Mya arenaria is also an infaunal burrowing mollusk that resides in intertidal, estuarine environments. This organism prefers sandier substrates and is capable of burrowing to 25 centimeters or deeper. *Mya arenearia's* shell is more elongate with the umbone situated closer to the anterior. Shell length attains 60 to 100 centimeters. The shells are typically white with a tan periostracum. The inhalent and exhalent siphons are attached and are capable of stretching 20 to 40 centimeters allowing for deep burial. As a result of the large siphon, the shell is agape at the posterior margin. *Mya arenaria* prefers more saline conditions and is often found in polyhaline to mesohaline environments within the preferred salinity range of 30 to 40 psu. *Mya arenaria* is an active suspension feeder with a diet of phytoplankton, small zooplankton, diatoms and other suspended organic matter.

Rangia cuneata is an epifaunal freshwater mollusc that has adapted to life in brackish environments of salinities no greater than 18 parts per thousand. *Rangia cuneata* has a robust shell 2.5 to 6 cm long that enables life in extremely turbid environments. Juvenile *Rangia cuneata* shells resemble *Mulinia lateralis* since they too tend to have flattened backslopes, but the shell thickness prevents confusion. Individuals generally live from 4 to 5 years up to a maximum of 15. *Rangia* is a non-selective filter feeder with a diet consisting of plant debris and phytoplankton.

4. Shell Structure

The mollusc shell serves to protect the soft parts of the organism. The shell framework is composed of calcium carbonate in the form of calcite or aragonite or both inter-layered with minor amounts of conchiolin. Conchiolin is best known as a brownish thin proteinaceous layer (periostracum) covering the outer surface of the shell complex or calcium carbonate ostracum. The periostracum serves to protect the shell exterior from dissolving under conditions of relative high local environmental acidity. The ostracum is usually composed of multiple layers (inner and outer layer as noted in schematic of Spissula solidissima in Figure 8).

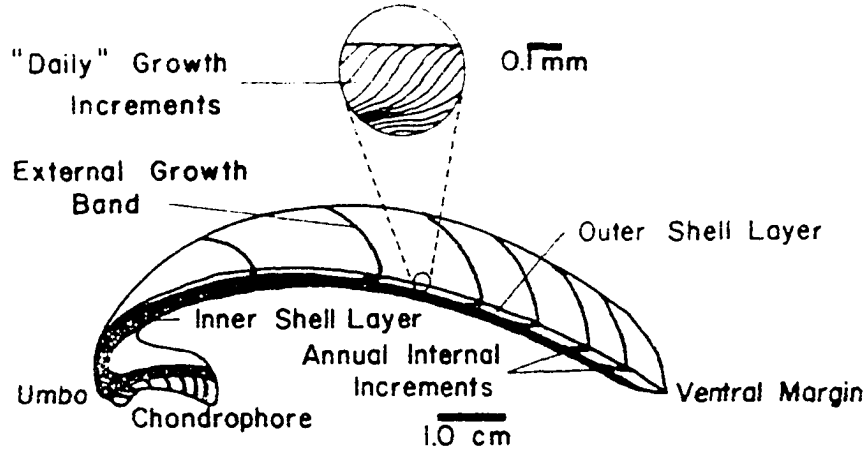

Figure 8. *Microstructure of mollusc shell. The top of the diagram represents the upper surface of the shell. From Bottjer, Hickman, Ward, 1985.*

Some species develop one at the expense of the other. The inner layer of the ostracum consists of microcrystalline calcium carbonate in micro-layers, again, sometimes inter-layered with conchiolin. The outer layer consists of robust crystals or quasi-crystals sometimes oriented perpendicular to the shell surface. The entire inner shell is lined with

a microscopic thickness of aragonite called the nacreous structure. This structure has a pearly luster and is sometimes referred to as 'mother of pearl'.

5. Trace Metals and bivalves

Since estuarine water flow is complicated by tides, and seasonal river flow within a restricted area, chemical variability in sediments is also complex. Filter-feeding or deposit feeding bivalves, i.e. *Macoma balthica*, inhabiting these localized, metal-rich areas are prone to metal binding as shown by Babukutty & Chacko (1992), Carriker, et al (1985), Adami et al, (1997), Barlow & Kingston (2001), Gundacker (2000) Luoma et al, (1990) and others. Benthic sessile or infaunal organisms have been shown to make good bio-indicators of contaminant concentrations and the estuarine species *Macoma balthica* and *Mytilus edulis* have been used as metal monitors (Goldberg, 1975 and 1978).

Metal uptake by molluscs is a complex function of bioavailability of ions, salinity, organism metabolic activity, and to a lesser extent temperature, and calcium and metabolic inhibitor uptake (Yang & Sanudo-Wilhelmy, 1998). The effects of these factors in metal uptake is not completely understood, nor are the resultant effects on metal partitioning into shells, soft parts and/or excretion (Wright et al, 1995; Leung et al, 2002). Bioavailability of metals in the Hudson estuary water column was measured by Yang & Sanudo-Wilhelmy (1998). They maintain that in times of low discharge, i.e. lack of runoff and winter snow melt, metals have the opportunity to build-up as dissolved constituent in the water column. The dissolved component is one possible source for metals that are available to benthic fauna. Pitts & Wallace (1994) shows that lead availability to *Mya arenaria* occurs as a dissolved fraction in water and that the

concentration partitioned in shells is at times 10,000 times the ambient water concentration.

Strontium is the most heavily examined divalent metal to substitute for calcium in aragonite skeletons (Dodd, 1965) and corals have been most extensively studied organisms because they tend to concentrate Sr in their skeletal structure (Speer, 1983). The environmental factor relating most to Sr uptake is temperature. Speer (1983) reports that Kinsman and Holland (1969) have determined that Sr uptake by corals is inversely related to temperature. The only other significantly applicable environmental factor is Sr/Ca ratio as a dissolved component, which relates directly to Sr partitioning. Palacios et al (1994) relates Sr/Ca ratio in shells to seasonal variations as an increase reflected once yearly in the summer season. Dodd (1965) establishes the relationship between temperature and salinity with magnesium and strontium uptake by *Mytilus edulis*. Temperature is the most important factor controlling the partitioning of Sr in this species and salinity has only a minor effect. Interestingly, for this species, the response to temperature varies depending upon the particular shell layer that is being deposited. Dodd shows that the outer prismatic layer concentrates more Sr as temperature increases. The nacreous layer, on the other hand shows the opposite effect. Magnesium concentration in the outer prismatic layer varies inversely with salinity and directly with temperature. The content in the nacreous layer is too small to measure and evaluate.

Luoma et al (1990) examined Ag, Cd, Cr, Cu, Pb and Zn deposition in river-estuarine bivalves from Suisan Bay in San Francisco. He determined that metal partitioning is most closely correlated with bioavailability of metals and to a lesser degree dependent upon estuary salinity and temperature.

Adami et al (1997) generates a map of heavy metals from the shoreline of the Bay of Muggia in the northern Adriatic Sea to the open ocean has established that the majority of observed heavy metal contamination is both localized in distribution and anthropogenic in nature. In this examination concentration of different divalent metals are evaluated, chromium (Cr), lead (Pb), Zinc (Zn) and Cadmium (Cd). The response of benthic animals to the observed heavy metal pollution is reflected in the population dynamics of the bio-indicator species, *Corbicula gibba*, a suspension feeding mussel whose distribution correlates strongly with the presence of Cr, Cd, Pb, and Zn in the sediments upon which this organism resides. Since *C. gibba* is strictly an obligate suspension feeder, the observed contamination can not be from metals bound to sediments, but from contaminated diatoms filtered from the bottom waters.

Other examinations of divalent metal uptake are undertaken by Leung, et al (2002), {Cd}, Gundacker (2000), {Cd, Pb, Cu, and Zn in freshwater molluscs} Bilos, et al (1998), {Cd, Cu, Mn, Cr and Ni in estuarine mollusc *Corbicula fluminea*} Blackmore (2001), {Cd, Zn, and Cu in inter-tidal mollusc tissue}. The former relates cadmium binding to salinity and shows that as salinity decreases Cd and other trace metal uptake increases in the gastropod *Nucdella lapillis*. This study reveals the significance of salinity fluctuation and metal uptake by asserting that estuarine organisms residing in regions that typically encounter fluctuating salinity are more likely to survive under heavy metal stress. Gundacker (2000) examined biologic assemblages instead of individual organisms relative to metal uptake and once again tissue values are evaluated. No data on shell carbonate is presented. Metal concentration in tissue correlates with degree of metal contamination and specifically particle size of the contaminant sediment,

i.e. ideal size of sediment ingested by deposit feeders. Wright et al (1995) has also established the correlation between increased metal uptake and decreased salinity for *Mytilus edulis* and *Macoma balthica* regarding most divalent metals. The mechanisms responsible for this relationship are still poorly understood. These estuarine bivalves are often used as bio-monitoring species in estuaries and coasts since metal uptake increases linearly with environmental metal availability.

Decho & Luoma (1994) examined Cd, Cr uptake as a function of bioavailability in estuarine molluscs and Bourgoin, et al (1991) examined lead uptake by *Macoma balthica*. In the latter study, the intent is to demonstrate the relationship between bio-availibility of lead and the sulfur concentration in the oxic layer of the sediments in the Restigouche River Estuary, Dalhousie, New Brunswick. This study is particularly significant to the present research since the Dalhousie study area characteristics are remarkably similar to the Hudson. Both estuarine systems contain substrates primarily composed of thin oxic organic silts to sands over thick anoxic black muds and contain populations of *Macoma balthica*. Lead is contributed to the Dalhousie study area through some of the same inputs as the Hudson, i.e. atmospheric deposition and runoff, but includes an additional source of galena from a nearby sulfide ore loading facility. This study basically established that the availability of lead is not the sole determining factor for lead uptake. Uptake is heavily influenced by the composition of the oxic upper layer that contributes to the diet of *Macoma balthica*. Although bulk lead in the region reflects nearness to the source of the contamination, *Macoma balthica* did not show the same variation. Essentially, the Pb bound to S in galena is not readily available to *Macoma*

balthica. This study elucidates the need to calculate metal concentrations in terms of bioavailability in addition to bulk availability parameters.

Decho & Luoma (1994) reveals that the presence of heavy-metal-laden humic and fulvic acids in estuarine sediments contributes to metal accumulation in molluscs since these compounds tend to act as a sink for heavy metals. These heavy-metal laden organic compounds are then consumed by deposit feeders. Experiments involving Cr and Cd adsorption show that organic coatings on particles greatly increase the bioavailability of metals from the surfaces of hydrous ferric oxides or silica. Cd availability is always increased through adsorption onto organic particles or organic coatings. Cr adsorption is very low for both inorganic and organic bound Cr.

Barium in the form of barite (BaSO4) is shown to cause damage by degrading the gill tissue of deposit-feeding *Macoma balthica* (Barlow & Kingston, 2001). Barite is used as a lubricant in drilling and once discharged it accumulates and persists in low-energy regions of ocean or estuary bottom. The damage to organisms results from the interaction of suspended barite-containing sediment to suspension feeders preferring sediment free water. *Macoma balthica* is a facultative species so the damage by uptake of barite is more greatly enhanced by the dual feeding strategies.

Metallothioneins (MT) are a specific group of proteins produced by microorganisms as a coping mechanism for environmental metal exposure. MT produced by aquatic organisms may influence the binding capability of metals and enable incorporation of metal ions including Zn, Cd, copper Cu, and mercury Hg, through the formation of metal-tholiate complexes (Leung, et al (2002); Bordin et al, 1997). The formation of these complexes results in metal detoxification by the binding process and

subsequent partitioning into mollusc shells and/or organic tissue. MT-like proteins in *Macoma balthica* increase both due to seasonal and short-term anthropogenic metal fluctuations. Bordin et al shows that bivalves living in less polluted environments respond much more readily than those accustomed to contaminants. Therefore, the fluctuation in MTs is greatest for those organisms in less polluted environments.

MT production in the freshwater mollusc *Corbicula fluminea* (Asiatic clam) reveals that MT production peaks during spring and early summer (Baudrimont et al, 1997). The seasonal peak production of MT correlates with the reproductive cycle of the organism, rather than the environmental presence of metals in a lake system. MT production may be further complicated by salinity fluctuations (Leung et al, 2002).

Although not central to the present study, it is well known that the metal concentration in soft tissue is not necessarily in direct proportion to the environmental metal concentration. Strongly metal-rich environments often fail to show similar anomalies in organic structures (Bordin et al, 1997). In many cases, the sediment wins the competition for metals. There is very little information as to the consequence of this competition to the resultant composition of the shell.

In the present study, we focus instead on correlations with water salinity, position in the channel (longitudinal location) and species-specific issues. Correlations with sediment are especially suspect in the estuarine setting since the molluscs are relatively immobile (restite) in comparison with grab samples of the bedload material which is mobile and may not de--- from the locality where it is collected (see Ashkan 2000 unpublished doctoral thesis).

6. Crystallography and bivalves

Scant studies regarding the characterization of crystal structure and unit cell parameters for mollusc shells have been undertaken. One such study, Babukutty & Chacko (1992), provides information based on IR spectroscopy to show the incorporation of metals in the aragonite structure. They show that carbonates such as cerrusite (Pb) that are isostructural with aragonite and involve metal cations with larger ionic radii than Ca are precipitated by molluscs in minor amounts. Mn substitution is also evident in aragonitic forms though rhodochrosite is isostructurally similar to calcite, not aragonite. Sr has been shown to substitute for Ca in the highest concentrations of all divalent cations (Lowenstam, 1981). For many marine species, the Sr/Ca ratio in the shell approximates water chemistry. Lowenstam shows that the 'species effects' cause variations in shell chemistry from that of the environment in higher organisms that precipitate calcium carbonate intracellularly. Less complex organisms rely on extracellular precipitation and therefore generate calcium carbonate that approaches inorganically precipitated aragonite.

Speer (1983) outlines recent shell structural characterization for divalent metal replacement of calcium. He determines that substitution is a function of ionic size and has established that the greater the deviation from the calcium ionic radius, the lesser the degree of substitution. This hypothesis works well for Sr and Mg, but not for Cu concentrations, which have been defined as inclusions of Cu complexes. Monovalent cations are included in aragonite as adsorbed ions and fluid or solid inclusions because their observed concentrations in shells have no correlation with ionic size and are hence assumed to exist outside of the crystal structure. Sodium is an exception since its ionic

size is quite similar to Ca and it has been proven to reside within the aragonite structure. Since Na is monovalent, the charge imbalance is rectified by the inclusion of the bicarbonate ion (HCO_3^-).

7. Distribution of Estuarine molluscs

Scant few current molluscan distributions are established for estuarine environments. Carriker (1985) reviews the ecology of benthic invertebrates which reviews works prior to 1964. Sanders (1960) mapped the distribution of soft-bottomed benthic fauna of Buzzards Bay, Mass. Another nearby study in the Hadley Harbor area of Massachusetts adjacent to Buzzards Bay conducted in 1967 by Parker et al maps the distribution of benthic fauna limited to the estuarine euhaline environment where salinities are over 30 psu (parts per thousand). Bivalve diversity in this region is also low dominated by only two species, *Yoldia limatula* and *Solemya velum*. Several of the organisms populating Buzzards Bay are also present in the Hudson Estuary, *Mulinia lateralis*, *Yoldia, Nassarius* and *Crepidula* species. The ecology of this region is markedly more diverse than estuarine environments. Richards & Riley (1967) mapped the distribution of epibenthic fauna of the Long Island Sound for determination of total biomass primarily to measure fish food availability and secondarily to establish the validity of their oyster dredge sampling techniques. Again, this environment exhibits much greater diversity than estuarine systems. Davies (1972) evaluates the molluscan fauna of the Rappahannock River Estuary, Virginia. He notes that the molluscan fauna are mainly associated with particular substrates. This finding is supported by this research. In the Rappahannock estuary, four mollusc species dominate with ranges that overlap between 30 and 40 kilometers from the mouth of the estuary. Except for slightly

different species specific to the region, the assemblages are quite similar and provide the best comparison to the Hudson. A more recent study of the estuarine assemblages along the North and South Carolina coasts was undertaken by Mallin, et. al (2000). This environment most closely resembles the Hudson and the benthic communities are similar based on the presence of *Macoma balthica.*

The most thorough Hudson Estuary investigations were undertaken by Shaw (1974, 1975), Weiss and Shaw, et al (1978) and The Boyce Thompson Institute for Plant Research (1977). The Boyce Thompson research identified *Mya arenaria* and *Macoma balthica* as the dominant estuarine species throughout the estuary with ranges that overlap in the mesohaline reaches. *Crassostrea virginica* and *Rangea cuneata* are absent from the distributions. The latter research is the motivating factor for this work. Shaw notes two assemblage zones, a high brackish community occupied by *Mya* and *Mulinia* and low brackish community dominated by *Mytilopsis*. The current research modifies these designations in Chapter 4.

CHAPTER 3: MATERIALS AND METHODS

A. Sample collection

Hudson mollusc species assemblages and general distribution and were first established in 1977 by F. Shaw (Rudolph and Shaw in preparation). In that study, the Hudson samples were collected from 34 east west traverses with a two-kilometer spacing from the Battery to Croton Point. Three to five sites were sampled along each transect depending upon the width of the channel at that latitude. Sampled segments comprise at least one from each near-shore and one in the navigation channel. Shells and sediment were collected using a spring-activated Petersen Grab sampler that entraps approximately one cubic foot of sample per enclosure. The focus of the 1974 – 1977 mission was to characterize the benthic distribution of organisms and establish assemblage zones for the observed associations. This initial monitoring was conducted monthly to assess the possibility of seasonal variations and establish replicability. Although the sample sites were located by GPS, pinpoint site replication was problematic due drift resulting from tides. Benthic composition is the likely culprit in gaps in organism distribution since the primary clam species in the Hudson estuary are both sediment type and salinity dependent. For large expanses of benthic environments with similar salinity, the small-scale variations in sediment type would hinder the colonization by burrowers.

The present study attempts to replicate the monthly collections of the Shaw (1977) in two comprehensive summer/fall sampling trips, one each in 1997 and 1999 and a select re-sampling replication trip in August of 1998. The 1997-1999 team includes the author, advised by Dr. Frederick C. Shaw, Lehman College, CUNY, Dr. John A. Chamberlain, Brooklyn College, CUNY, and Dr. Jeffrey C Steiner, CCNY, CUNY. Two

additional doctoral students participated, Fatemah Ashkan, Brooklyn College, CUNY, and Paul Feinberg, Queens College, CUNY. The project was divided into three components: 1) The sediment geochemistry of the Hudson Estuary assigned to Fatemah Ashkan, 2) Mollusc soft tissue geochemistry assigned to Paul Feinberg, and 3) Mollusc distribution and shell geochemistry performed by the author. In 1997, the resurrected survey was initially conducted from September 1 through 4 on a small vessel, operated by the New Jersey Science Consortium. This vessel is a small 10-foot powerboat with 2 outboard motors and a small Petersen Grab sampler. This vessel traversed approximately ¼ of the study area, approximately 30 kilometers per day for the first two days, sampling three sites along each transect (one on each coast and one in the channel). The final two days of 1997 sampling along with one day in 1998 and two in 1999 were conducted on the R/V *Lionel A. Walford*, a vessel owned and operated by the New Jersey Science Consortium, Sandy Hook Field Station, Fort Hancock, NJ, and captained by Jim Hughes. This vessel is substantially larger and slower so that per day sampling was dramatically reduced to approximately twenty samples per day, one from each coast along a series of ten transects. The sample grid was modified with inception of *Walford* sampling by elimination of navigation channel sampling since the channel samples contain only shell hash and other debris, with no live organisms. Again, the Petersen grab sampler was used to collect benthic samples aboard the Walford. Although a fairly disruptive method by principle, a weighted spring activated clamping claw snaps shut upon striking the bottom and grabs approximately one cubic foot of sample, the Petersen grab method did not result in a disruption of the upper silty, oxidized layer, one to two centimeters thick. In fact, it remained in tact and the live clams were in living position, burrowed into the lower dark gray mud to as much as 10 centimeters. The mixture of surface

sand, mud, organisms and debris was initially emptied into a five-gallon bucket after removal of a representative amount of oxidized surface sediment.

During the 1997 sampling, 98 samples stretching from the Battery T34 A-C to just north of Croton Point T20 A and C were gathered, one sample from each shoreline and one or two from the navigation channel (see Figure 9) depending upon width of the channel along the transect.

The 1998 sample set included west-coast shoreline samples from T34 to T25 (Figure 10). The purpose for the 1998 sampling was to determine and document the success of sample replication primarily in reference to surface sediment heavy metal concentration. The 1999 sample set comprises 61 shoreline samples from T34 to T16. The 1999 mission revisited all shoreline locations from the battery to Croton Point, NY (Figure 11).

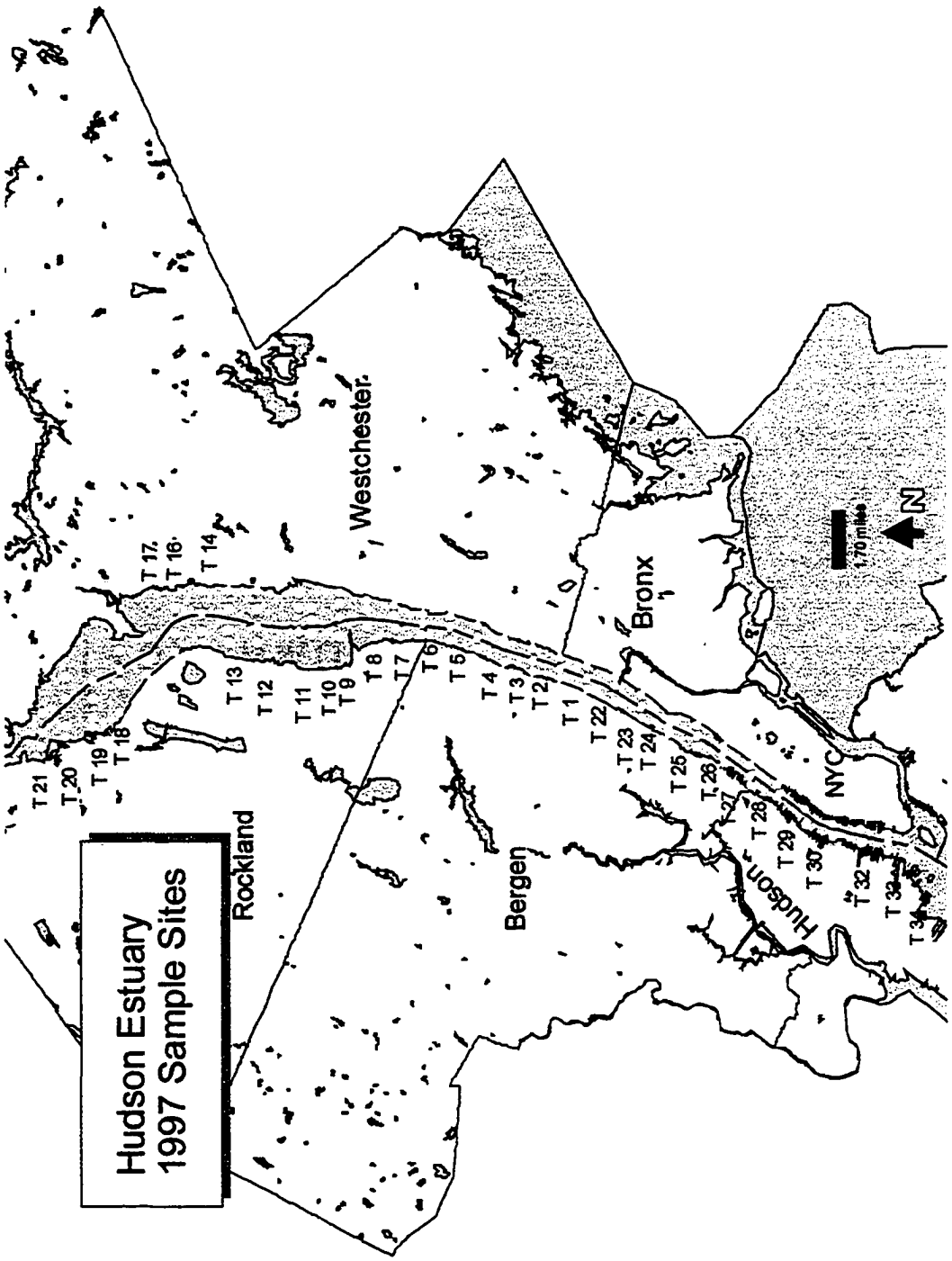

Figure 9. *1997 Sample sites. Research area includes T34 at the NYC Bight to T20 Haverstraw, NY.*

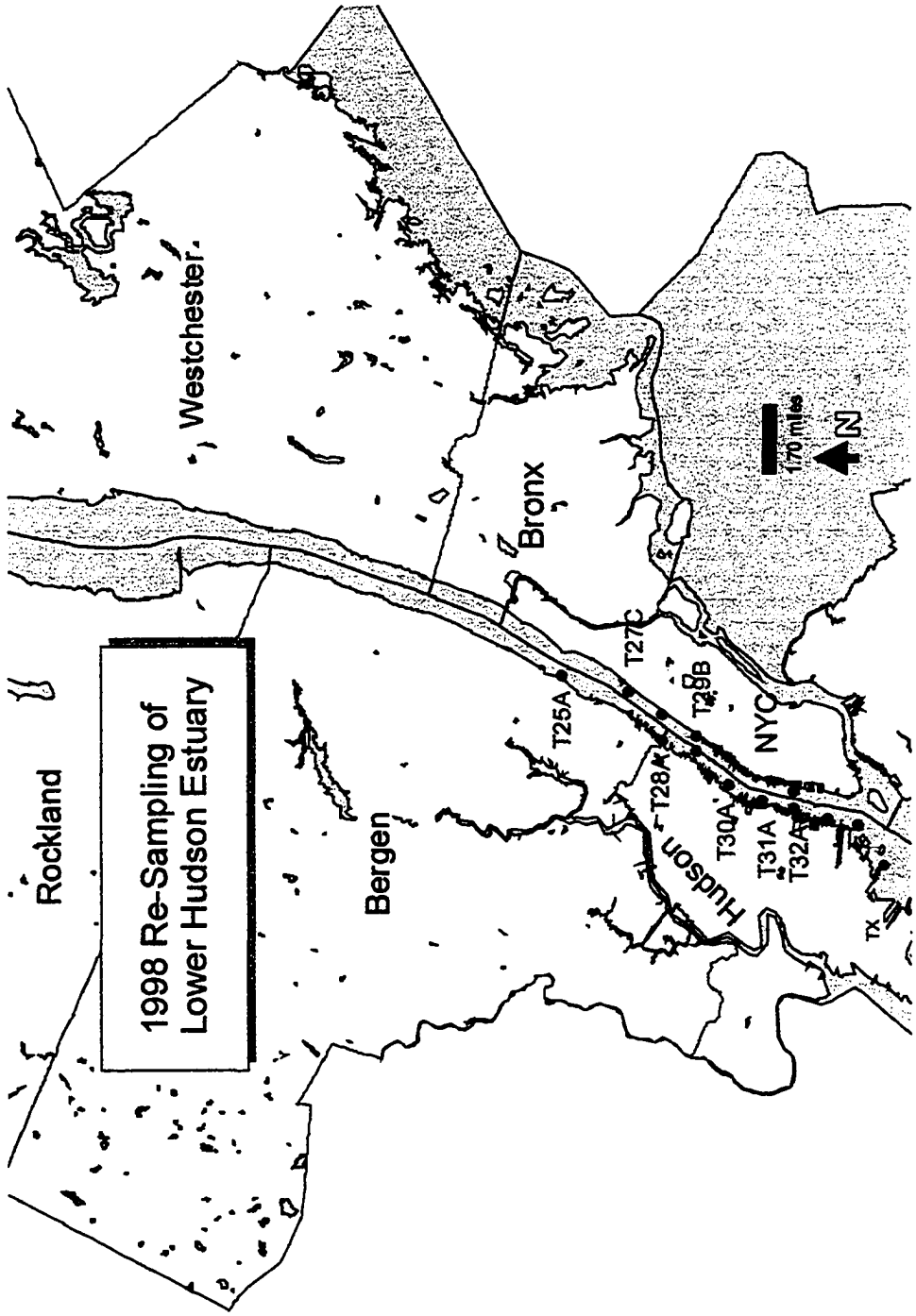

Figure 10. *1998 Sample Sites: 15 lower estuary locations*

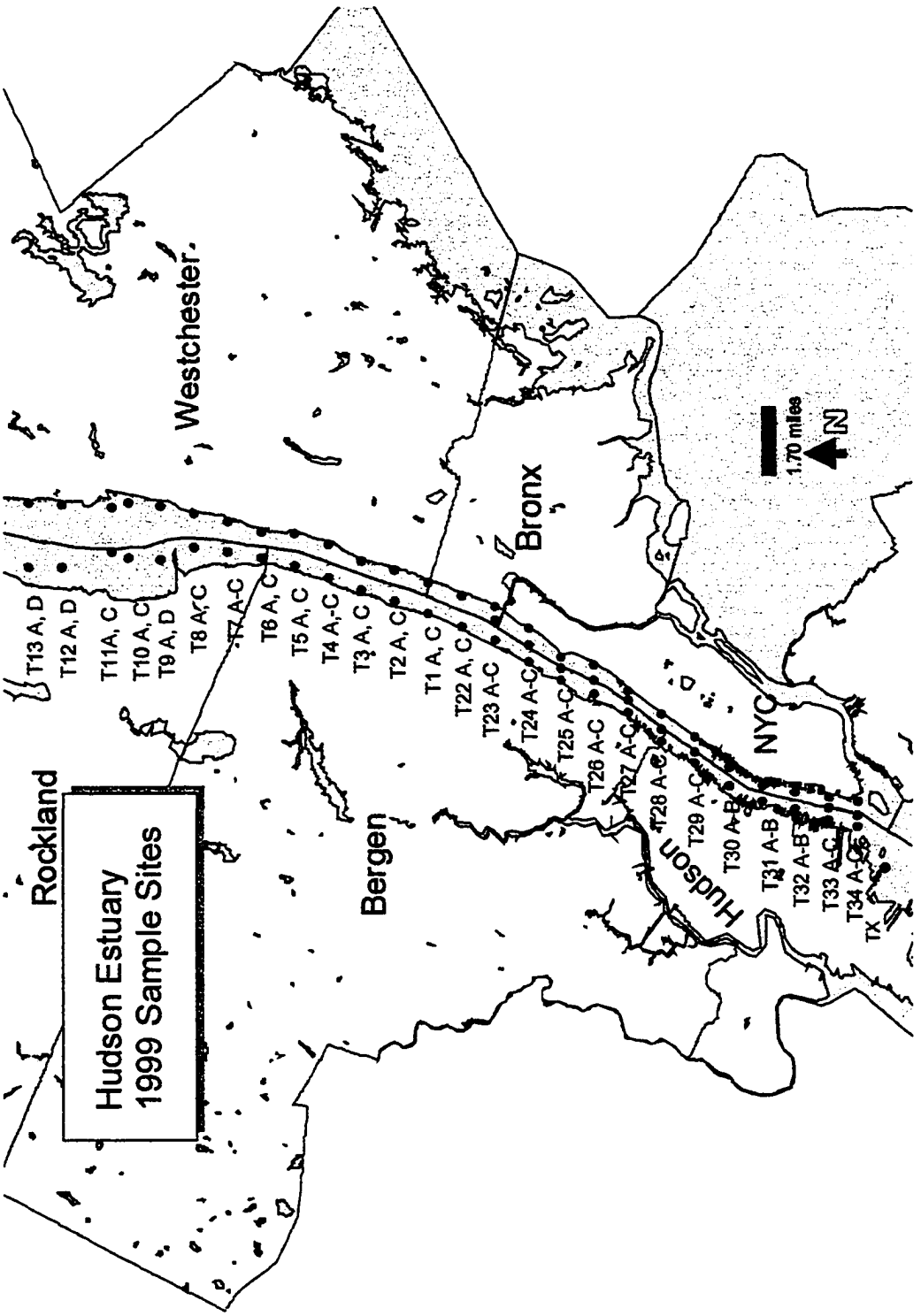

Figure 11. *1999 Sample sites: Re-sampling of most of the Hudson Sites, omission of channel sites north of Manhattan*

Upon reaching the locations first sampled in the 1970s using shipboard GPS, the Petersen Grab was released and brought forth to remove one shovel-full, approximately one cubic foot of sediment. A one-liter random sample was hand separated and transferred to a worktable for rinsing. Organisms were sorted using a 0.25 inch wire sieve to remove the macro organisms; a second sieve, 0.097 inch, 32 mesh, collected the finer fraction. Both fractions were bagged and labeled. Samples were stored on ice to preserve the soft tissue of live organisms.

In the lab the molluscs were sorted identified and counted; only the live organisms are used in the present study. The samples are archived in bags and plastic containers at CCNY in room J924. Organism counts are archived in Lotus Approach Database named *Hudson.*

B. Analytical Techniques and Sample preparation

1. X-Ray Diffraction (XRD)

X-ray diffraction patterns depicting the aragonite structure of final growth year shell material for all live Hudson molluscs are archived in Appendix 1. The collection of diffraction data evolved as a consequence of the desire to establish that metals other than Ca are contained in shell aragonite in minor quantities. The diffraction patterns elucidate the crystal structure of the aragonite and any deviations of the expected calcium carbonate pattern are interpreted as the result of ancillary minerals or inter-layered organic compounds. In general, the bivalves examined possess structures that conform to the aragonite structure. There are minor differences in diffraction spectra that can be attributed to trace substitutions for Ca in the aragonite structure.

A Panalytical (formerly Philips Electronics) modified PW10 diffractometer with an XRG300 generator operated at 35 kv and 15 ma is used to characterize shell materials. As discussed earlier, the outer growth year is abraded into a 2.5 cm mortar and pulverized under

STANDARD REFERENCE MATERIAL 660

LaB_6 reference standard for X-ray diffraction

Calculated Diffraction Angles and Relative Intensities

(T = 299 K)

hkl	I (rel)	2 theta
100	54	21.358
110	100	30.384
111	41	37.441
200	22	43.506
210	46	48.957
211	24	53.988
220	8	63.217
300	23	67.546
310	16	71.744
311	10	75.843
222	2	79.868
320	6	83.844
321	13	87.79
400	2	95.669
410	8	99.64
330	7	103.658
331	3	107.746
420	4	111.93
421	9	116.241
332	3	120.719
422	3	130.404
500	3	135.795
510	10	141.769
511	6	148.657

Table 1. *LaB_6 X-ray standard: hkl values, intensity and 2-theta locations determined by X-ray diffraction*

acetone for approximately 5 minutes with lanthanum hexaboride applied as an internal standard (LaB_6, Reference Standard 660). The dispersion (average 20 micron powder size)

is transferred by dabbing (using the pestle to drop the mixture) onto a quartz holder. The polished quartz holder is designed to be oriented such that background spectra emanating from the sample holder are minimized.

Samples are analyzed over a range of two theta from 20 to 65 degrees at 10 seconds per 0.2 degree step. The hkl value, location and intensity of each expected peak for the LaB_6 is output from the APD Panalytical Data-Analysis program. The individual peak refinement option is not employed. The values are the standard peak-selection output values (raw output in 2-theta is collected in ASCII files with an 'RD' extension). The LaB_6 standard diffraction maxima (Table 1) are compared to experimental values and found to produce a standard error of 0.002 in slope and 0.09 in intercept using the linear fit function in either EXCEL or MICROCAL ORIGIN. The correlation coefficient method approaches 0.9 to the linear condition (see Table 2 and Figure 12).

T9a Macoma balthica				
Correction for T9A Macoma balthica unit cell				
Table Shows Corrections for LaB6				
			x-independent	y-dependent
		La B6	La B6	
		Standard	Observed	Delta-Obs
hkl	I (rel)	2 theta	2 theta	
100	54	21.358	21.2245	0.1335
110	100	30.384	30.24	0.144
111	41	37.441	37.3	0.141
200	22	43.506	43.34	0.166
210	46	48.957	48.775	0.182
211	24	53.988	53.8	0.188

Table 2. *Table of Diffraction Peak Correction for LaB_6 for Hudson mollusc Macoma balthica at T9A*

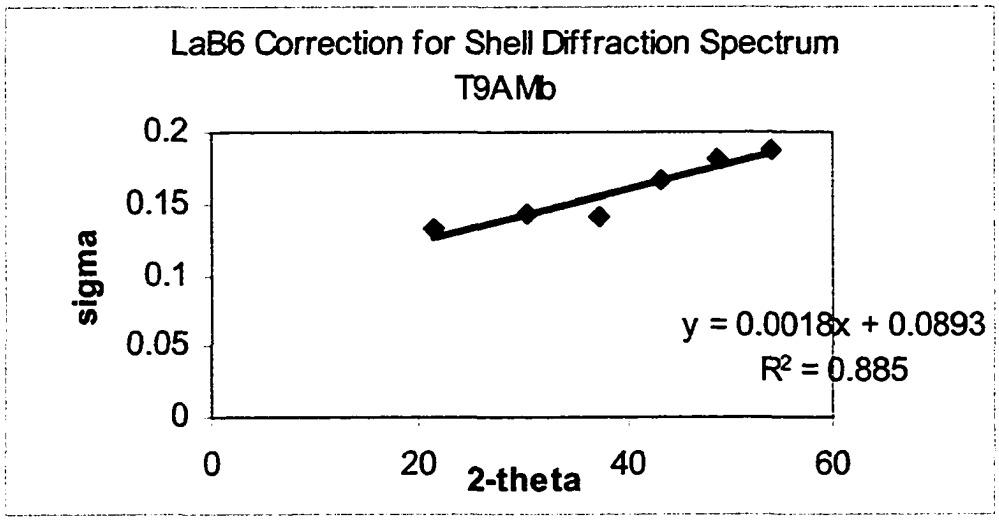

Figure 12. *Correction curve for T9A Macoma balthica using linear correction of LaB6 reference standard peak locations*

Once corrected the newly derived two-theta locations for the hkl values for molluscan aragonite are collected in **.txt* files for unit cell refinement (Table 3).

Sample: t9amb	
hkl	d-spacing
1 1 1	3.397735
0 2 1	3.269887
0 0 2	2.872987
0 1 2	2.704328
2 0 0	2.490449
1 1 2	2.375896
1 3 0	2.32993
2 1 1	2.187859
1 3 1	2.160295
1 2 2	2.108139
2 2 1	1.97883
0 4 1	1.88296
1 3 2	1.816332
1 1 3	1.745211
0 2 3	1.728049
0 0 0	

Table 3. *Text file for T9Amb (Macoma balthica) for Unit Cell determination*

The d-spacing for the material is evaluated using *UNIT CELL*, a DOS program that derives unit cell parameters from diffraction data and calculates the difference from ideal lattice parameters (Table 4).

Table 6: Output from Unit Cell
method of TJB Holland & SAT Redfern 1995

Sample Title: T9AMb.txt

mimiising the sum of squares of residuals in d-spacing

parameter	value	sigma	95% conf
a	4.9708	0.0044	0.0097
b	7.9506	0.0081	0.0177
c	5.759	0.0039	0.0086
cell vol	227.2079	0.2567	0.5602

residuals: strandard, average, and maximum deviations:-
sd(d) = 0.0029 aad (d) = 0.0021 maxdev (d) = 0.0060
sigmafit = 0.003194
students t = 2.18

Table 4. *Spreadsheet table 6: Sample Unit Cell output showing a, b, c lengths in angstroms and differenced from aragonite unit cell parameters.*

Select shells of live organisms are isolated for X-ray examination. Shell treatment begins with the separation of the two valves and removal of soft tissue. The protective outer proteinaceous layer is carefully removed with tweezers and an *exacto* knife. The entire shell is gently washed with warm tap water and rinsed with distilled water. Preliminary examination using a binocular scope capable of 2.5X magnification was conducted in order to establish the absence of all external material and to identify the growth bands. Most molluscs evaluated in this study are 1 to 4 years old and possess

clear summer-winter growth bands separated by fine indentations. The outer growth band signifying the final year of life is carefully sampled from one of the valves and processed for x-ray diffraction analysis. The remnant shell and second valve are archived for additional analyses. The approximate weight of sampled shell varies from 0.09 to 0.15 grams. The shell is powdered with methanol in a four-inch agate mortar with pestle for several minutes until achieving a uniform slurry consistency and particle size of 20 to 45 microns. After drying, the powder is scraped into two-milliliter centrifuge tubes, labeled and archived in room J924. Only a small fraction, less than 1/2 of the preparation is required for x-ray diffraction. The powder is once again converted to slurry by adding methanol and 0.005 grams or less of LaB_6 XRD standard reference material 660 is added as an internal standard. LaB_6 has a strong and characteristic x-ray spectra, with peaks completely out of the aragonite range resulting in a reliable peak location corrector. The sample-standard slurry is applied to a quartz window x-ray diffraction Type 9425.036.60100 zero background specimen holder and allowed to dry. The window contains a micrometer-sized depression capable of holding a thin layer of material.

2. Electron Microprobe

Electron Microbe analyses are performed on a Cameco electron Microprobe owned and operated by the American Museum of Natural History. Microprobe analyses are not the most economical for the purpose of establishing element variations in shells because of the high cost, and ultrafine points of examination. These analyses were invaluable for confirming XRF, SEM and Neutron activation results, and revealing micro-scale variations of rare earth elements (REE).

Several representative live organisms were selected for experimental microprobe analysis to verify element concentration determinations by other methods and to elicit details regarding the variation in chemistry at the micro structural level. For this limited work, representatives from two key Hudson species were selected. One shell of each *Macoma balthica* and *Rangia cuneata* were sent to Spectrum Petrographics for microprobe thin section preparation. *Macoma balthica* was chosen because of its general pervasiveness to the Hudson and *Rangia cuneata* as an unexpected newcomer. Additionally, *Rangia cuneata* has a robust shell enabling good sample preparation. The preparation technique involves embedding the shells in colored epoxy, making a vertical slice from beak to ventral margin, cementing the slice to a glass slide and finally polishing the slice to a thickness of less than 100 microns. The slide is carbon coated to create a conductive surface for analysis.

3. Scanning Electron Microscopy (SEM)

Scanning electron microscopy (SEM) images and chemical data are collected using a new computerized Zeiss SEM fitted with an EDAX energy dispersive analyzer owned and operated by Lamont Doherty Earth Observatory. The SEM attained 30,000+ magnification and qualitative chemistry either normalized by oxides or individual element concentrations. The SEM operates by generation of an electron beam that is focused and centered using a series of magnets. The resultant beam scans the surface of a sample that has been rendered conductive with the addition of a thin sputter coating of carbon, gold, or silver. Qualitative chemistry collection is enabled with the EDAX energy dispersive analyzer that detects elements by recognizing the characteristic energy emitted by backscatter electrons of different elements.

Most valuable to the interpretations was equipment maneuvering and scientific input from Dee Breger, SEM operator and administrator. She has 35 years of experience at the SEM and was able to distinguish between surface and structural compounds and aided in the interpretation of shell layers.

The microprobe mounts described in section c were also used for SEM analyses. The scanning electron microscope revealed patterns of microstructure that have been characterized for other species, *Mercenaria mercenaria* and *Spisula solidissima* (Dodd 1965). Additional less labor-intensive sample preparations for representative mollusks were also undertaken. Small sections of the last growth year (half-year) are cemented to glass slides in various orientations to elicit information regarding structural and chemical variations. Some ventral margins have been shaved at an angle with an *Exacto* knife to reveal the inner structure of the shell's final growth year. Others were left intact for detailed surface evaluation. In all cases the periostracum was not removed and the organic interlayers were intact in order to determine whether these regions exhibited any microstructure or housed heavy metals or atypical elements.

4. Neutron activation

Shells of live specimens of Macoma balthica from the 1999 collection were sent to Oregon State University Radiation Center Lab for element examination. The purpose was to collect data for elements that are more easily collected by this technique and otherwise below the detection limit for XRF. Neutron Activation is a technique based on the collection of characteristic gamma rays that are emitted as a stable nucleus is bombarded with neutrons causing it to become radioactive (Figure 13).

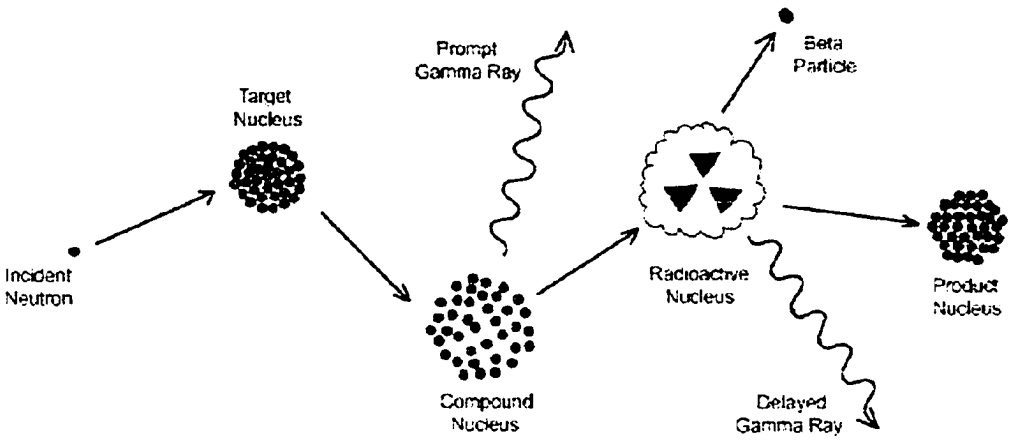

Figure 13. *Nuclear basis for neutron activation from http://www.missouri.edu/~murrwww/pages/ac_naa1.shtml*

C. X-ray fluorescence Spectroscopy (XRF)

Element information is collected by XRF, using an automated wavelength dispersive Philips PW1400 X-Ray Fluorescence Spectrometer. The XRF technique provides element information based on the fluorescence phenomena resulting from the release of photons of energy as an electron, excited by x-rays is ejected from an inner orbital and is replaced by a higher energy electron. This energy represents characteristic X-ray radiation for the element in question because the energy difference between the ejection of an electron from an inner orbital and replacement by a higher energy electron is fixed (Figure 14).

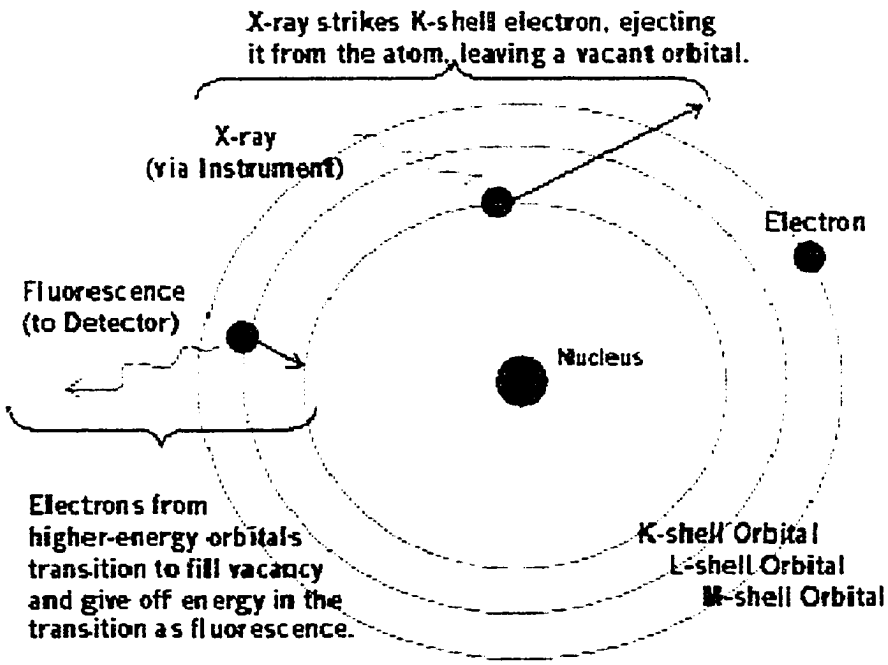

Figure 14. *Schematic of generation of X-rays in X-ray fluorescence spectroscopy http://www.nitonuk.com/html/information_documents/how_xrf_works.html*

Therefore, elements may be identified using XRF by determining the wavelength of the

emitted radiation. XRF is extremely useful as it provides a relatively quick, inexpensive, non-destructive means of element data collection. XRF output is in relative intensity, kilocounts per second, and therefore, needs to be converted to comprehensible values. The correction process includes multiple steps beginning with careful sample preparation. Shell preparation for x-ray fluorescence is similar to x-ray diffraction in that both techniques utilize powdered samples, in XRD to minimize mineral grain orientation, and in XRF to create a thin film. At the outset of this research, preparation and/or analytical strategies applicable to the examination of shell material were unavailable. Of the few shell studies, the predominant analytical technique is atomic absorption and GC mass spectrometry; virtually no x-ray fluorescence studies were found. Initial element analyses were undertaken using whole, unprocessed shells fitted into the XRF platinum sample holder with 25mm window such that the region in question is exposed through the opening. Analyses are begun by first examining, the umbo region. Subsequent shell layers are examined by rotating the area of interest to the sample holder opening. Each measured location is permanently labeled with indelible ink with a circle. Approximately three to four circles are marked per 4-5 year old organism. All the data are ratioed to calcium counts to establish element variability throughout the mollusc lifetime. This technique worked well for bulk estimation, but several flaws were revealed. XRF is a 'surface technique' and penetrates to a maximum depth into the sample of less than 1mm. The shells are actually several millimeters thick and therefore the chemistry is not completely represented. This bias in information collection resulted in the search for a technique that might more appropriately characterize the bulk chemistry of the shells. Secondly, the XRF technique works best on extremely flat surfaces. Bumps on the

analyzing surface cause analysis 'shadows' in adjacent areas. This renders shell surface analyses less accurate as the shell surface contains numerous ridges and depressions.

Much of the new XRF research involves examination of 'thin film' samples. Thin film thickness is generally less than 0.5mm. This thickness represents the maximum penetration achieved by the generated x-rays at the kilavolt-milliamp settings utilized in our programs. Therefore, the entire sample is considered.

To create thin film preparations, the shell-alcohol slurry with particles ground to 20 micron nominal is dabbed onto a pre-weighed 25 mm Millipore filter. A vacuum pump attached to a Millipore filtration flask enables even dispersal of the shell slurry as it is applied to the filter with the pestle in individual, uniform weight 'dabs'. This technique allows for uniform application of shell powder. The weight of shell sample is recorded after the sample has dried. Several applications are prepared for each sample for replication, to aid in calibration and to verify XRF results. The justification for this repeat preparation is that at some minimal weight of material, the element concentrations will approximate zero and at some maximum weight, the kilocounts per second will level off to a maximum. We therefore, sought to achieve a systematic range of samples with a regular difference in weight. The measured element concentrations, therefore, should range from nearly zero and level off at a maximum value for the sample that contains just enough material to produce one uniform layer the exact dimensions of the analyzing window. Any amounts exceeding the later described weight should produce the same intensity values since the x-ray beam does not penetrate to the deeper depths. The only additional possibility might result from x-ray absorption by the upper layers of the sample as the generated x-rays exit the sample on route to the detector. Avoiding the

aforementioned condition forces careful, accurate sample preparation. The relationship should be linear until maximum amounts are achieved and intensity levels off.

Incremented samples by weight are achieved through the newly devised 'dab method'. The 'dab-method' is described above. Collections are made on 25 mm filters in one dab intervals until a maximum amount of sample is achieved. The weight is recorded and archived for each filter. The filter is then placed onto a SPEX Certiprep aluminum holder filled halfway with Ultrabind, a background-minimum pressing medium prepared by SPEX Certiprep, Inc., exclusively for XRF. The entire assembly is flattened with a hydraulic press reaching a pressure of 25 tons. The permanent sample is perfectly flat and ready for repeated examination by XRF.

Data collection is a simple combination of acquisition of needed information with least wear on equipment. To this end, each preparation is examined using analytical programs written in element clusters based on element similarities, such as those that co-exist in minerals, etc. To minimize crystal changer wear, elements are further subdivided according to the analyzing crystal required. Finally, to reduce collimator locking, elements are organized in order of increasing two-theta angle. The data is corrected first by subtracting values obtained from a background preparation that is identical to the shell preparations minus sample material. The measurements are weighted as a function of actual shell material applied to the filter. This weighting is necessary since the kilocounts per second measurement is a function of the thickness of the preparation as well as the actual element concentration. The corrected kilocounts per second are converted to parts per million by fitting the data into a plot of USGS standards also prepared by the thin-

film method and analyzed with the same XRF programs. Standards and samples are re-examined for replicability.

X-ray standards are prepared in the same manner as shell samples, that is, multiple preparations of increasing weight values based on the addition of one dab increments to the filters. It was through the initial examination of standards that the shell protocol was developed. Each of the following USGS standards has 3-5 such preparations: AGV-1, Guano Valley andesite; BHVO-1, Hawaiian basalt, COQ-1; Canadian carbonatite; SCO-1, Cody shale; DNC-1, Braggtown dolerite; G-2, Rhode Island granite; GSP-2, Silver Plume granodiorite; BIR-1, Icelandic basalt; QLO-1, Oregon Quartz latite; RGM-1, Glass Mountain rhyolite, STM-1, Table Mountain syenite; and W-2, Virginia diabase. Each USGS standard has been examined by one or more analytical technique; bulk and individual element concentrations are compiled and published on the NIST (National Institute of Standards and Technology) website and in several publications.

Shell preparation protocol and XRF analytical program design were devised by preliminary USGS sample analyses with the CCNY, EAS department's newly acquired, (2000) partially automated, used x-ray fluorescence spectrometer donated by Philips Laboratories in Briarcliff Manor, NY. Our initial objectives were to 1) devise a quick preparation technique for all, (or most) samples collected in our lab, 2) to calibrate the spectrometer to achieve collection of reliable and replicable results 3) to calculate the range of detection for the various elements for the equipment. To meet these ends, the dab-method sample preparation was developed.

Analytical programs measure element concentrations by user request. Each element can be identified by characteristic x-rays emitted based on the specific electronic

transition. For example, if the innermost electron, from the K orbital is ejected and subsequently replaced by an electron from the L orbital, K alpha radiation is emitted with its characteristic wavelength and energy. An element's specific characteristic x-rays are identified by the resultant peak location intensity minus the background intensity. These parameters are both computer assigned by the element channel function and user calibrated. Peak location adjustments to channel parameters can be achieved through the use of standards. Each time the XRF generator is used the characrteristic peak location for the elements to be examined must be recalibrated using the CAN function (calibrate angle-two-theta). Calibration proceeds by placing into the sample chamber, a mineral known to contain the element in question. Calibration time and range are set and the spectrometer performs a qualitative scan to identify the two-theta location that marks the highest intensity. When completed, the new angle is selected and data generation may begin.

Analytical programs are designed to measure element concentration over a set collection time interval. Elements that are higher in concentration need less counting time than trace elements. Typical counting times are between 50 and 300 seconds. Background collection is typically counted for only $1/10^{th}$ the time of the peak collection.

The USGS sample preparations were used to establish the validity of the thin-film technique. Each USGS sample was analyzed by XRF for mineral forming element and heavy metal concentrations. Weight incremented samples were utilized. The data were plotted together and a trend noted for each element. The data were fitted by linear regression in *MICROSOFT EXCEL*. *EXCEL* calculates the equation and goodness of fit

for the line. Figure 15 shows the silicon correction chart used for the dual purpose of calibrating for Si detection and establishing the validity of the new sampling technique.

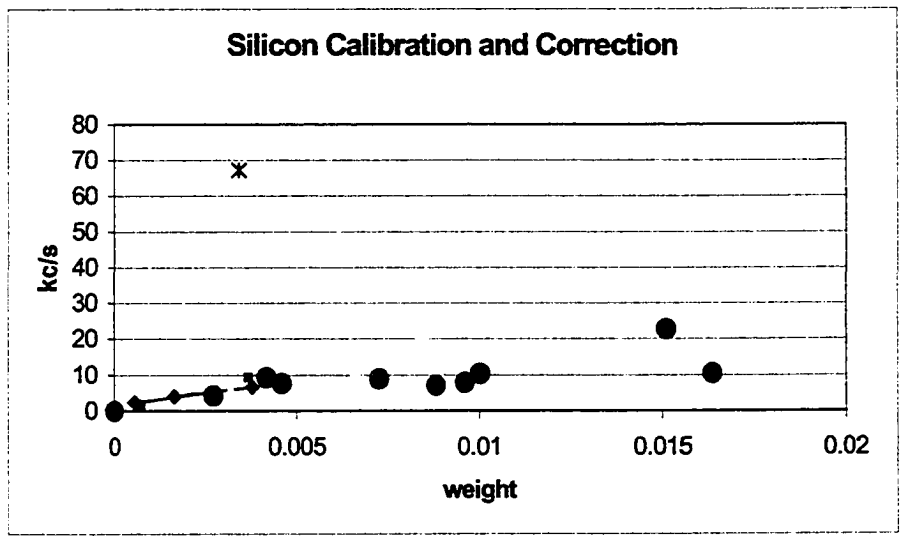

Figure 15. *Si calibration. Each pattern represents a different USGS sample in increasing weight increments*

The overall correlation of element weight per sample to kc/s XRF intensity is shown in Figure 16. In this sample assemblage, only the best-fitting sample preparations are retained. The detailed examination weeded out the heaviest and lightest preparations and helped to establish the protocol that is currently in use for thin film preparations.

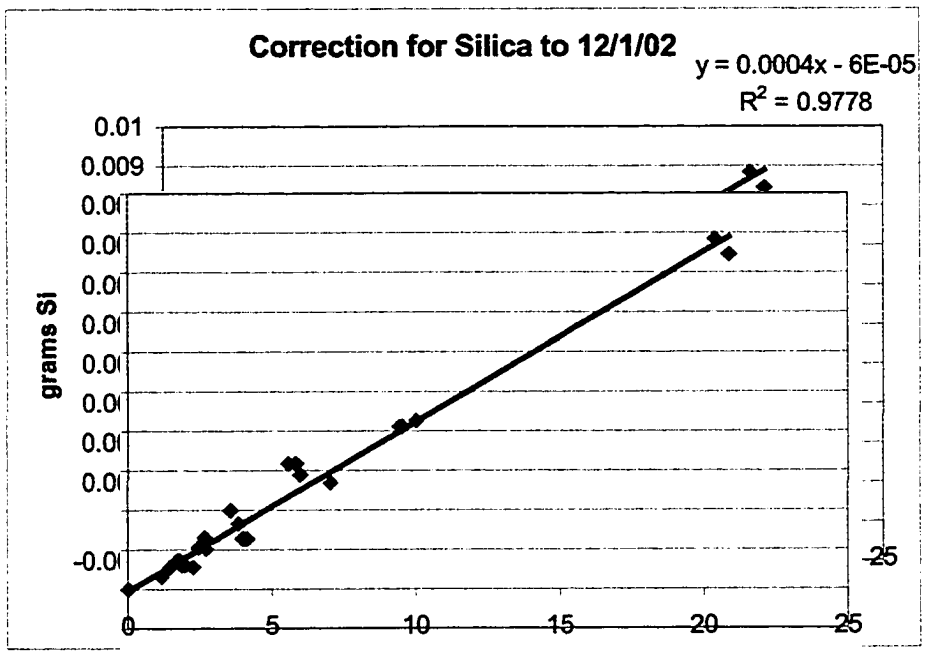

rock standards.

CHAPTER 4: RESULTS

A. Hudson Estuary Sediment and water parameters

The distribution of benthic organisms and resultant assemblages are a function of environmental parameters, most importantly salinity and sediment composition. Dissolved oxygen, pH and water depth are of secondary importance and need to be addressed.

Water parameters were collected at the surface and bottom at each sample location using a shipboard Hydrolab. In 1997, measurements sites were sampled in a zig-zag pattern; the boat located the traverse latitude, then along the traverse at the various stations, then north again this time along the other margin. In 1999, a different approach was taken; the ship samples all western margin sites on the trip north and all eastern margin sites on the trip south so that minor variations due to waxing or waning of the tide was encountered. Even with the time difference from measurement at the west sites over the east sites, remarkably little actual variation occurred. For the benthic communities, this means that there is not a dramatic flux in any single water parameter over the research interval.

Salinity of the Hudson bottom is outlined in Background section 1 (see Figure 5). The asymmetric orientation of bottom salinity is not significant. Instead it is an artifact of the gap in measurement between the western and eastern margin sites as explained above. A comparison to the 1974-5 work of Shaw shows an insignificant change in salinity (See Figure 17)

Bottom pH has an interesting pattern showing the lowest levels in the middle of the survey area, at the Bronx and into Westchester County (also on the west, the border

between NY and NJ) (Figure 18). Both north and south of this region, pH values increase from the mid 7s to a high of 8.4 though, on the average, pH is not dramatically variable. The lower salinity region roughly compares to the distribution range of *Macoma balthica.*

Depth is a function of location within the Hudson channel, particularly, distance from the shore and navigation channel. Depth varied from 2.4 meters along the Hudson margin at northern locations to 21.1 meters in the navigation channel in the southern extent of the survey region (Figure 19). At least one southern margin site at less than 4.4 meters in an otherwise deep portion of the Hudson can be explained by the silting near the mouth of an entering tributary.

Dissolved oxygen, (DO %) in the bottom water shows a steady increase northward except for a few unusually high dissolved oxygen values at the mouth (Figure 20). The anomalous shallow depth site at T 28 A also shows correspondingly higher dissolved oxygen percent (Figure 21).

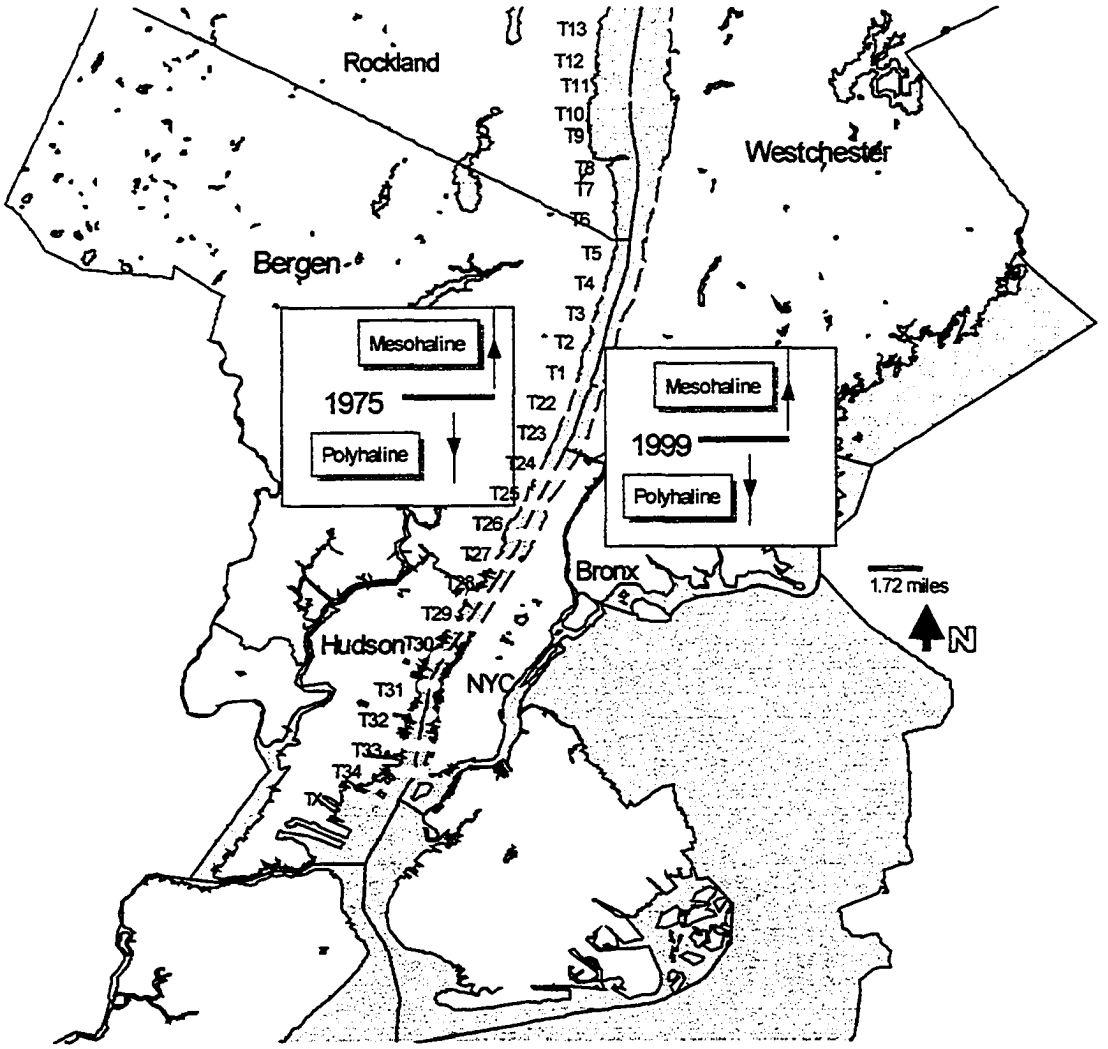

Figure 17. *Salinity comparison, 1999 and 1975 showing similar separation line between polyhaline and mesohaline zones.*

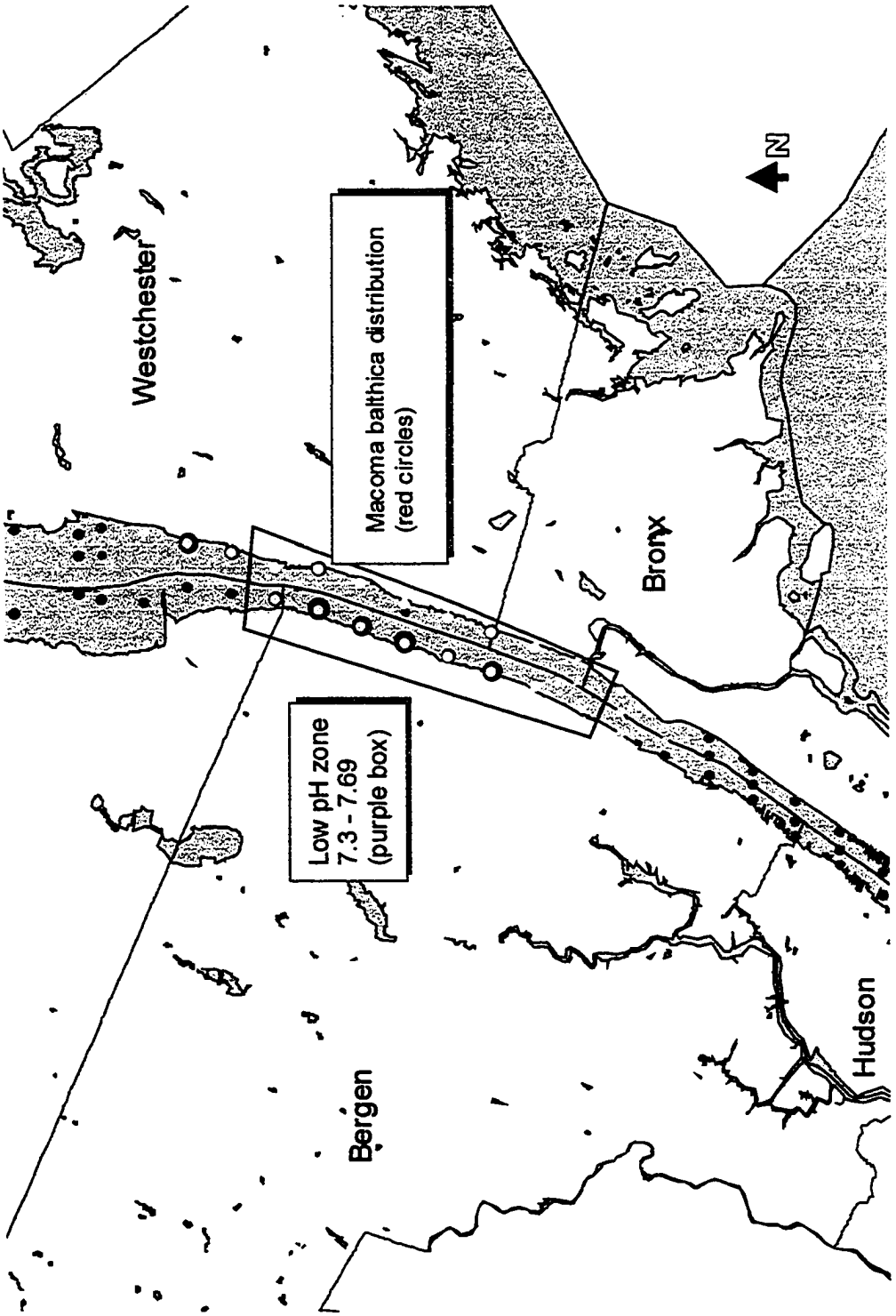

Figure 18. *Overlay of bottom pH and Macoma balthica distribution showing correlation*

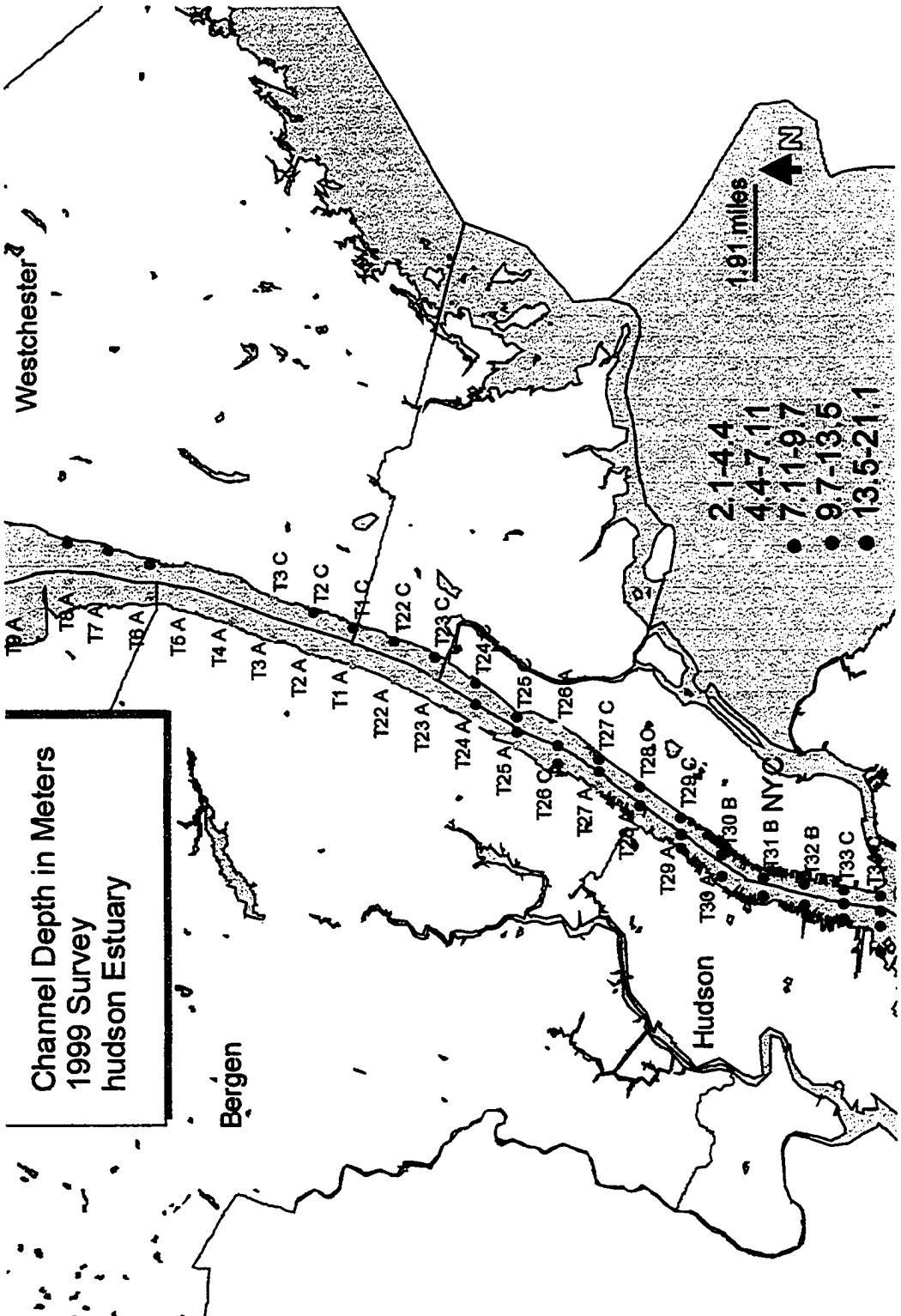

Figure 19. *Channel Depth of Hudson Estuary Sample Sites, 1999. Depth shows no distinct pattern.*

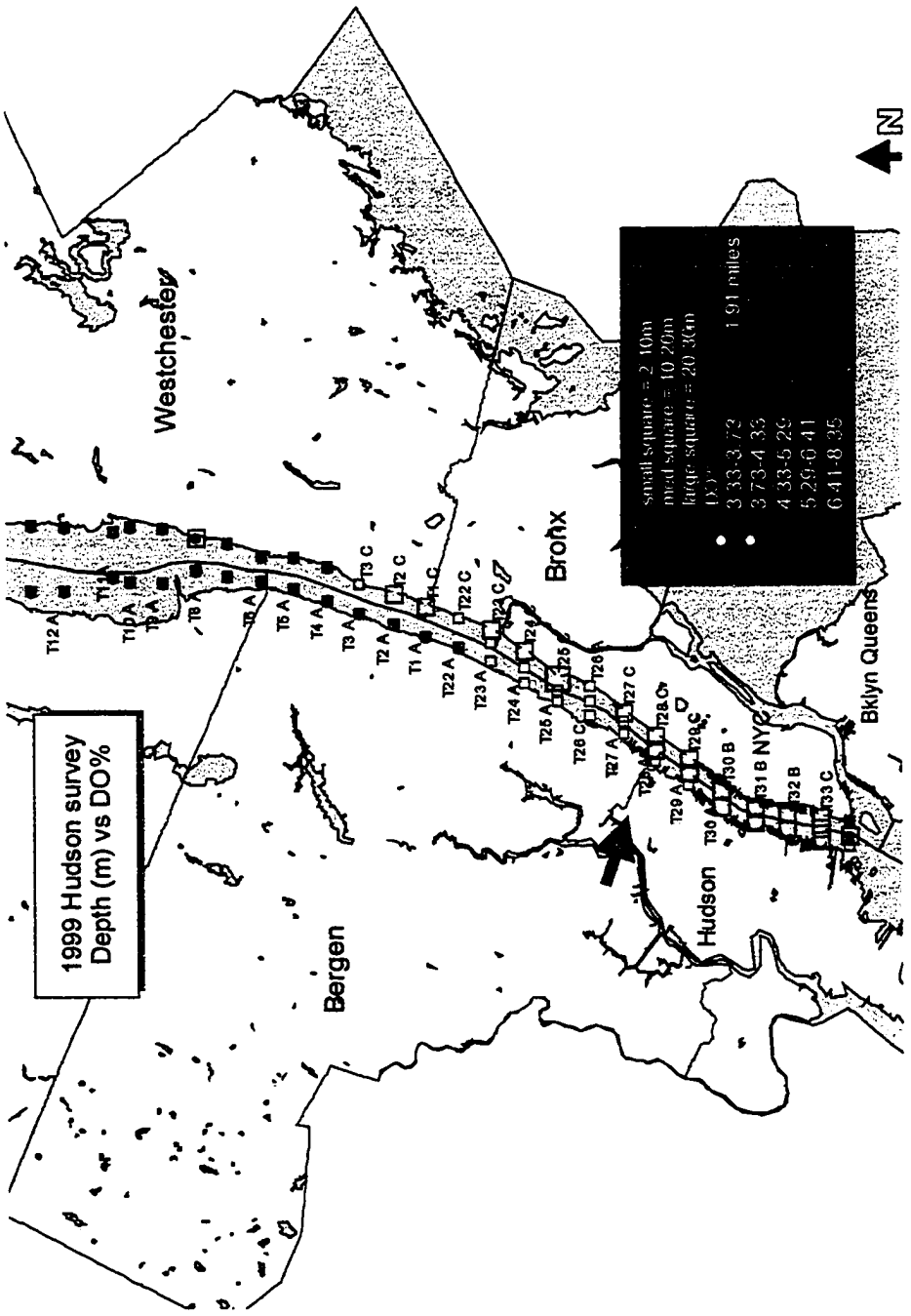

Figure 20: *Comparison of DO% and Channel Depth. Map shows a general correlation up estuary of higher DO% and shallow depths, western shore T22-T12. Lower estuary depths are greater and DO is lower, note exceptions at the bight region T34-T32 where depths are great and DO is higher than 4.33%*

Notice that the anomalous high DO% is located at the entry of a subsidary stream into the Hudson main channel (see red arrow in Figure 20). The range of DO % in the survey area spans from 3.33 to 8.35. As illustrated by this work, infaunal organisms densely occupy regions containing 3.73 to 5.29% dissolved oxygen in the center of the study area and at the mouth of the Hudson. The one new resident, *Rangia cuneata*, occupies a northern region where dissolved oxygen percents range from 6.41 to 8.35% but its occurrence more likely reflects salinity (Weiss and Shaw, 1978).

Finally, temperature shows a similar pattern to dissolved oxygen, exhibiting a steady increase from south to north ranging from 23.55 to 26.08 degrees Celsius (Figure 21). Overall, this range is not striking; temperature variation is expected to be highly variable throughout the year and all of the benthic organisms can adapt to these temperatures.

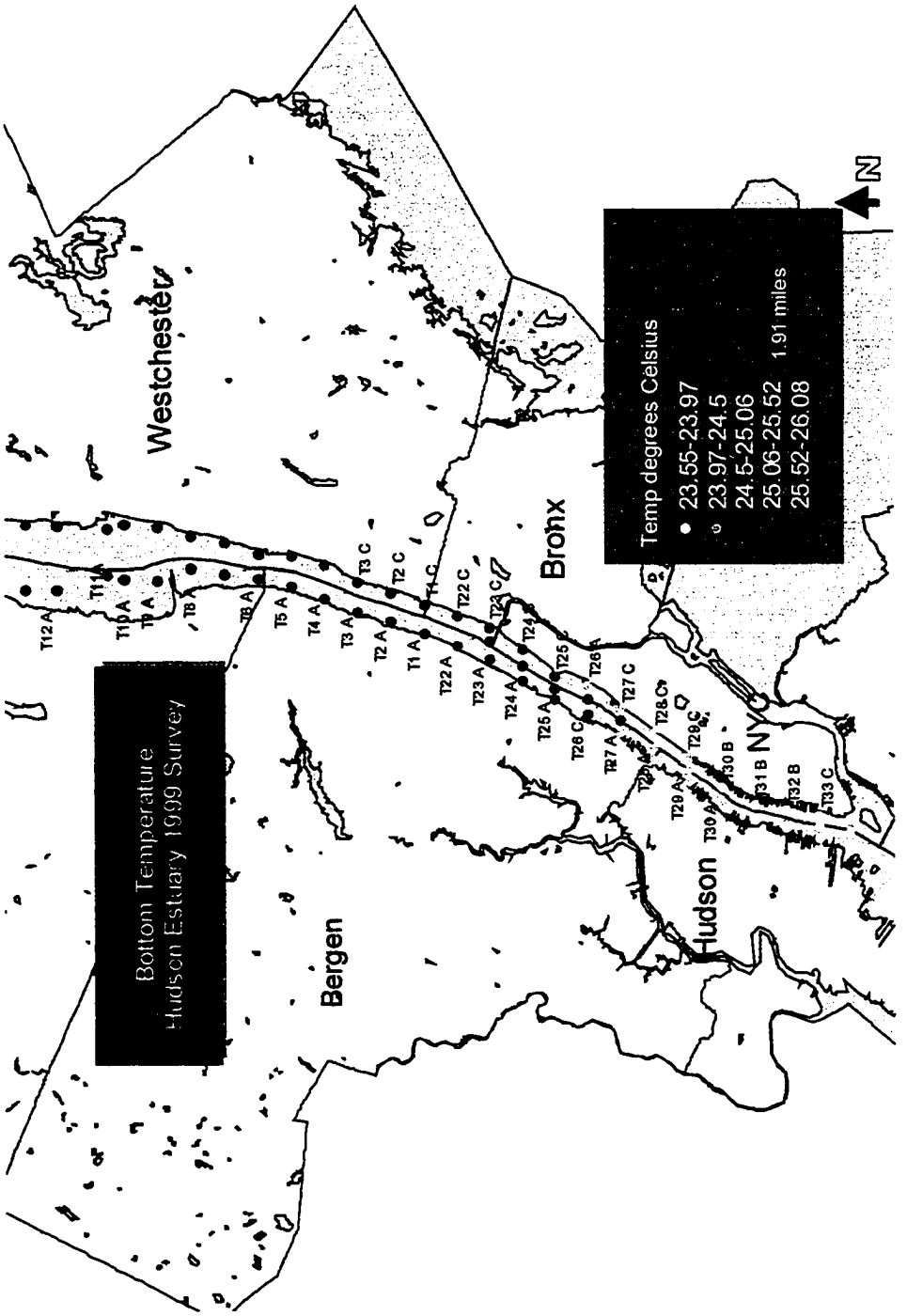

Figure 21. *Bottom temperature 1999. Note increase in temperature moving north from the bight.*

B. Mollusc Distribution

Six to eight mollusc species coexist in the Hudson Estuary. In this study we relate their present distribution to salinity and to sediment composition, and draw comparisons with the earlier, 1974-1977 surveys, though for the 1974 research, the intention was more focused on monthly monitoring. The results presented here consider only summer 1997, October 1998 and August 1999. The results of the 1970s surveys are presented in Appendix 5 and are partially re-plotted in current distribution maps (Figures 25-28).

A plot of the live tallies from the 1997 and 1999 surveys (Figure 22) demonstrates a remarkable division of species based on estuarine salinity. The benthic communities consist of small pockets of individual and to a lesser degree, co-existing species. Distributions and assemblages are a strong reflection of sediment properties, and the Hudson benthos contains a fair amount of sediment variability, therefore, contouring the benthic macro-fauna is problematic, unrealistic and presumptuous.

The overall mollusc distribution plot shows that the southern assemblage in the most saline portion of the polyhaline zone (closest to marine salinity) is dominated by *Mytilus edulis*. *Mulinia lateralis* coexists with Mytilus in this region, but in lower numbers (only three to six organisms recovered at three sites)(see Figure 23 for enlargement). Immediately to the north in the salinity range of 19 to 26 ppt no live molluscs were recovered. This species-absent zone corresponds to almost the entire length of Manhattan with the exception of 2-3 *Macoma balthica* specimens at location T26 A (just south of the George Washington Bridge). The Manhattan species absent zone signifies a notable change in the benthic distribution reported by Shaw and others, 1974-1978 (Figure 23, 25-27). The northern reaches of the lower estuary, salinity 5 to 18

ppt, are dominated by *Macoma balthica* and *Rangea cuneata* slightly to the north. A single sample recovery returned five specimens of live *Crassostrea virginica*, at T4C, otherwise none were found in the survey region (Figure 24). Disarticulated valves of *C. virginica* were recovered, but the degraded state of most of the shells indicates severely reworked old shells, possibly eroded out of the benthic muds in adjacent areas. Though once dominant in the historic past (200 ybp), *Crassostrea virginica* numbers have declined due rising levels of pollution in the estuary that has eliminated oyster farming in the Hudson. The newly adapted freshwater mollusc, *Rangea cuneata* (not previously reported) was found in the extreme north regions of the study area. Since the 1997 sampling *Rangea* has increased in live numbers.

Remarkably, we presently find that very little overlap exists among mollusc species though in theory many species are capable of co-existing. Interestingly, species habitat is exactly defined by salinity boundaries.

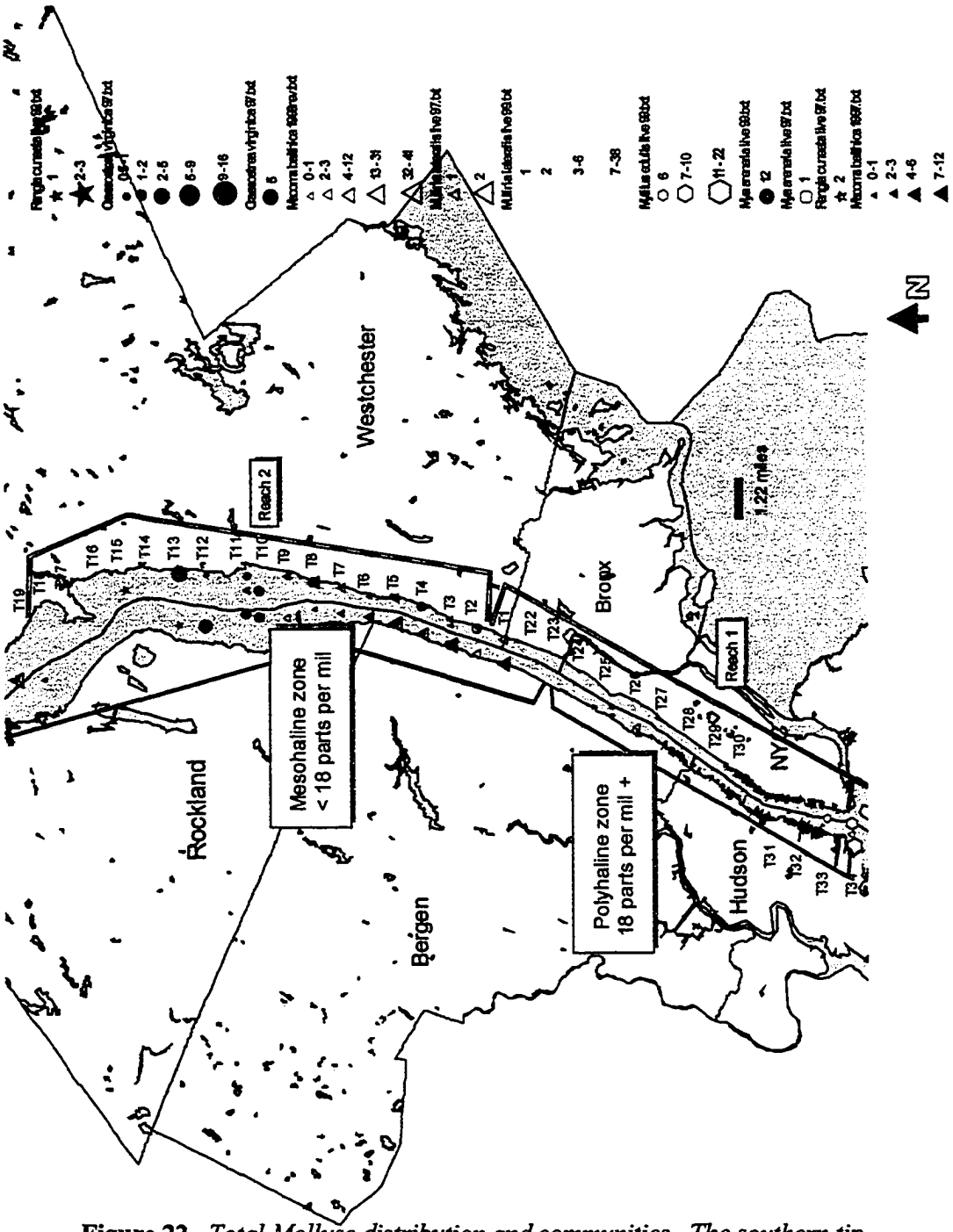

Figure 22. *Total Mollusc distribution and communities. The southern tip of Manhattan comprises the Mulinia lateralis/Mytilus edulis zone; Mytilopsis/Rangea zone occurs north of the Mulinia/Mytilus zone. Macoma balthica occurs in both in the 1970s, but is exclusively in the Mytilopsis/Rangea zone in the current survey. The remainder of the Hudson bottom was devoid of bivalves.*

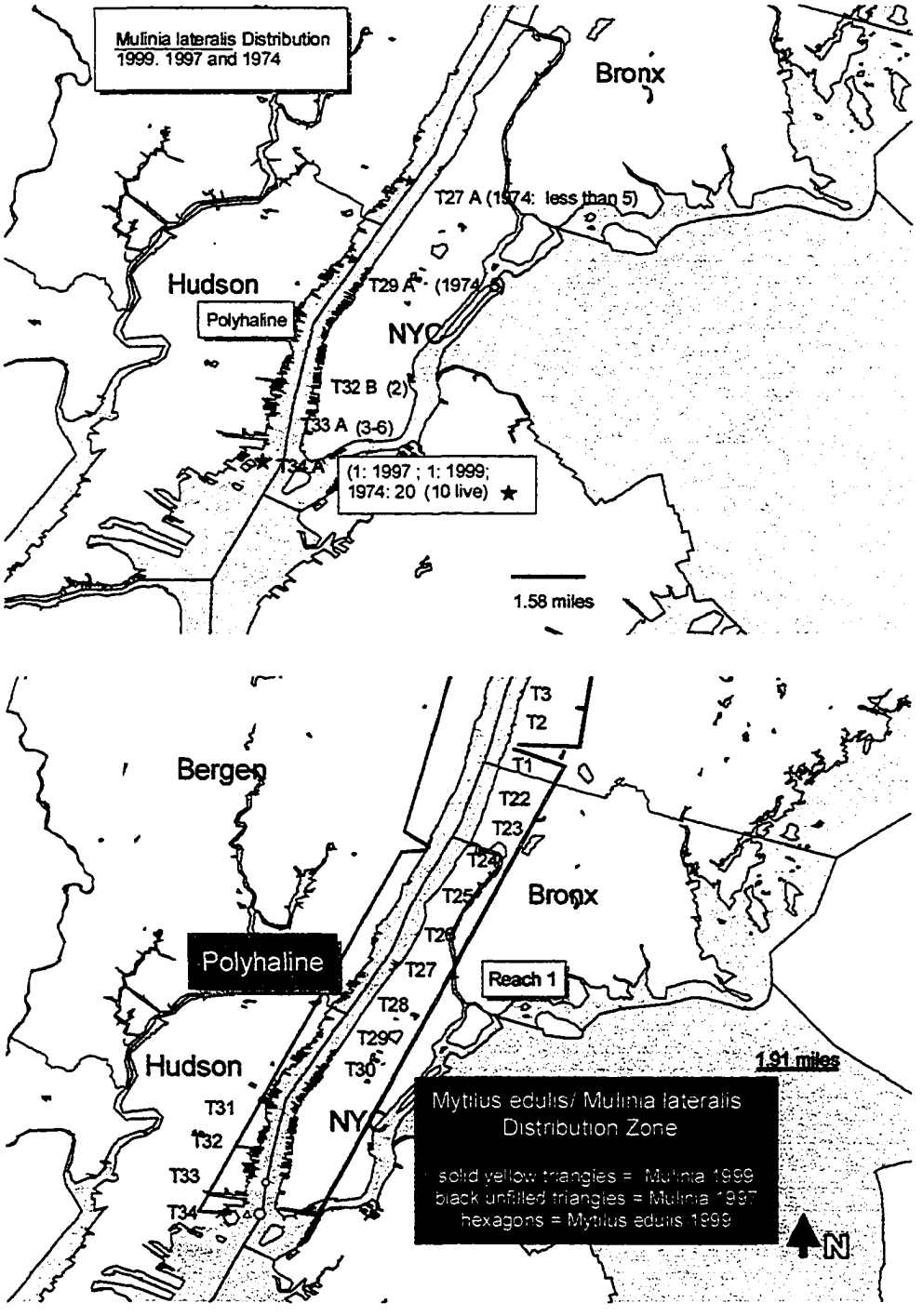

Figure 23. *Polyhaline community: Mulinia lateralis-Mytilus edulis assemblage zone also including 1970s data for comparison.*

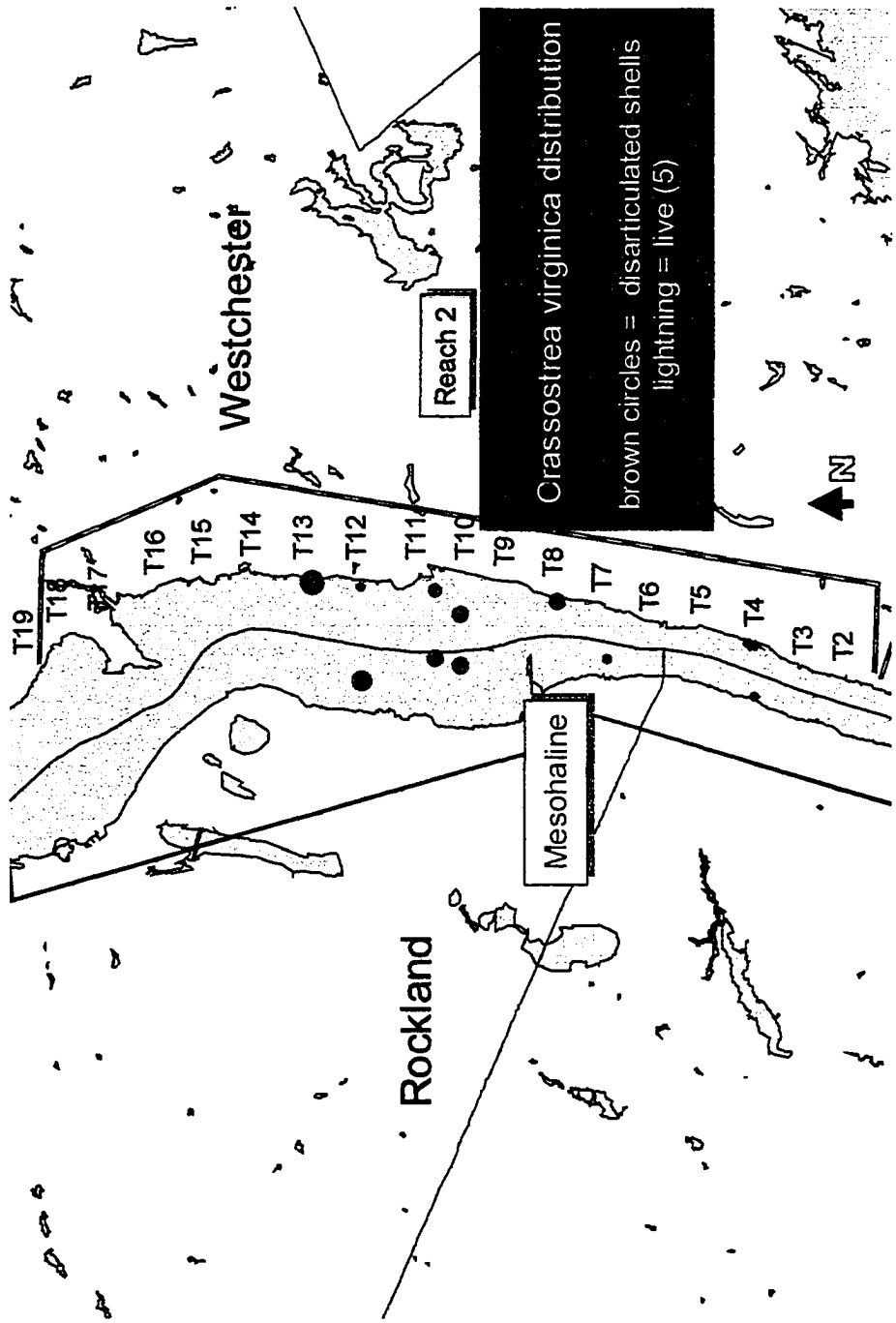

Figure 24. *Crassostrea virginica distribution, 1997. Brown circles mark locations where disarticulated shells were recovered. 5 small, immature, live specimens were recovered at T4 C, just north of Hastings-on-Hudson. Unfortunately, no live Crassostrea were recovered in 1998 or 1999.*

Mytilus edulis-Mulinia lateralis zone (formerly including Mya arenaria)

The Battery region houses the *Mytilus/Mulina zone*. In the 1970s *Mulinia* and *Macoma* and *Mya* were all well established in this zone (Figure 23). Instead, in the current survey *Mya arenaria* only two occurrences are to the north in the mesohaline zone just the north of Spuyten Duyvil (T23) at the highest salinities of 'Ristich' Reach 2 (See Boyce Thompson report, 1977). The mussel *Mytilus edulis* and clam *Mulinia lateralis* are the only bivalve occupants of the NYC Battery region. *Mytilus edulis*, a filter-feeding, byssally-attached mollusc, is found in great numbers and at all ages. However, it is found only at a limited number of locations around the Battery (Figure 23, green hexagons). The live organisms are confined to the navigation channel since mussels require rocky or at least hard substrates to enable byssal attachment. The navigation channel contains substrates composed of shell hash, debris and gravel in a sand matrix, ideal for mussel attachment. *Mytilus* occurs in clusters affixed to large rocks, debris fragments, or to other attached individuals. In 1999, young *Mytilus*, designated by small size and lighter color, were located at the mouth of the Hudson where tidal flow and near-ocean interaction bring great quantities of nutrients in suspension. Live *Mytilus edulis* were not recovered in 1997 possibly as a result of sampling difficulties encountered in the initial stages of the 1997 survey. In the 1970s *Mytilus edulis* is also present, but in smaller numbers and mostly south of the Battery (out of the current sample range). Therefore, it appears that *Mytilus edulis* has expanded in population and location since the 1970s.

Mulinia lateralis occurrence is also confined to the lower reaches of the study area (Figure 23) in 1999. Though its salinity tolerance is similar to *Mytilus, Mulinia* occurs at shoreline locations away from the navigation channel. Here, the sediment is more uniform in size, predominantly sand, and suitable to the epibenthic habit of *Mulinia lateralis*. 1997 numbers are also minimal; only two sites contain live organisms. *Mulinia lateralis* numbers have seriously declined and its range reduced since the 1970s (Figure 27). In the 1970s surveys this species occurred as north as Piermont in low numbers. Where it is found at the Battery, individuals numbered over 20. In the present study, the range is reduced to a small section at the southern tip of Manhattan. Shaw (1974-1977) has classified *Mulinia lateralis* as an opportunistic species; the presence or absence of *Mulinia lateralis* is a reflection of the health of the environment. In the present case, the decline of *M. lateralis* may indicate that the Hudson's benthic health is at least less acceptable for this species than in the 1970s. The other possible explanation for its absence is the encroachment of other species into the ecological niche of *M lateralis*. *Mytilus edulis* has shown an increase in population, but its occurrence at channel locations that are undesirable to *Mulinia* precludes it from attributing to the demise of *Mulinia*. Figure 25 shows a comparison of the *M lateralis* distribution from Shaw, 1974-1978 and the present study illustrating the marked decline in *M lateralis*.

Mytilopsis leucophaeta-Rangea cuneata zone (formerlyMytilopsis only)

Though the bivalves in this zone can tolerate a broad range in salinity from fresh water to marine, *Macoma balthica*, *Mya arenaria* and the recent opportunistic species, *Rangea cuneata* coexist predominantly in the mesohaline zone, 5-18 parts per thousand. *Mya arenaria* distribution is limited to sites T3 and T2, (Figure 23 check mark). In

contrast, *Macoma balthica* is widely distributed (Fig 23 red crosses and circled stars). *Macoma balthica* numbers have grown to an excess of 30 individuals per liter of sample at many locations, (T1A, T3A, T5A). Organisms are uniform in size and age, predominantly falling into two size/age categories, a 4-year age group at an approximate length of one inch, and a 1-year age group less than 1cm long. The sediment of preference for this organism is soft mud; *Macoma* were not recovered from navigation channel sites. *Macoma* distribution, Figure 25, shows a preferential though not dramatic occurrence of organisms on the west shore of the Hudson. Relative to the 1970s, *Macoma* population has dramatically increased based on live counts but the distribution range has reduced and the population center has moved seven miles north from the Bronx Manhattan border to the Bergen County (see Figure 26 for comparison). The former range spanned a distance of 24 miles from approximately midtown Manhattan (40^{th} street) to Upper Nyack. The present study finds *Macoma balthica* distribution spanning from the Bronx-Westchester border to Upper Nyack, a distance of just under 12 miles. In the 1970s, the majority of *Macoma balthica* organisms occur at locations adjacent to upper Manhattan (Figure 26) near the raw sewage discharge pipe that has since become the North River Water Treatment Plant. This suggests that Macoma balthica's occurrence at that location was directly related to nutrients derived from sewage. In the present study, no Macoma balthica were recovered from this location and the center of maximum *Macoma balthica* concentration is located off the west shore adjacent to north Bergen County, NJ. Individual numbers are also significantly higher in the present study. Population density has increased from a maximum of ten individuals at a given location to twenty-five to thirty in some locations. Though *Macoma balthica* is by far the most

prevalent Hudson bivalve species, its tendency to reside in multiple salinity zones hinders its use it in assemblage designation.

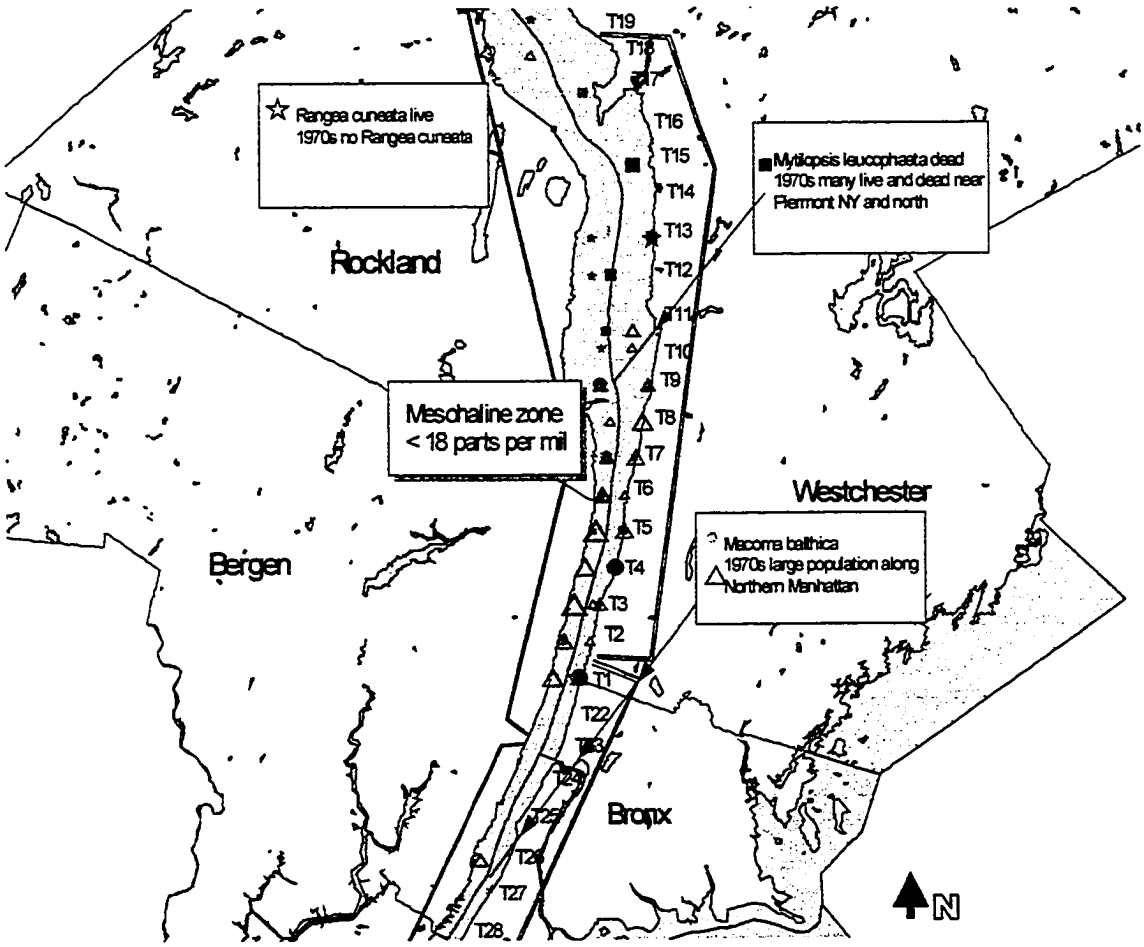

Figure 25. *Mytilopsis-Rangea assemblage zone_ 1997-1999 and comparison to the 1970s.*

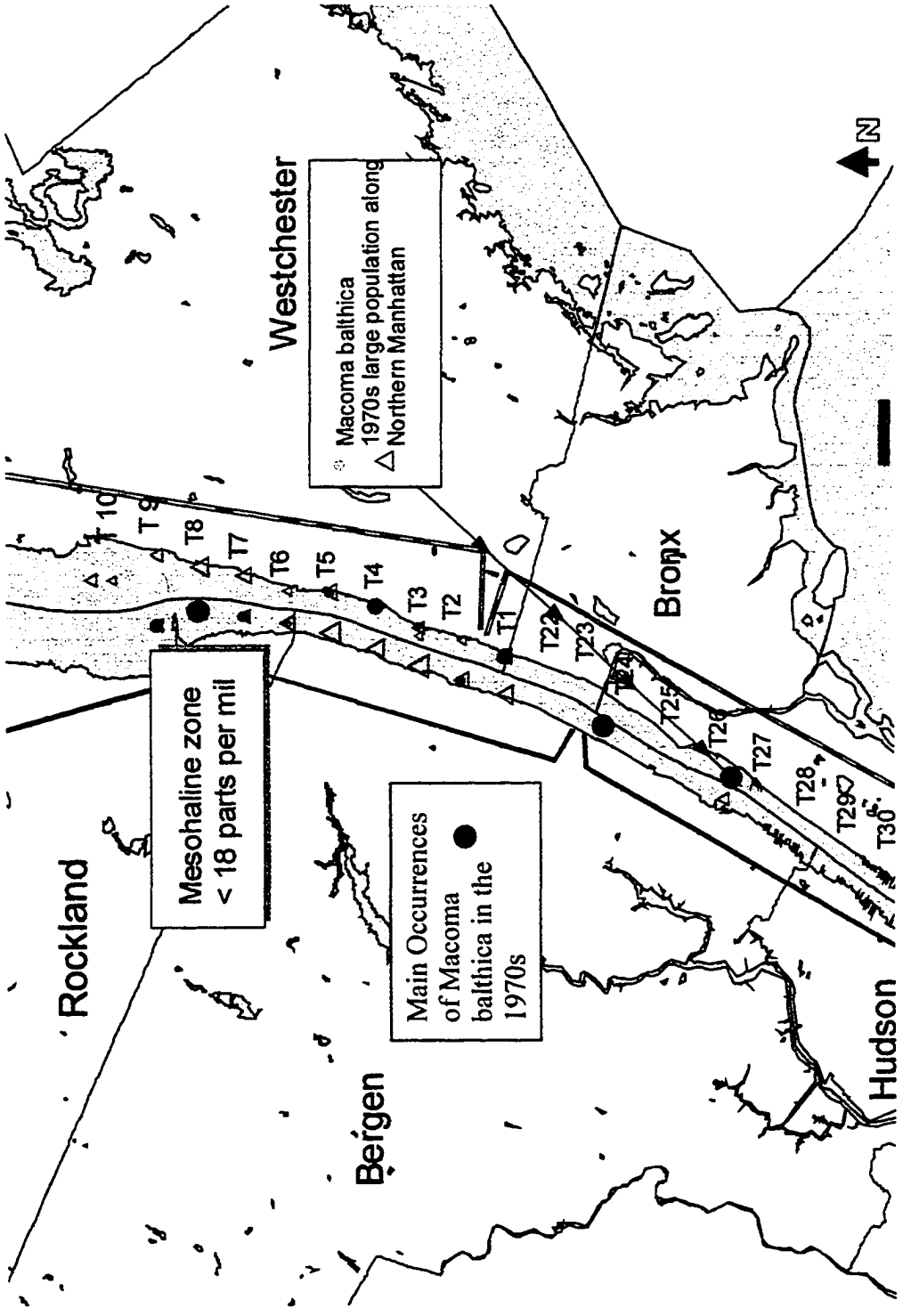

Figure 26. *Comparison of Macoma balthica distribution 1970s to 1999 showing shift in distribution center*

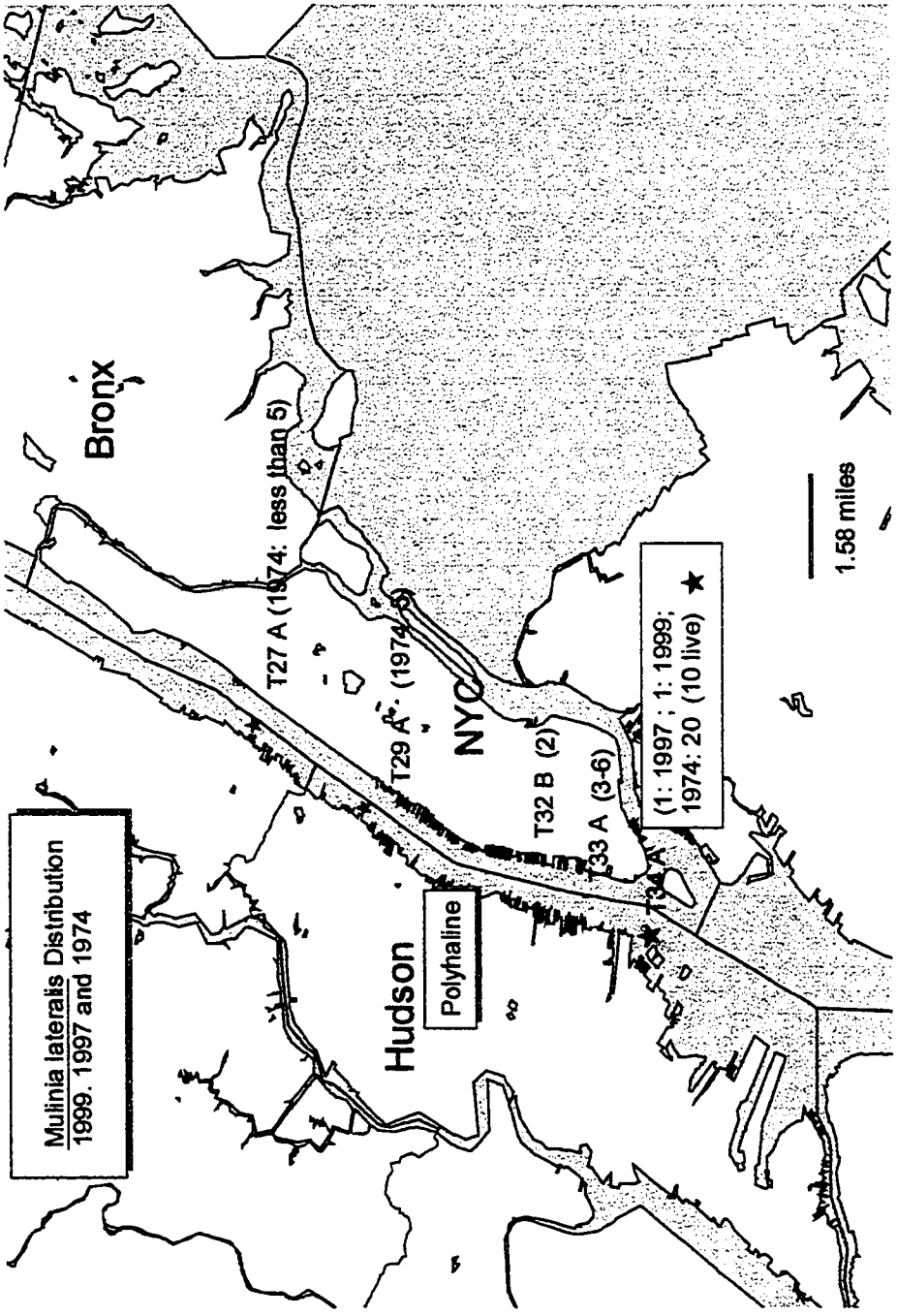

Figure 27. *Mulinia lateralis distribution comparison 1970s to 1999 showing decline*

Mya arenaria, on the other hand, shows both a move into less saline waters, and a dramatic reduction in occurrence. In the 1974-1977 study, *Mya* occurred in the Hudson from the Battery to Dobbs Ferry and individuals numbered as many as 100 or more in the channel during November of 1974 (see Appendix 5) at the Battery and greater than 20 on the east shore near 77th Street (see Figure 25 and Appendix 5). From 1997 to 1999, there is a minor increase in population density of *Mya* that occurred near Yonkers; only one live *Mya* was recovered in 1997 and 12 in 1999. With the addition of disarticulated valves, numbers increase slightly, but overall there is a substantial decrease from the 1970s survey. Disarticulated *Mya* valves were recovered at T4 and T24, immediately north and south of the live occurrences respectively. These occurrences extend the range of *Mya* to 7.5 miles exclusively in the mesohaline salinity range of Venice, 1959. The absence of *Mya* arenaria is not puzzling when considering its sensitivity to both substrate composition and water quality, in the present case the former is the likely culprit. Through laboratory experimentation Swan (1952) proved that *Mya arenaria* success is directly related to sediment composition. *Mya* thrives in sand environments while growth is dramatically inhibited in mud environments or where silt is entrained in bottom water. The majority of benthic samples were composed of thick black mud topped with a very thin < 1cm green organic silty oxidized layer. The absence of thick sand beds might explain the lack of *Mya arenaria* and at the same time the expansion of *Macoma balthica*, a bivalve that prefers muddy substrates.

Rangea cuneata is a freshwater mollusc, generally found in southern fresh and estuarine waters, that has adapted to brackish portions of the Hudson. It is often found in

marshes and in near shore sands. Until 1997, it was absent from the Hudson but by 1999 it has increased its numbers from a single live occurrence at T15, (see Figure 25) just south of Croton Point, to 2-3 live occurrences scattered throughout the northern portions of the mesohaline section of the study area. The recovered organisms are 2 to 2 ½ inches long with shells up to 0.25cm thick. The size and growth rings indicate mature organisms 3-4 years old. Recent wash-ups of thousands of juvenile *Rangea cuneata* valves in 2002, at Croton Point, New York further establishes the fact that *Rangea* has expanded in the Hudson (Shaw personal correspondence). At present, David Strayer of the Institute for Ecosystems Studies in Millbrook, NY is investigating the possible causes for the demise of so many juvenile *Rangea cuneata.*

Mytilopsis leucophaeta, a mesohaline mussel that had, in combination with Mya arenaria, defined the entire lower Hudson estuary assemblages in the Shaw 1974-1978 studies is entirely absent save for substantial numbers of disarticulated shells in the northern portion of the study area (See Figure 25). At sites T13D, and T12C, over 50 and at T20B over 250 disarticulated valves were recovered, but no live *M leucophaeta* were recovered. Despite the absence of live specimens, numbers are large enough to suggest that *M leucophaeta* is living in the mesohaline environment of the lower Hudson. Death assemblages, especially shells showing little reworking represent inhabitants of an environment and there is no reason to think differently here.

In order to quantify the assemblages, numerical values for species richness and diversity are calculated. The diversity index DI is given by the formula

$$-\sum \text{Pi ln(Pi)}$$

where Pi is the proportion individual numbers for each species to the total numbers of all individuals in the population based on a one liter random sample. Species richness for the total Hudson sample region is 8, determined by adding the total number of species found throughout the system. For such a high richness value, the Shannon-Weiner Diversity Index (DI) for the region as a whole is relatively low at 1.12 (Table 5).

Shannon-Weiner Diversity Index $-\sum$ Pi ln(Pi)

	individuals	Pi		ln(Pi)	Piln(Pi)
Macoma balthica	267	0.70	0.70	-0.352923	-0.247975
Mya arenaria	31	0.08	0.08	-2.498152	-0.20544
Crassostrea virgin	25	0.07	0.07	-2.721295	-0.179033
Rangia cuneata	7	0.02	0.02	-3.994261	-0.073578
Mulinia lateralis	22	0.06	0.06	-2.849129	-0.16495
Mytilus edulis	19	0.05	0.05	-2.957018	-0.153687
Nassarius sp	5	0.01	0.01	-4.330733	-0.056983
Crepidula sp	3	0.01	0.01	-4.841559	-0.038223
	379	1.00	1.00		-1.119869
					1.12

Table 5. *Shannon-Weiner Diversity Index for Hudson Study Area. The greater the index value, the greater the diversity. The greater the variety of species occurring at relatively equal numbers, the greater the diversity.*

The Dis of the individual assemblage zones are also low since no more than 2 species occur at any given site with one species always dominating (See Figure 22). The greatest diversity based on species richness and numbers of individuals occurs at the mouth of the Hudson where the two species, *Mytilus edulis* and *Mulinia lateralis* coexist in fairly high numbers.

Over the portion of the Hudson replicated in this study, even fewer species coexist since the Shaw 1974-1977 surveys. Specifically noted are the absence of *Mya arenaria* in significant numbers; the reduction in population of *Mulinia lateralis*; a diminished

Shannon-Weiner Diversity Index		$-\sum$ Pi ln(Pi)		
	individuals	Pi	ln(Pi)	Piln(Pi)
Macoma balthica	267	0.81	-0.2	-0.17
Mya arenaria	31	0.09	-2.4	-0.22
Crassostrea virginica	25	0.08	-2.6	-0.2
Rangia cuneata	7	0.02	-3.9	-0.08
Mulinia lateralis	0	0.00		
Mytilus edulis	0	0.00		
Nassarius sp (gastropod)	0	0.00		
Crepidula sp, (gastropod)	0	0.00		
	330	1.00		-0.67
				0.671

Table 6. *DI for Hudson Mesohaline assemblage zone. Diversity remains low for each site and the entire system, though numbers of individuals is on the rise for some species*

Mytilus edulis range (though this may be due to the elimination of channel sampling); and a total absence of live *Mytilopsis leucophaeta.* The species that do persist occur in greater numbers than in the mid to late 1970s (Figures 25-26). In particular, *Macoma balthica* has increased in population three-fold at several locations. *Rangea cuneata* is a new opportunistic resident of the Hudson. The first occurrence is reported here as 2 live adult organisms at T15C, in 1997. Its range had expanded in 1999 to sporadic live adult occurrences at T18, T13, T12, T10, and 3 live adults at T13C. There is good evidence to suggest that *Rangea* continues to thrive in the upper Hudson estuary with the recent findings of thousands of shells from juvenile *Rangea* along the beach at Croton Point.

C. Shell Chemistry

1. X-ray Fluorescence Spectrometry: Initial results, Programming protocols, raw data

The bulk of elemental analyses were performed by X-ray fluorescence spectroscopy. In the early phases of analytical work, a non-automated, Philips XRG 300 combined diffraction/fluorescence spectrometer was utilized. The two-theta angle, and counting time for each element is manually set and the data is read off the digital dial in counts per second. Corrections are accomplished by evaluating rock and mineral standards of known composition thereby enabling the determination of element concentration in parts per million (ppm) or relative percentage of element present. Preliminary data is presented below (See Tables 7 and 8). First pass interpretation of this initial analytical strategy revealed a general reduction in concentration of Ca from beak to commisure, for *Rangia cuneata* and *Macoma balthica*, and *Mya arenaria*, an increase in Fe concentration for all mollusk shells except *Rangia cuneata* and an absence or unchanging concentration of magnesium throughout the shells. The original intent was to reveal variations in elemental concentrations through the life of the clam.

All organisms examined are located north of the Bronx-Westchester county border in salinities ranging from 15 to 18 parts per thousand. *Mya arenaria* at location T3C (Yonkers) has no magnesium and even low kc/s intensity readings are essentially zero values. The variation in calcium is understandable given the variation in thickness of most mollusc shells with the thickest shell at the beak and substantial thinning toward the commisure. *Mya arenaria*, however does not show a marked difference in shell calcium between the beak and mid section (Table 7).

Whole shell analyses	Intensity: concentration Kc/S	*Rangia cuneata*_T10a	*Macoma balthica*_T8C	*Mya arenaria*_T3C	*Mya arenaria*_T6C	*Macoma balthica*_T4A
Beak	**Ca**	127.4865	196.704	203.1859	200.2681	175.9055
	Fe	1.9723	0.5623	0.3515	0.5194	0.4051
	Mg	0.52	0.1793	-6.421	0.3422	0.0918
Middle	**Ca**	119.6663	180.865	199.2447	203.156	170.652
	Fe	1.0813	0.8147	0.4629	0.5116	0.512
	Mg	0.5571	0.2541	-6.3325	0.228	0.09264
Commisure	**Ca**	100.1868	132.227	144.4367	171.9173	153.8221
	Fe	1.1837	1.278	0.8174	0.545	0.7891
	Mg	0.4856	0.2504	-6.2364	0.195	0.09011

Table 7. *Whole shell data for select Hudson molluscs showing expected decrease in shell Ca over the life of all molluscs, and general increase in Fe. Shell Mg is constant over the life of the organism. (All negative and low values for Mg are essentially zero values)*

The actual elemental variations are more accurately depicted upon examination of the ratios of the given element to calcium (table 8). The ratios reveal a consistent increase in Fe for all molluscs but *Rangia cuneata* shells instead show a decrease. Magnesium concentration is too low for detection by this technique, though the ratios are provided. Since the analyses were of the exterior of the shell and Mg is expected, it may be present in different portions of the shell, not examined by this technique.

Whole Shell Ratios	*100	*Rangia cuneata*_T10a	*Macoma balthica*_T8C	*Mya arenaria*_T3C	*Mya arenaria*_T6C	*Macoma balthica*_T4A
Beak	Fe/Ca	1.547066	0.285861	0.172994	0.259352	0.230294
	Mg/Ca	0.407886	0.091152	-3.16016	0.170871	0.052187
Middle	Fe/Ca	0.903596	0.450447	0.232327	0.251826	0.300026
	Mg/Ca	0.465545	0.140492	-3.17825	0.112229	0.054286
Commisure	Fe/Ca	1.181493	0.966523	0.565923	0.317013	0.512995
	Mg/Ca	0.484695	0.189372	-4.31774	0.113427	0.058581

Table 8. *Whole shell element ratios relative to calcium content showing consistent increase in Fe from beak to umbo for Macoma balthica and Mya arenaria at site T3C and inconsistent Mg content*

Rangia cuneata shell contains approximately five times more magnesium than the other species. This may be due to species-specific uptake or the fact that site T10A is the most northern and least saline location examined in this preliminary study.

At the close of the whole shell preliminary study, the City College acquired a newer, automated Philips PW 1400 X-ray Fluorescence Spectrometer run by Philips X-40 software. The sample chamber assembly holds up to four samples and rotates automatically. To achieve more accurate results, permanent ultra-flat samples were prepared and the whole-shell analysis was dropped for shell 'final growth year' bulk determination.

2. Relationship of Salinity to Mollusc Shell Sodium

Although sodium carbonates and bicarbonates occur in nature, a clear link has not been established between sodium in mollusc shells and the ambient salinity of the growth environment. We presently evaluate the sodium content of the last year of growth in bivalves from the polyhaline and mesohaline environments, and tentatively include the last growth year from fossil bivalves recovered at the mouth of the Hudson for consideration. The latter shells are recovered from a depth of no more than 10 cm and are shells that are configured exactly as living organisms (two shells attached and encased in mud, in living position and undisturbed and undegraded). These shells are considered to be approximately 3 to 5 years in age and directly comparable to the living shell suite.

As noted earlier, the salinity profile represents a collection acquired at differing tide and time conditions creating a scatter in the trend of salinity points. A comparison of the sodium concentration within the three sets (Tables 9) shows an almost one-to-one correlation with declining salinity (Figure 28) over the range of salinity values (1000 to 20000 ppm Na). To reduce scatter, the comparison is made using a running average (average of 3 samples; Table 9) that steps from the first sample as Station 1 to the last station for which a triplicate average is possible, Station 19. These stations are shown as points at indreasing distance from the Battery in Figure 28. As reviewed earlier, trace metals may be embedded interstitially or form as part of a complex solid solution series. The variation appears to show a linear decrease up-estuary as illustrated in Figure 29. A greater degree of scatter is evident in *Macoma* shell Na, but the same decreasing trend related to the estuarine salinity gradient is reinforced. This result clearly shows that the

Table 7. Relationship of Salinity to Sodium in Mollusc Shells					
	Raw Data			Running Average	
Station	salinity	Na/300	Na	salinity	Na/200
1	26.2	18.15	5446.2	25.4	25.4
2	25.7	35.55	10665.98	24.7	23.1
3	24.2	22.36	6707.93	24.1	27.8
4	24.3	11.42	3426.54	23.1	31.6
5	23.8	49.57	14869.76	21.8	34.8
6	21.1	33.67	10100.79	20.4	19.9
7	20.5	21.2	6360.29	19	14.2
8	19.5	4.84	1452.72	17.3	12.9
9	17.1	16.63	4989.62	16.7	16.6
10	15.4	17.26	5177.7	16.1	12.8
11	17.6	15.92	4776.6	15.8	15
12	15.3	5.12	1535.84	15.2	13.2
13	14.4	23.94	7182.84	14.8	16.5
14	16	10.41	3123.63	15.2	13.3
15	14.1	15.21	4561.77	14.6	15.9
16	15.4	14.21	4263.88	13.9	14.3
17	14.3	18.2	5461.41	13.4	11.6
18	12	10.42	3127	12.7	9.2
19	13.9	6.31	1893.73	12.9	6.6
20	12.1	10.83	3250.37		
21	12.7	2.8	840.85		

Table 9. *Showing sodium content of mollusc shells relative to station position; peach: polyhaline section, green: mesohaline*

sodium content of shells is a marker of the salinity of the estuary, and supports the inclusion of the fossil shells at the mouth of the Hudson as a reflector of recent environmental change.

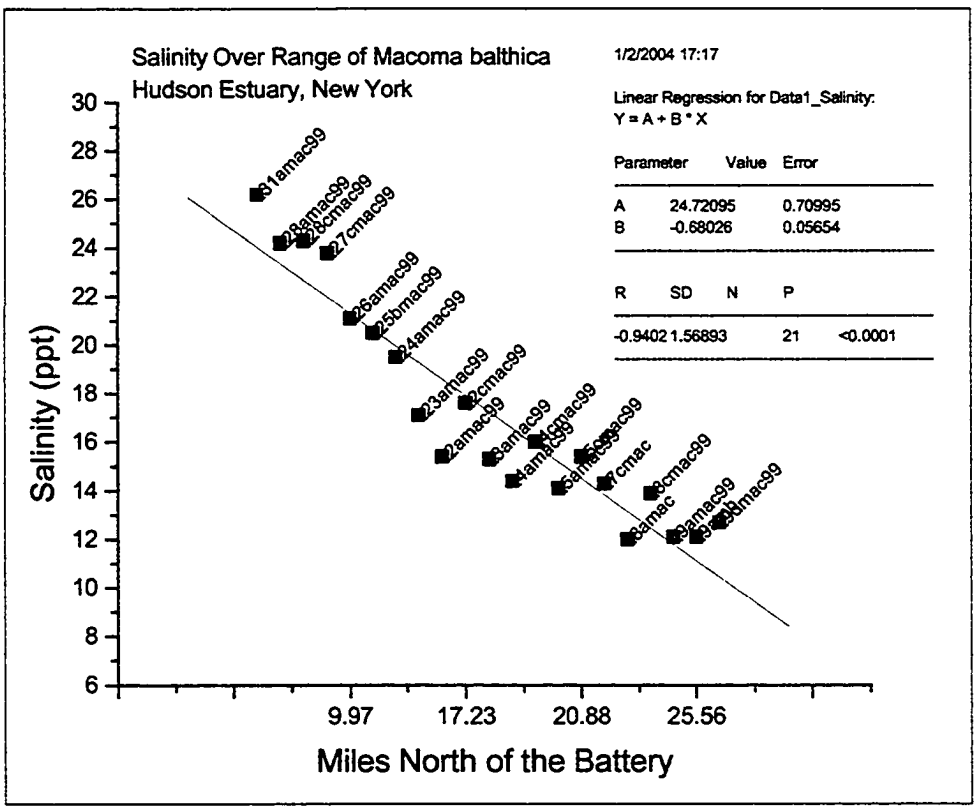

Figure 28. *Salinity as a function of distance from the Battery*

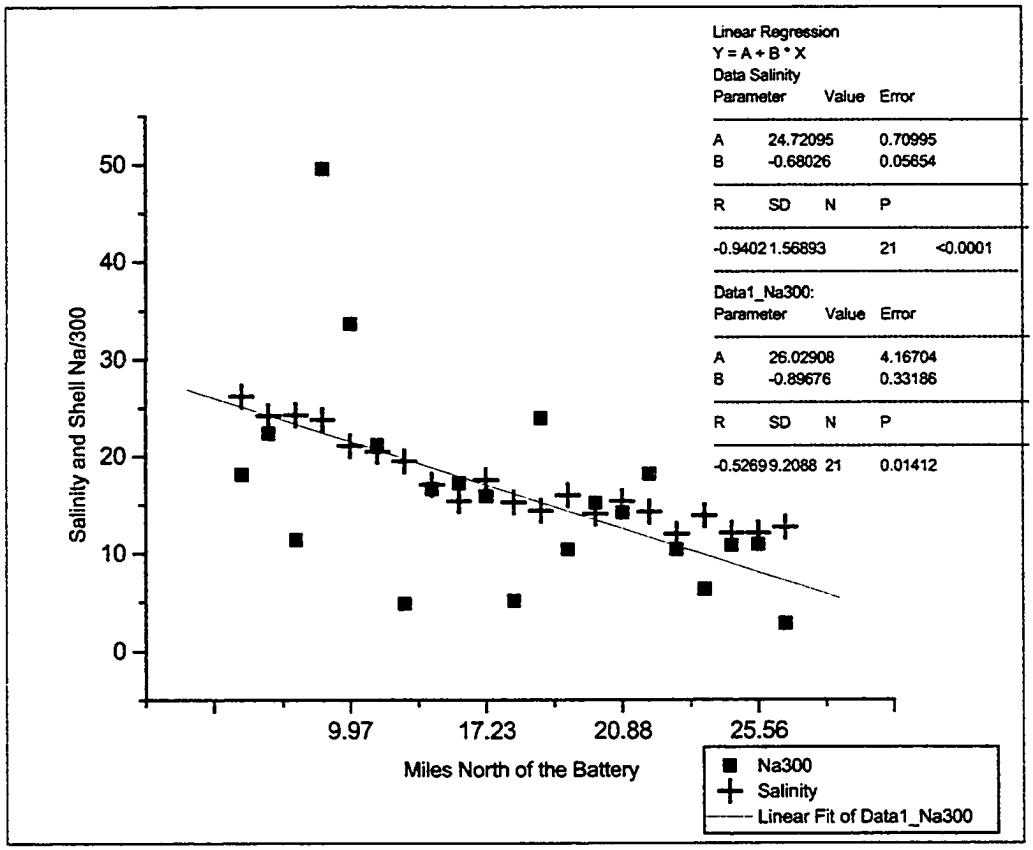

Figure 29. *Decrease in the sodium content of bivalve shells related to the decrease in salinity with distance from the mouth of the Hudson*

3. Relationship of Trace Metals Fe-Al-Ti to Shell Chemistry

Based on ionic size and charge considerations, dissolved magnesium and to a much lesser extent ferrous iron are capable of directly substituting for calcium in the shell structure. In contrast, aluminum substitution requires an associated substitution of a monovalent cation to retain electrical neutrality. If we assume that the sodium in the foregoing discussion is largely interstitial, then potassium is potentially available for creating an ionic balance for the substitution of aluminum. If the sodium is actually

bound in the aragonite structure then it is available for the same ionic balance for the substitution of aluminum. Speer (1984) indicates that the latter is probably the case since he shows that Na, after Mg most prevalently substitutes for Ca in aragonite. The elements iron (Fe 2+), aluminum (Al 3+), and potassium (K+) are trace metals in this system relative to Mg(2+) and Si(4+) and are considered farther along. We examine them as a group to determine whether they behave substitutionally as a group and whether their abundance in shells is also a function of salinity.

The calcium content of shells can fluctuate in the presence of major substitution of donor ions, such as magnesium (Dodd, 1965; Speer, 1984) and possibly other metals. Indeed, the bivalve shells from the Hudson show a fluctuation in calcium with distance up the estuary that ranges from 12,000 to 400,000 ppm (Figure 30 black squares) that does not trend with salinity (See Figure 28). Moreover, the calcium level is generally indifferent as well to fluctuations in trace metals (Figure 30). The sum of Al and K ppm concentrations are so much lower than Ca that their variation has little affect on Ca concentration. For elements with greater concentrations, variance is noted. The Fe-Al-K trace metal group tends to vary proportionally at several locations where upsurges in concentration are noted as peaks at mile 19.69, 23.21 and 25.56 and dips at 3.47 and 7.25 (Figure 31). In only one case (mile 19.69) is this increase associated with a calcium increase. Therefore, the group Fe+Al+K group comprises a reasonably covariant set showing spikes in composition that punctuate the length of the section, but the occurrences are not strongly linked to the changing salinity. The metal content

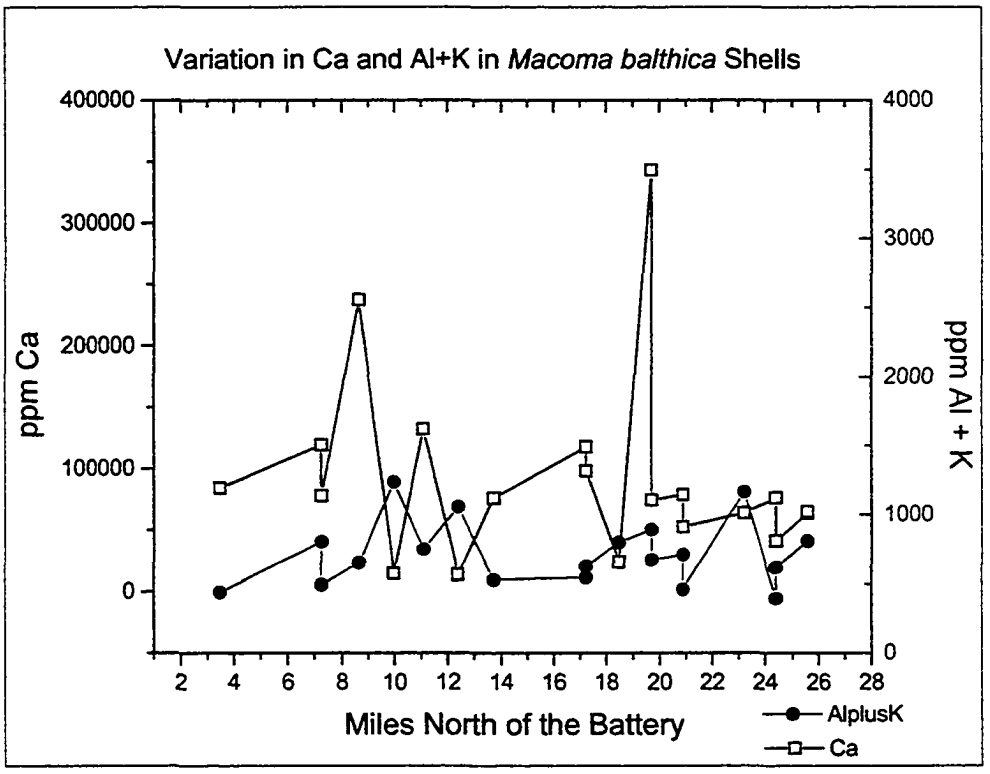

Figure 30. *Fluctuations in trace metals aluminum (Al(3+), and potassium {K(+)} showing somewhat systematic variation with calcium {Ca(2+)}; covariation of Al(III) and K(I) supports the possibility of ionic substitution in shells.*

of the Fe-Al-K set therefore decreases with salinity but at a rate that is not directly parallel to the salinity change in the estuary.

Most of the individual mineral forming metals examined, magensium {Mg (2)}, Iron {Fe(2+)} and silicon {Si(4+)}, have a weak relationship to salinity (Figures 32, 33, 34). Mg and Fe appear to increase with increasing salinity much the same as Na. Si shows an inverse relationship. The correlations are extremely weak and therefore lead to the conclusion that salinity is not a major factor in the uptake of these metals, though uptake is in most cases significant, (thousands of ppm).

The covariance of Al and K constitutes some support for the possibility that these are related by substitution neutrality (Figure 32):

$$Ca = Al + K$$

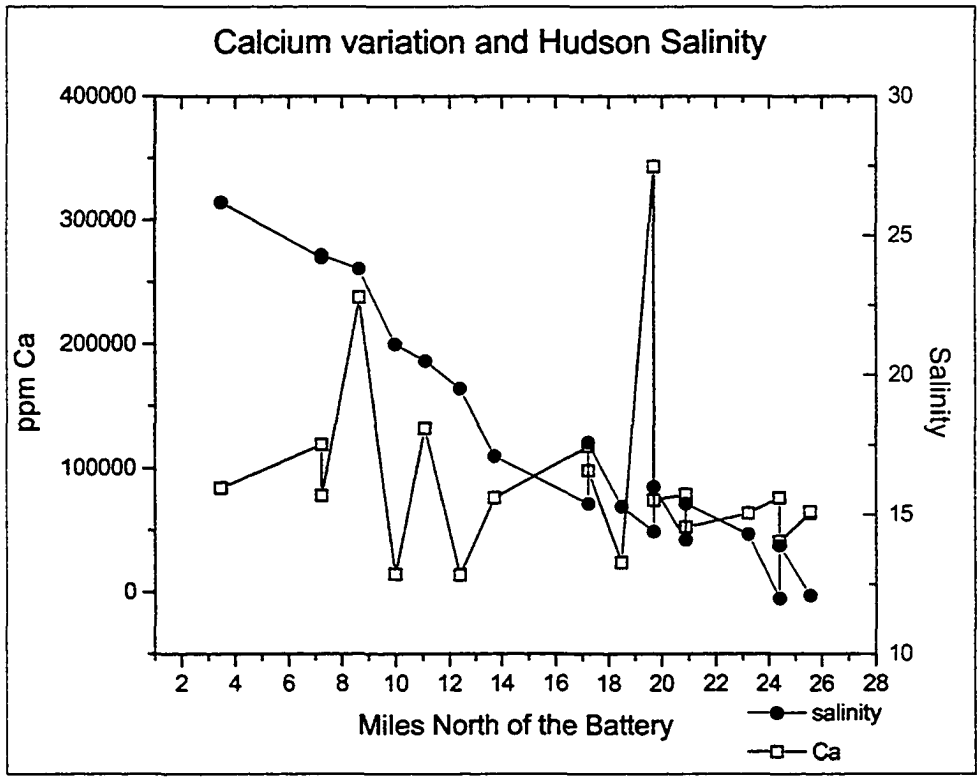

Figure 31. *Calcium variation and Salinity. Calcium concentration bears no relationship to changing salinity.*

This possibility will be evaluated in relation to scanning electron micrograph study of the shell material in a later section.

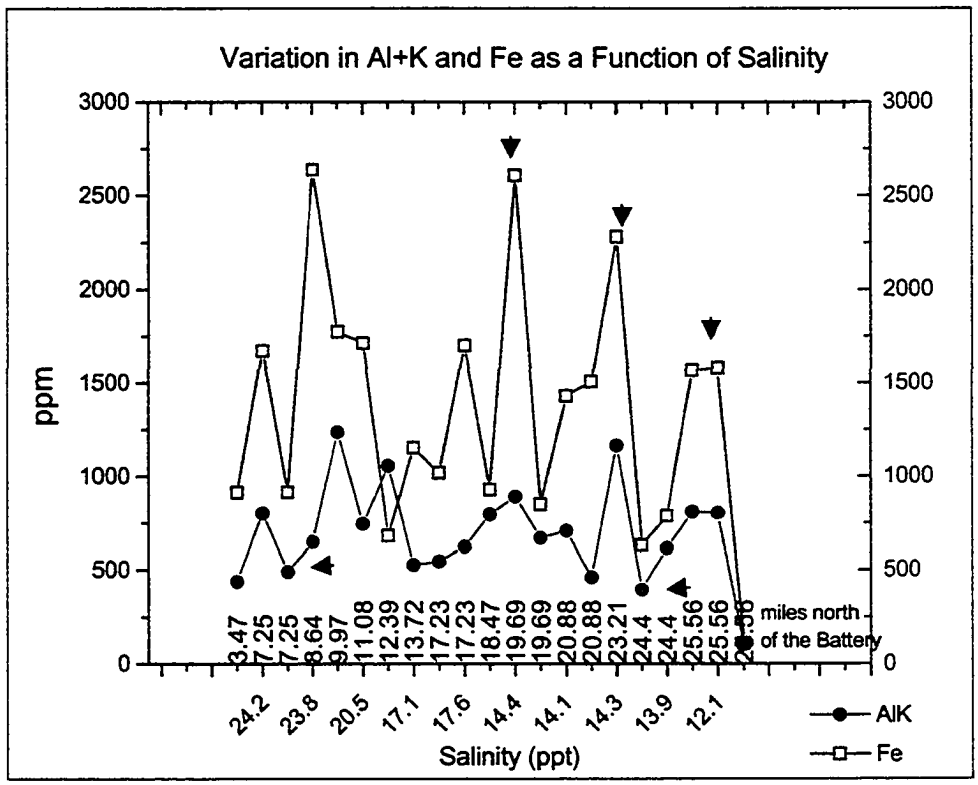

Figure 32. *Concentration of Al+K and Fe as a function of salinity illustrating covariance at several locations (arrows).*

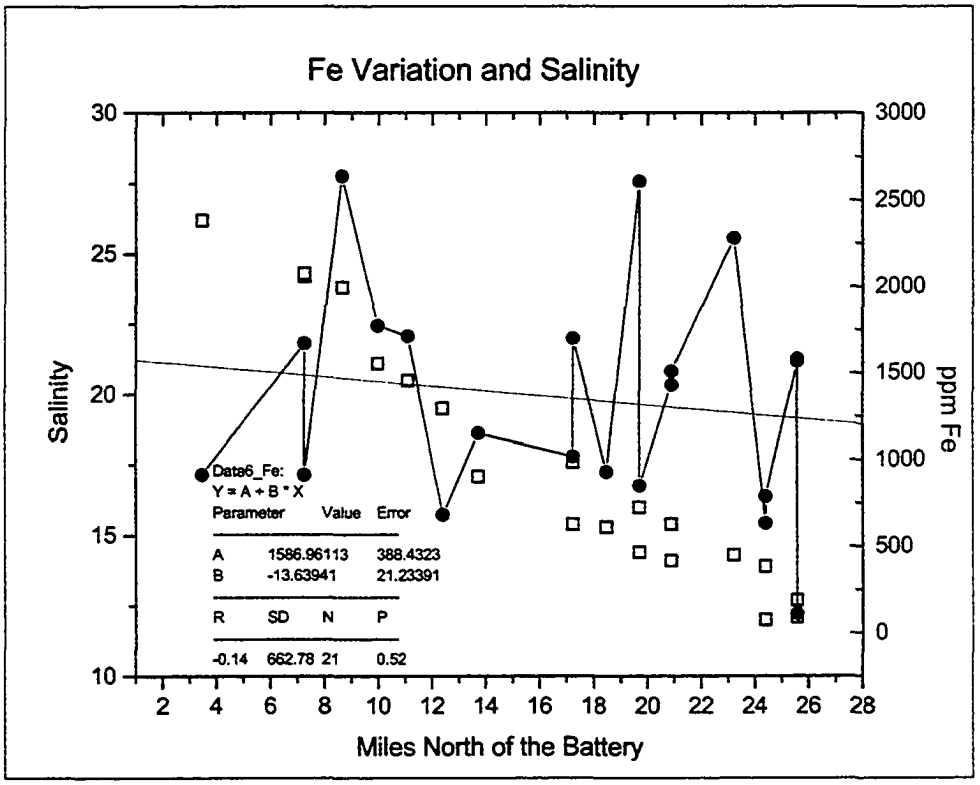

Figure 33. *Fe variation as compared to Salinity demonstrating lack of correlation.*

4. Magnesite Component of Shells

Previous studies of the shell chemistry have shown that certain species preferentially incorporate magnesium ion in inverse relationship to salinity (see Dodd, 1965). As with prior studies, we measure the bulk inorganic chemistry without examining the shell crystalline component of the bulk material. Work in progress, as outlined here, shows that the assumption that the organic component is inconsequential may not be justified.

The incorporation of magnesium in shells is an important factor in determining the temperature at which shells are produced (Dodd, 1965). In most treatments, the proposed relationship is

$$\left[Mg/Ca\right]_{Shell} = \left[Mg/Ca\right]_{Water}$$

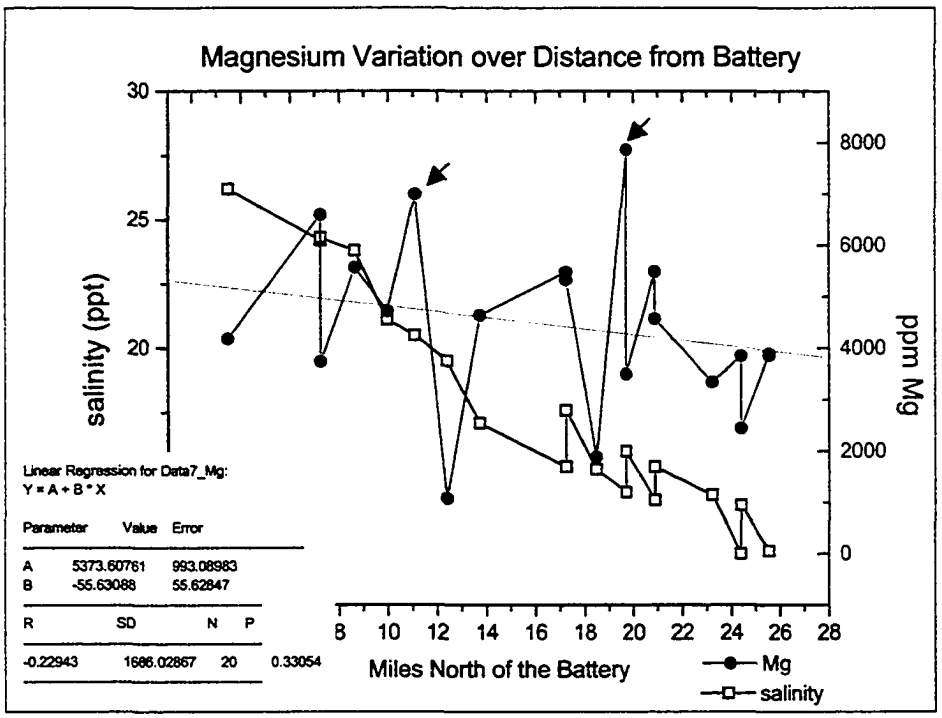

Figure 34. *Mg variation over salinity illustrating weak decreasing trend*

after Kinsman and Holland (1969) and Weizer (1983). However, the expression for filter feeders, such as *Macoma balthica*, is more appropriately

$$\left[Mg/Ca\right]_{Shell} = \left[Mg/Ca\right]_{Water} + \left[Mg/Ca\right]_{Seds}$$

Unfortunately, the data necessary for this comparison are not yet available. At present, we examine the possible relationship of the molecular magnesium percent to salinity. The concentration of magnesium, perhaps as magnesite ($MgCO_3$) appears to this author to be strongly variable in character (see Figure 34). Average Mg concentration in the crystalline material of about 4000 ppm seem totally in line with published data (Dodd, 1965). Above this background, there appear to be spikes that may reflect magnesium entrained by the organic matrix (Figure 34 arrows). If correct, this observation contradicts published work on other shell material that shows an increase in magnesium with decreasing salinity (Dodd, 1965) that indicates either a response specific to Macoma balthica that may reflect sediment chemistry. Work is presently underway that will investigate both the chemistry of the organic material, the quantitative geochemistry of shells by electron microprobe, and the chemistry of associated sediments. These investigations are intended to clarify this issue.

5. Silicon Content of Shells

Silicon is not usually considered to be an important major elemental constituent of shells, in part due to its poor potential for ionic substitution in a calcitic matrix. However, present data demonstrates that, after magnesium, silica is the most abundant minor shell component (Figures 35 and 36). Moreover, the environmental characteristics in the Hudson that create fluctuations in the magnesium percentage in shells for the most part create opposing fluctuations in silica. The correspondence is not perfect, but is sufficient to suggest that the uptake of these metals may be related to each other and perhaps to special conditions in the Hudson at somewhat periodic intervals, i.e. drought,

influx of freshwater and muds or any other such variable. These preliminary data are being replicated for the other shell growth years.

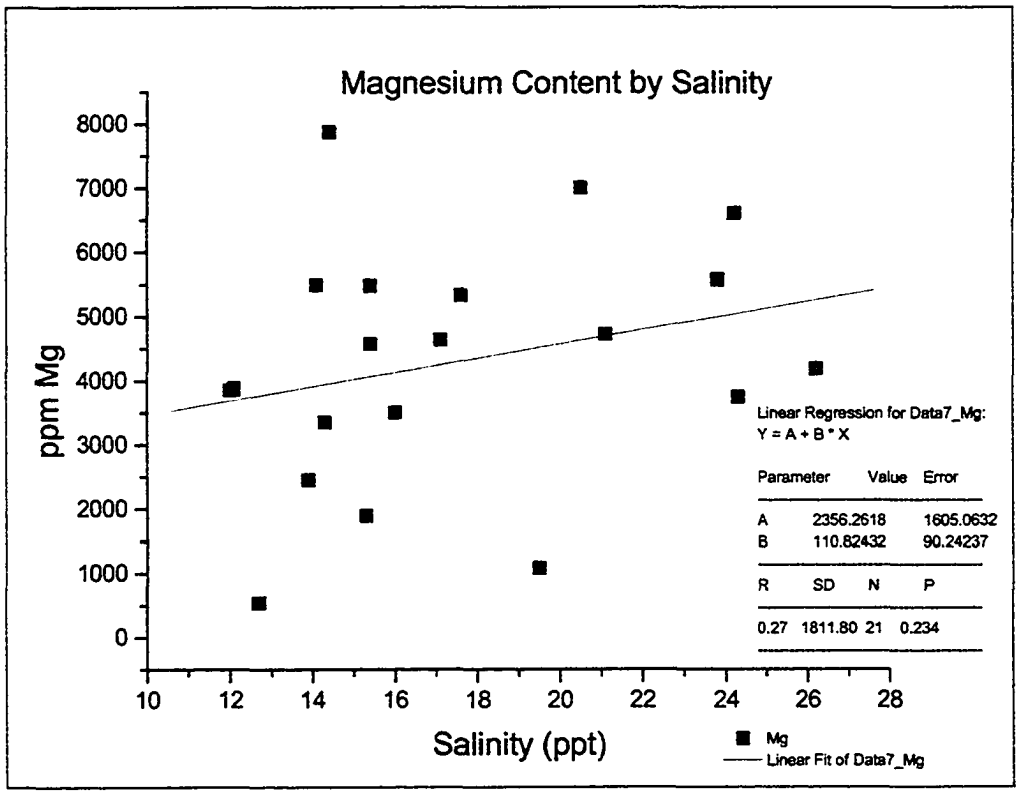

Figure 35. *Mg as a function of salinity showing slight increase with increasing salinity.*

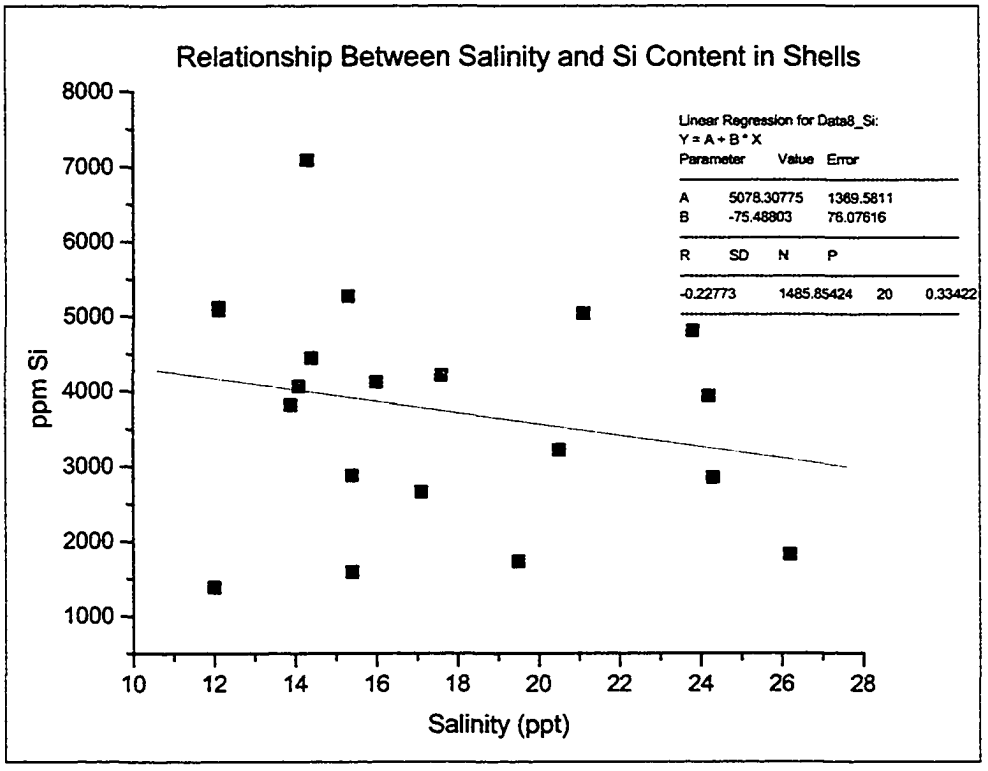

Figure 36. *Silicon concentration as a function of salinity illustrating the opposite trend to magnesium*

6. Zr, Rb, Ba, Sr variation in Macoma balthica shells

Zircon, rubidium and barium show fluctuating concentrations in *Macoma balthica* shell material. All elements spike at T1C, an eastern shore site adjacent to the Bronx-Westchester border, and further north at T6C, another eastern shore site this time adjacent to Hastings-on-Hudson (Figure 37). Though there appears to be no obvious reason for the spikes in metal concentrations other than a possible point source discharge of metals into the estuary near that location, it is clear from Figure 37 that the elemental concentrations are correlative. Later discussions regarding the unit cell structure of shell

aragonite will address the possibility that these divalent metals may have altered the unit cell for shell aragonite.

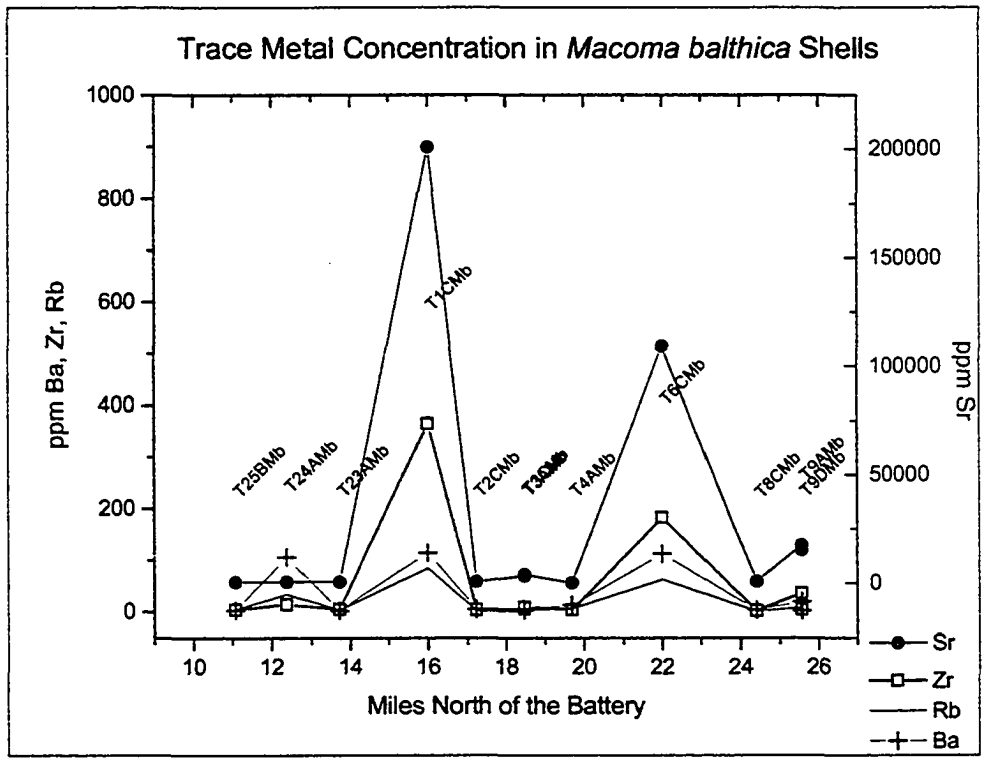

Figure 37. *Variation in Zr, Rb, Ba and Sr. No relationship to salinity can be established, however, elements appear to be correlative. Spikes are a probable function of point source inputs at T1C and T6C and the incorporation of metals may infact be reflected in unit cell dimensions (Chapter 4 part 6).*

Sr has also been shown to increase in concentration with increasing temperature (Dodd, 1965) but that relationship is not evident in this sample set. Since temperature does not fluctuate greatly within the *Macoma* distribution range this relationship may be irrelevant.

7. Lead, Cadmium and Silver in shells of Macoma balthica

Lead {Pb(2+)} is the heaviest divalent metal under investigation in this study. Since its concentration is in parts per billion, it was necessary to calibrate lead XRF analyses independently. Figure 38 shows the correction for lead determined by a colorimetric

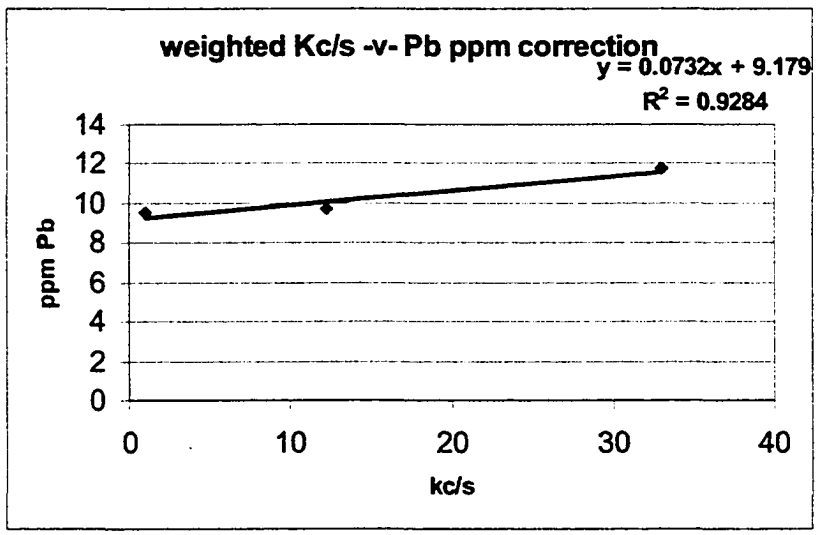

Figure 38. *Colorimetric calibration of Pb see Appendix 3 for data.*

method on select Hudson bivalves. The data sheets for the determinations are found in Appendix 2. Corrected lead values show a level distribution over the range of *Macoma balthica.* Concentrations are low, in the 9-13 parts per billion

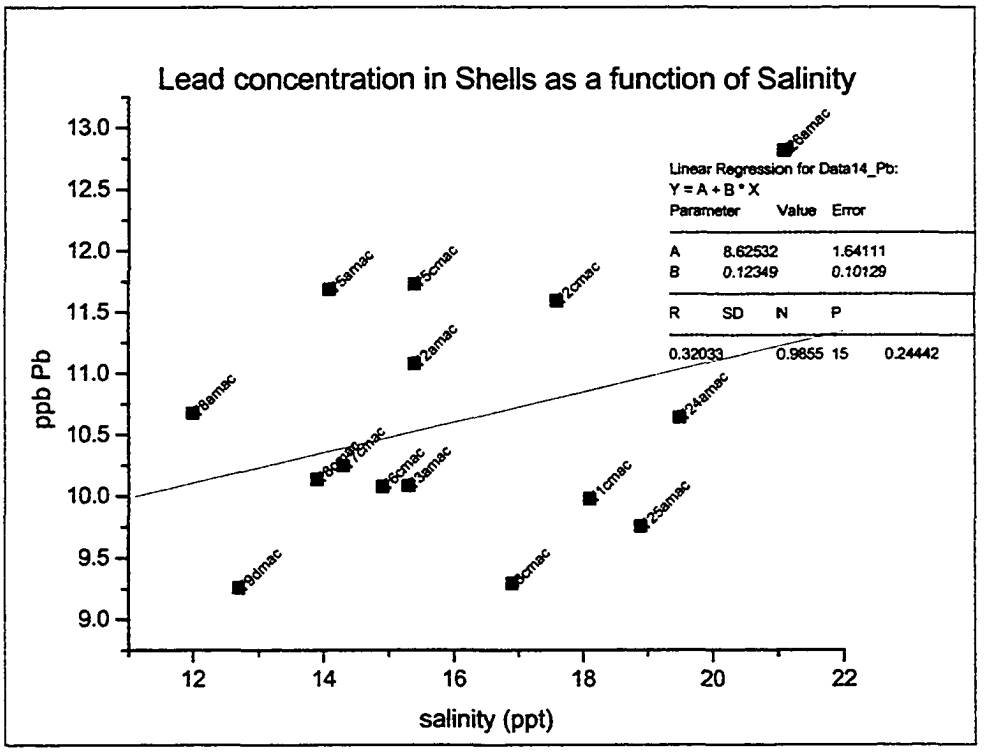

Figure 39. *Pb distribution in Macoma balthica shells.*

range (Figure 39), levels above the standard allowable for drinking water. A poorly correlated direct relationship of lead to salinity is depicted in Figure 39. The source of the lead is not completely understood, but lead is primarily bound to sediments and only to a much lesser extent found as a dissolved component in seawater. Therefore, *Macoma balthica* is exposed to this metal through filter- and deposit-feeding, but the latter is likely to assert more of an influence.

Cd and Ag show patterns that would suggest that metal incorporation in *Macoma* shells decreases as salinity decreases (See Figure 40). In addition, these

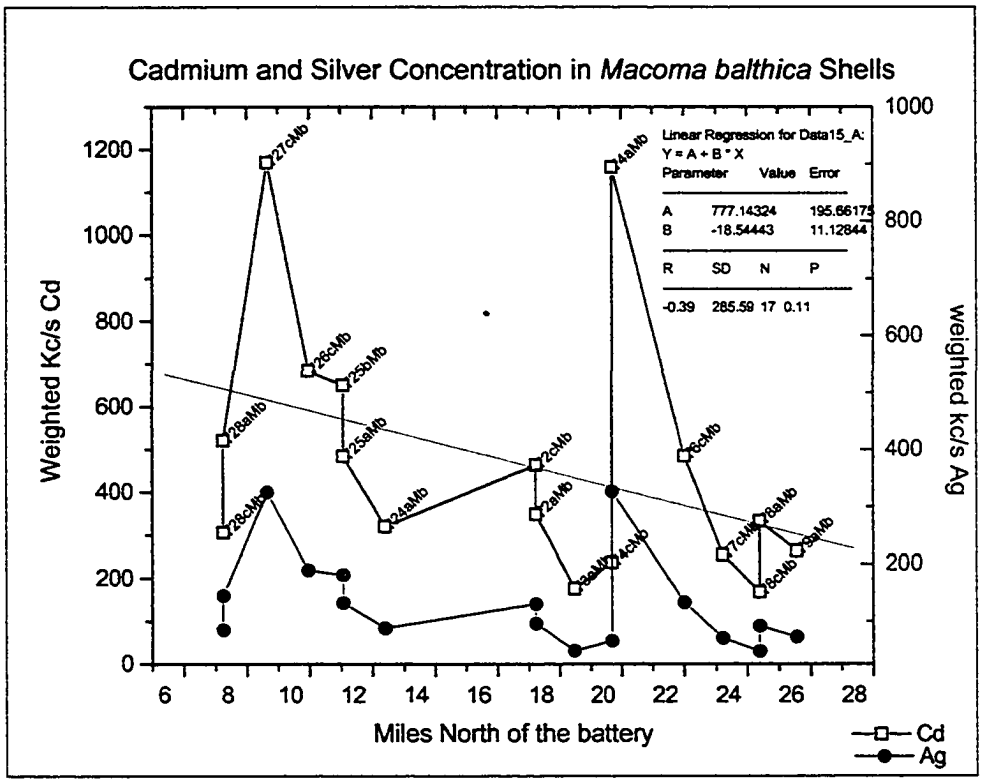

Figure 40. *Cadmium and Silver concentrations in weighted kc/s to show variation with distance from the Battery (decrease in salinity)*

elements appear to have related modes of uptake since their distribution patterns are almost identical, despite differing concentration intensities.

Of all of the elements examined, shell concentrations of only three mineral forming elements other than sodium (magnesium, silicon and iron) and two heavy metals (silver and cadmium) show correspondence with salinity. Magnesium and iron show a weak direct correspondence with salinity while silicon, cadmium and silver vary inversely. Barium, strontium, zirconium and rubidium show concentrations that are independent of salinity content of the bivalve living environment. These findings are

inconsistent with other published data that link increases in shell metal concentration with increasing salinity (except for magnesium which shows the reverse trend) (Dodd, 1965; Speer, 1983; and others).

D. Scanning Electron Microscopy

Analyses of the last growth year of the *Macoma balthica* shells has shown several interesting and new chemical and structural features at Scanning electron (SEM) magnifications and with qualitative chemistry using energy dispersive (EDS) microanalyses. SEM supports the unusually high concentrations of Mg, Fe, and Si revealed through XRF (See Figure 44). Na is also pervasive to shell material, and is

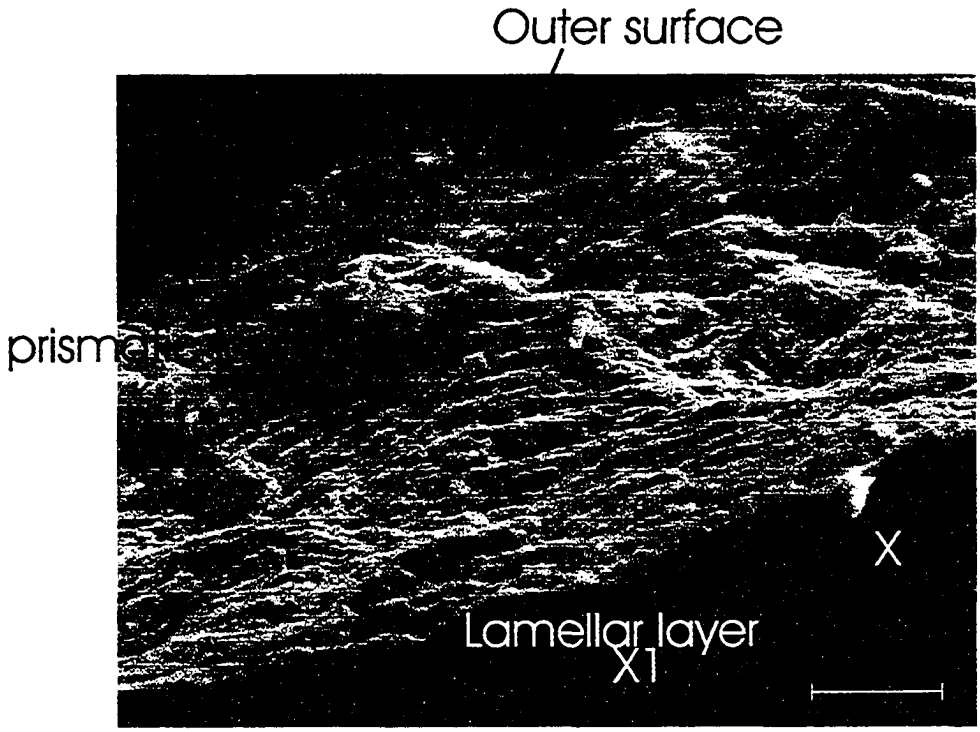

Figure 41. *Macoma balthica final growth year. Lower right interior of shell. Exterior of shell upper left. Inner prismatic layer center.Each lamellae represents periodic aragonite secretion.*

definitely not in carbonate form (See Figures 40, 44, and 48). The most interesting finding is that the common mineral forming elements do not appear to be part of the carbonate cell, but instead occur as isolated particulates affixed to the shell surface or bound in the organic matrix as denoted by heavy-element bright particles in Figures 41 and 45.

In the present study, SEM/EDS is used to substantiate and to some degree calibrate the Philips X-ray fluorescence chemical data, and to obtain information on elements previously shown to be potential marker elements in shells (Si, Al, K, Na, Mg).

Mollusc shells are complex admixtures of amorphous, micro- and quasi-crystalline aragonite with proteinaceous organic interlayer films. One of the purposes of the SEM/EDS study is to determine whether metals tend more to be structurally bound (crystalline), diffusely disseminated in the organic matrix, or present as minor localized inclusions or imperfections. The intent is also to look for broad chemical zonations related to seasonal changes in water chemistry. Specimens were selected for SEM/EDS study that show either enhanced major element concentrations via XRF analysis, or structural anaomalies by x-ray diffraction. Since little shell research has been conducted and *Macoma balthica* has emerged as a predominant and pervasive species in the Hudson it is a logical focus in this investigation.

A backscatter image of the interior surface of the final growth year for a *Macoma balthica* from Hudson location T1C (See Figure 3, near shore, eastern Hudson channel, approximately 10 miles south of the Tappan Zee Bridge) shows the carbon-rich nacreous lining of the shell interior as a dark layer, location X (See Figure 41). The remaining layers comprise the inner prismatic section of the shell representing major growth/shell

building periods. At this magnification (8,000X), each band represents a periodic growth increment of prismatic aragonite. Bright areas scattered along the inner surface represent locations dominated by compounds containing elements with relatively high atomic number. Bulk analyses at points X and X1 (Figure 41) give characteristic values for these heavy-metal-enhanced zones. The dominant aragonite components at X1 are Ca (40.08[1]), C (12.00) and O (16.00); the extraneous components are Na (23.00), K (39.09), and Cl (35.45). The atomic weight of calcium carbonate is thus 100 and the relative concentration of heavy metal (Ca) is 40 percent (Figure 42).

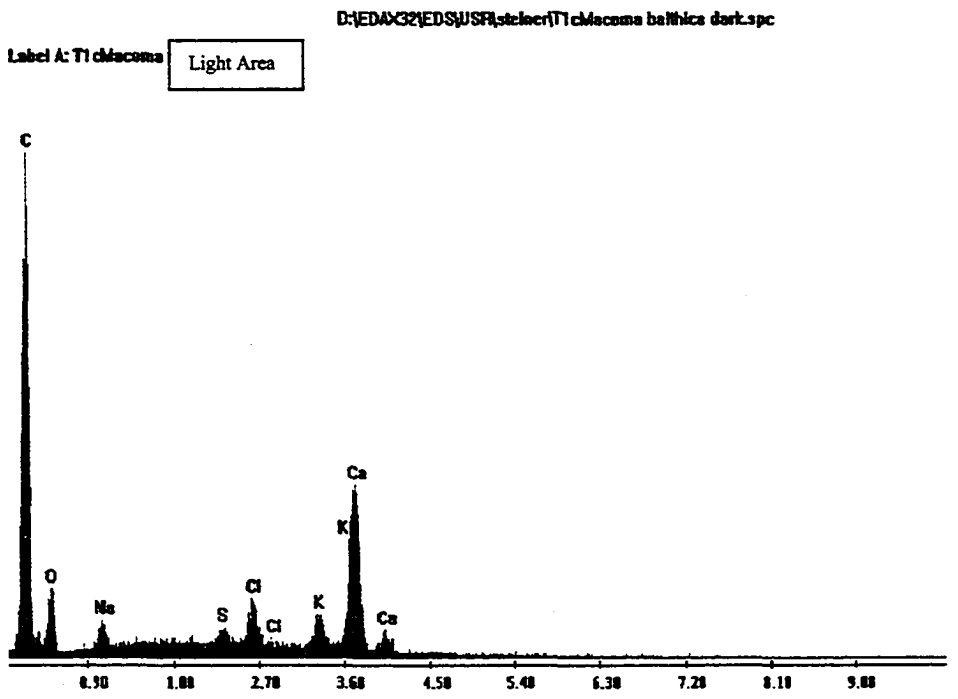

Figure 42. *Energy dispersive spectrum for light are on Macoma balthica shell interior marked X1 (Map location T1C, Fig 3) showing Na-K-Ca chloride or sulfide in clusters within the overall shell matrix*

[1] Atomic weight of calcium.

In contrast, the Na-K-Ca zone, indicated by the bright point at X1 (Figure 41) comprises a net increase in heavy elements (e.g. Cl (35.45) replacing C (12.00) and O (16.00). At this magnification it is not clear whether this agglomeration represents a crystalline modification of carbonate, an intergrowth of minerals, for example an alkali salt and calcium sulfide, or an amorphous aggregation of elements. In addition to chloride/sulfide aggregates, portions of the nacreous layer are clearly 'cleaner' than other portions containing a lesser concentration of extraneous elements. Position X is darker than the surrounding shell (location X, Figure 41) and shows a spectrum consistent with an interpretation of pure calcium carbonate (Figure 41). This agrees well with x-ray fluorescence data discussed in Chapter 4 Section C (Results-Shell chemistry) that shows that the average shell contains significant amounts of Si and Fe

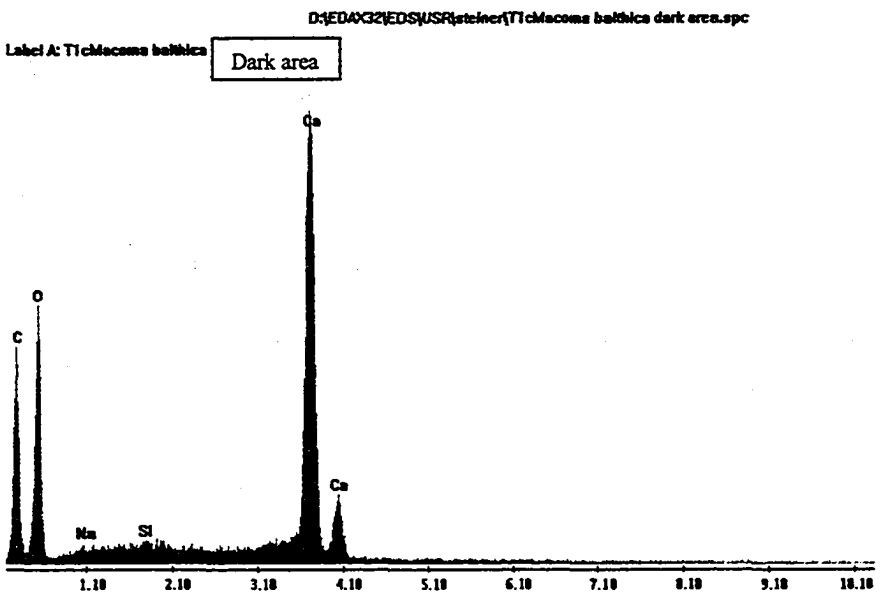

Figure 43. *Energy dispersive spectrum for dark area X from Figure 41 indicates pure aragonite*

Small bright areas may represent inorganic inclusions. Several locations, x-1, x-2, x-3, were analyzed to concentrations of Cu and Zn, 5.07 and 3.96 percent by weight, respectively (Figure 43). The spectrum shows that Cu and Zn are oxides incorporated by the aragonite matrix, but that the range of dispersed compounds is limited to a few highly resolved elements (C, Zn) but also FeO and SiO_2. Magnification of the exterior portion of the last growth year reveals the cyclic deposition of organic matrix complex interlayers (See Figure 44).

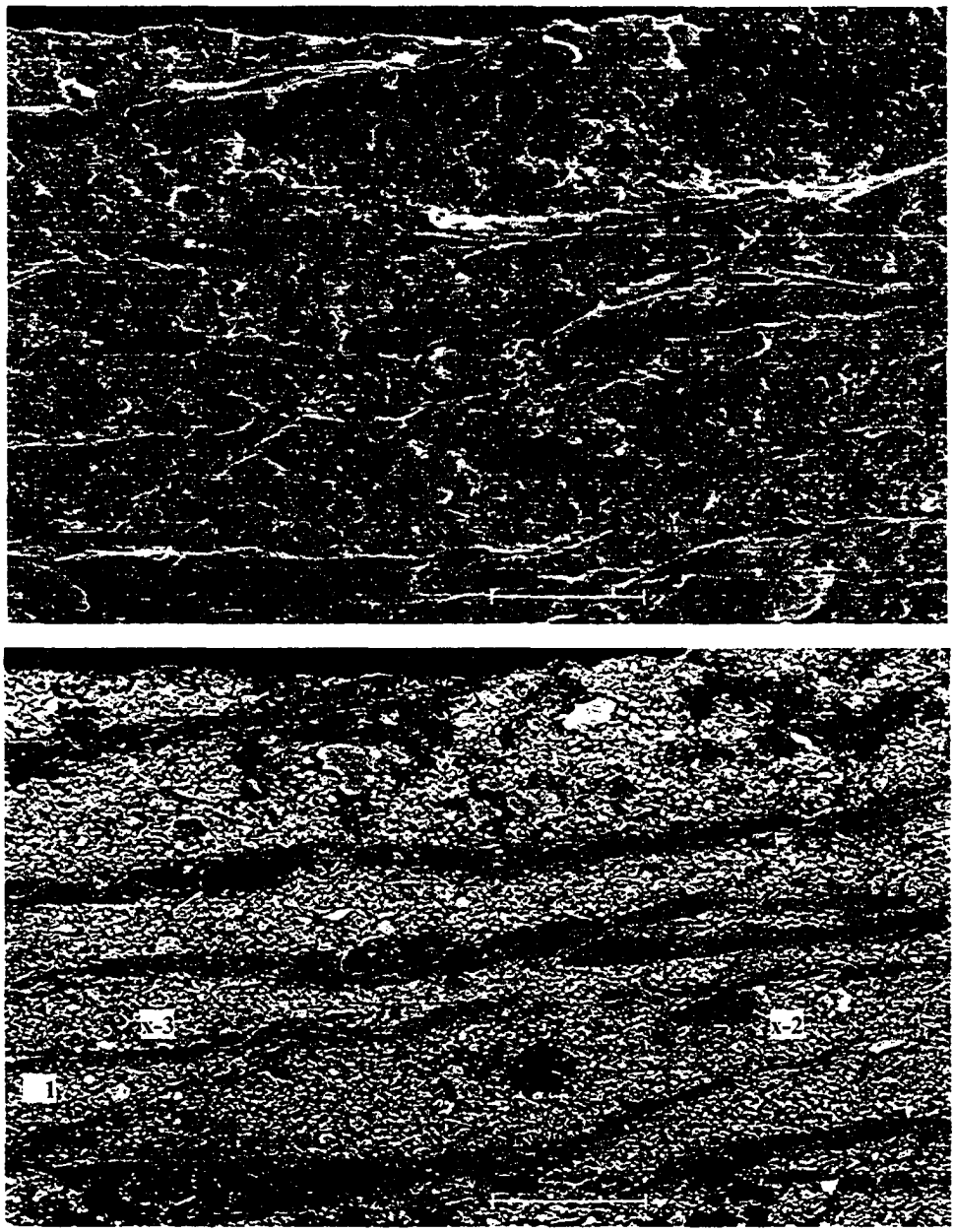

Figure 44. *Secondary(top) and Backscatter(bottom) micrographs of exterior surface of the final growth year of Macoma balthica shell from T1C, eastern shore – ten miles south of the Tappan Zee Bridge (Map Fig. 3) – illustrating scattered heavy metal source areas (brighter regions in right image); Microstructure is evident as noted by obvious linear bands which are inter-layered proteinaceous material (conchiolin).*

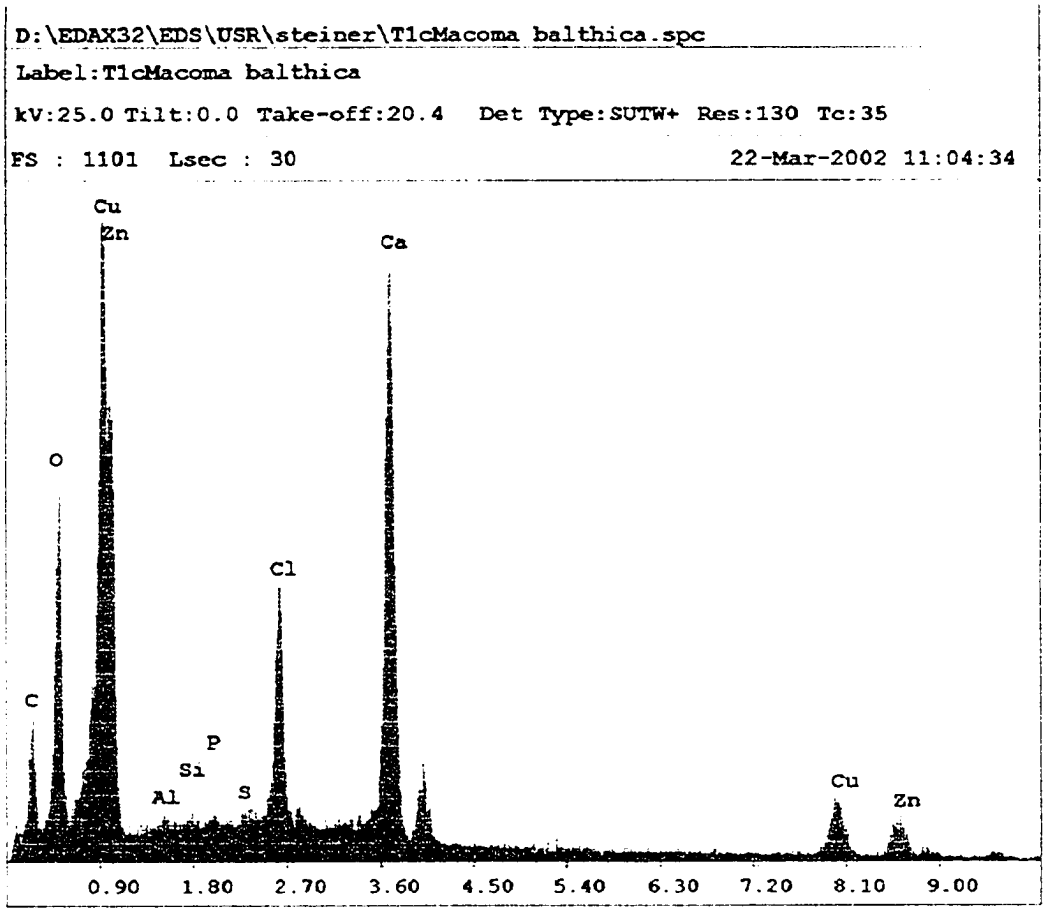

EDAX ZAF Quantification (Standardless)
Element Normalized
SEC Table : User D:\EDAX32\EDS\USR\dallas\4-2.sec

Element	Wt %	At	K-Ratio	Z	A	F
C K	28.23	41.00	0.0710	1.0354	0.2427	1.0005
O K	43.89	47.84	0.0702	1.0196	0.1568	1.0002
Al K	0.50	0.32	0.0017	0.9527	0.3661	1.0020
Si K	0.41	0.26	0.0020	0.9811	0.4920	1.0036
P K	0.29	0.16	0.0017	0.9492	0.6234	1.0063
S K	0.37	0.20	0.0027	0.9743	0.7437	1.0106
Cl K	4.53	2.23	0.0355	0.9251	0.8368	1.0106
Ca K	12.75	5.55	0.1169	0.9525	0.9603	1.0022
Cu K	5.07	1.39	0.0435	0.8459	1.0140	1.0000
Zn K	3.96	1.06	0.0341	0.8469	1.0162	1.0000
Total	100.00	100.00				

Figure 45. *Energy dispersive spectrum for Bright areas labeled x-1, x-2, x-3 fig 42.*

The bulk chemistry of the outer surface by SEM/EDS (Figure 45) corresponds within analytical error to the x-ray fluorescence determinations (Chapter 4, Section C). This indicates the relatively high concentration of rock-forming elements (Si, Al, Mg, Fe, Na, and K) and the approximately equal quantities of Ca and Si by weight (ca. 7 percent). Al and Fe are present in lesser, approximately equal, proportions. The aragonite layers between the perisotracum contain the majority of the bulk silica; the Fe and Mg values are distributed primarily into the periostracum relative to the carbonate host. The SEM micrographs do not reveal the mode of attachment of Fe and Mg in the periostracum, whether in chemical combination or in entrapped particulates.

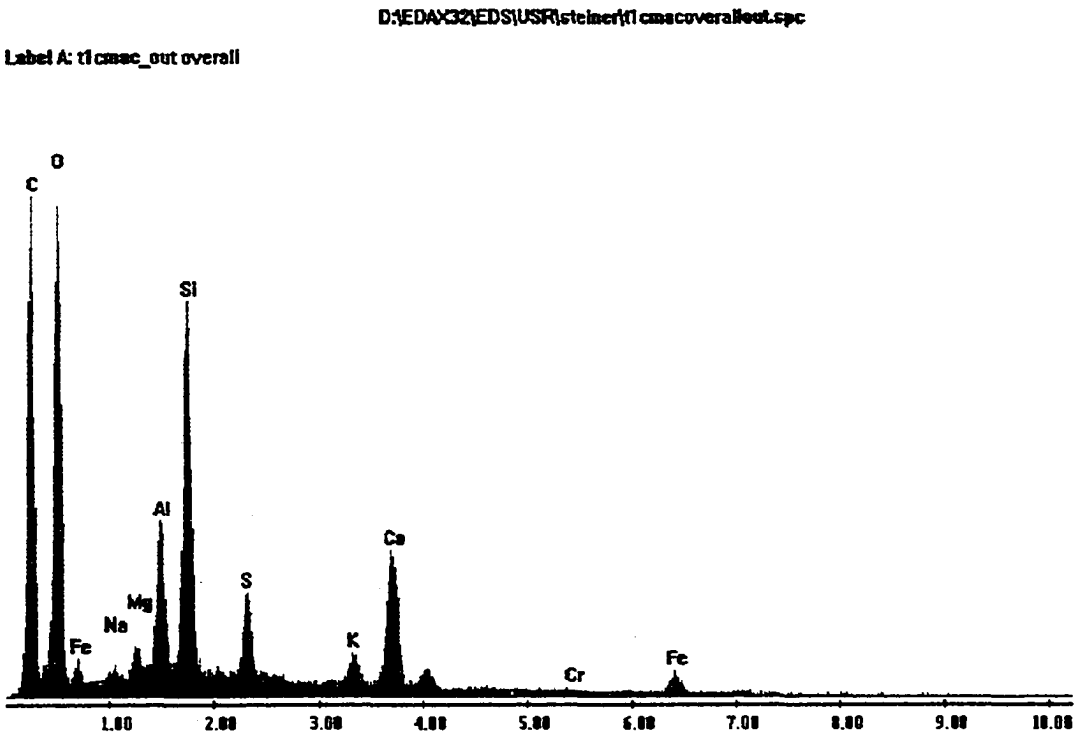

Figure 46. *SEM/EDS spectrum for Macoma balthica shell exterior (figure 44). Significant rock forming elements present, Si at 7% by weight, approximately equal to Ca.*

The average aragonite structure of the outer growth segment of the second *Macoma balthica* sample from T25B (Figures 47 and 48) is shown to be distorted by 0.54% elongation of the C-axis of the orthorhombic unit cell (discussion, Section 5). The SEM/EDS analysis reveals the multi-layer character of the last growth layer, comprising an outer ultra-microcrystalline horizontal surface layer, and the last growth layer, comprising an outer ultra-microcrystalline horizontal surface layer, and an underlying prismatic layer (Figure 46). The prismatic layer comprises an array of elongate microcrystalline aragonite columns with numerous randomly inter-dispersed heavy and light element concentrations.

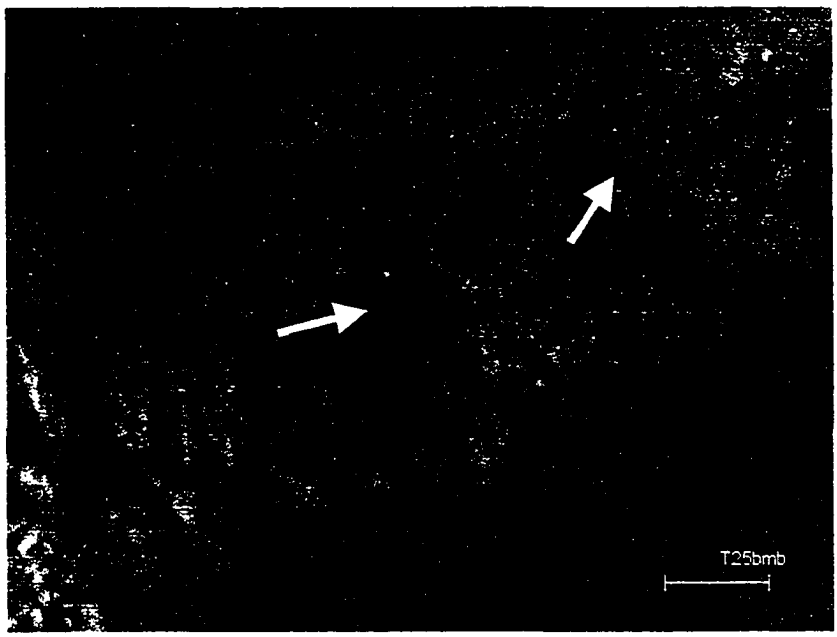

Figure 47. *Backscatter image of a Macoma balthica shell from T25B showing a portion of the outermost growth segment for the last growth year, (see figure 45); the segment comprises a horizontal uniformly gray outer layer (lower right) and an underlying layer made up of clusters of vertically standing (relative to the surface) aragonite prisms (lighter gray with light and dark inclusions) representing prismatic layer below lamellar layer.*

The secondary image, showing primarily surface structures, indicates that the irregularities are embedded in the crystalline structure as a probable source of the distortion of the crystal edge and corresponding unit cell distortion (Figure 48).

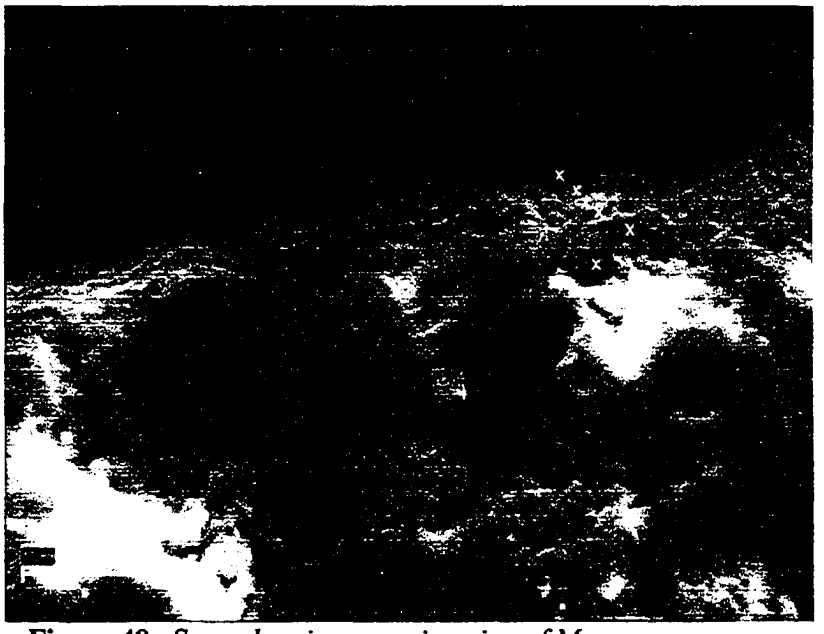

Figure 48. *Secondary image re-imaging of Macoma balthica T25B showing the location of chemical analyses (series of x's, upper right) illustrating the lack of expression of the 'light and dark' inclusions evident under backscatter imaging.*

Whereas individual elemental concentrations within the prismatic layer have yet to be determined, an EDS bulk analysis shows that Ti, Fe, Na, Al, Si all substitute within the aragonite structure. Given the expression of both chlorine and sulfur, and only potassium halite structures in the x-ray diffraction record (Appendix 1), the extraneous metals other than Na may to reside within lattice domains that are almost continuous with the aragonite host. High-resolution X-ray diffraction data are being collected to evaluate this proposition (Rudolph, in preparation).

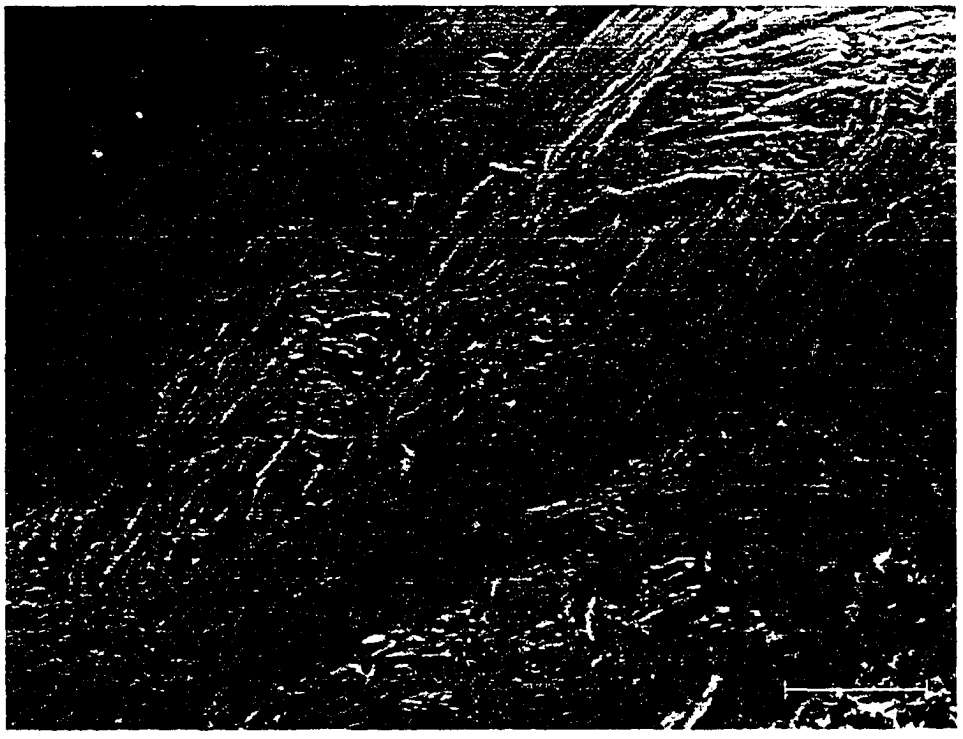

Figure 49. *Enlargement of last growth year for Macoma balthica from T8C, slightly inclined upper surface outer perimeter of uncut shell. Magnification in secondary mode shows convolution of aragonite layers of prismatic layer.*

The daily growth record for T8C *Macoma balthica* is apparent in the SEM image (Figure 46), a specimen from T8C. Analyses of these individual growth sections shows evidence for daily variations in oxidizing conditions that causes the mantle to secrete calcium carbonate as metabolic activity ensues and then during localized, temporary anoxic episodes, calcium carbonate production is replaced by organic matrix emplacement and possibly some carbonate dissolution. The conditions under which calcium carbonate is created do not support perfectly ordered structure and result in the incorporation of S, Si, Na, Mg, and Al by the shell medium as is found in other analyzed

Macoma balthica shells. The apparent convolution is generated by the perpendicular orientation of the prismatic layer relative to the surface of the shell and the general lack of regular alignment of crystals see Figures 46 and 48). This is easily supported by the general nature of shell formation.

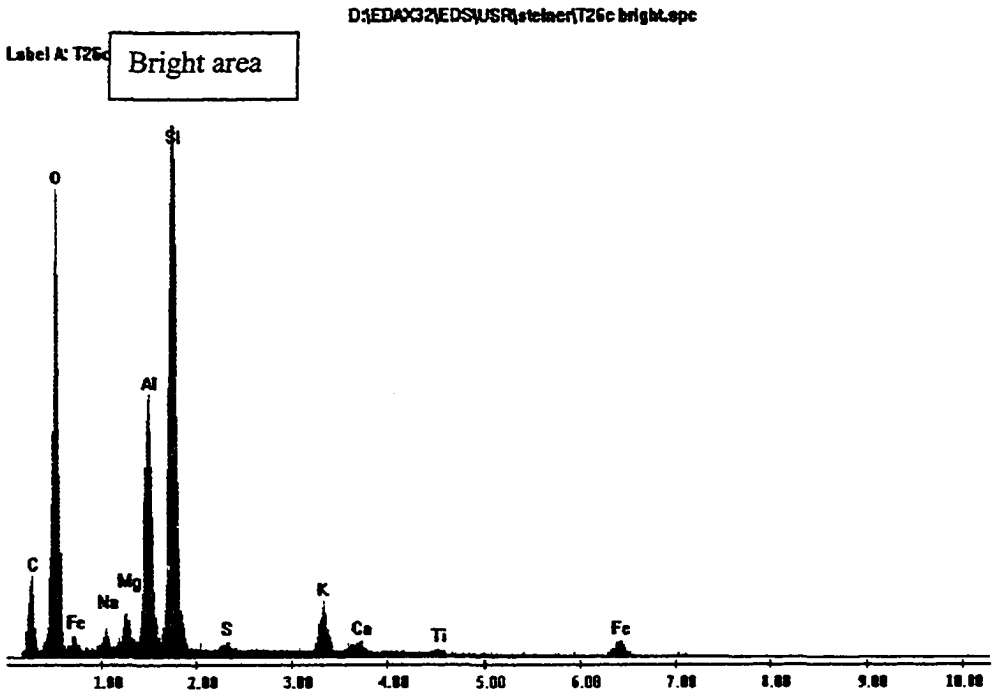

Figure 50a. *EDS spectra for Macoma balthica at T26C. Scan shows comparative chemistry of a typical bright particles composed primarily of Aluminum and Silicon with minor Mg, Na, Fe, K, and Ti.*

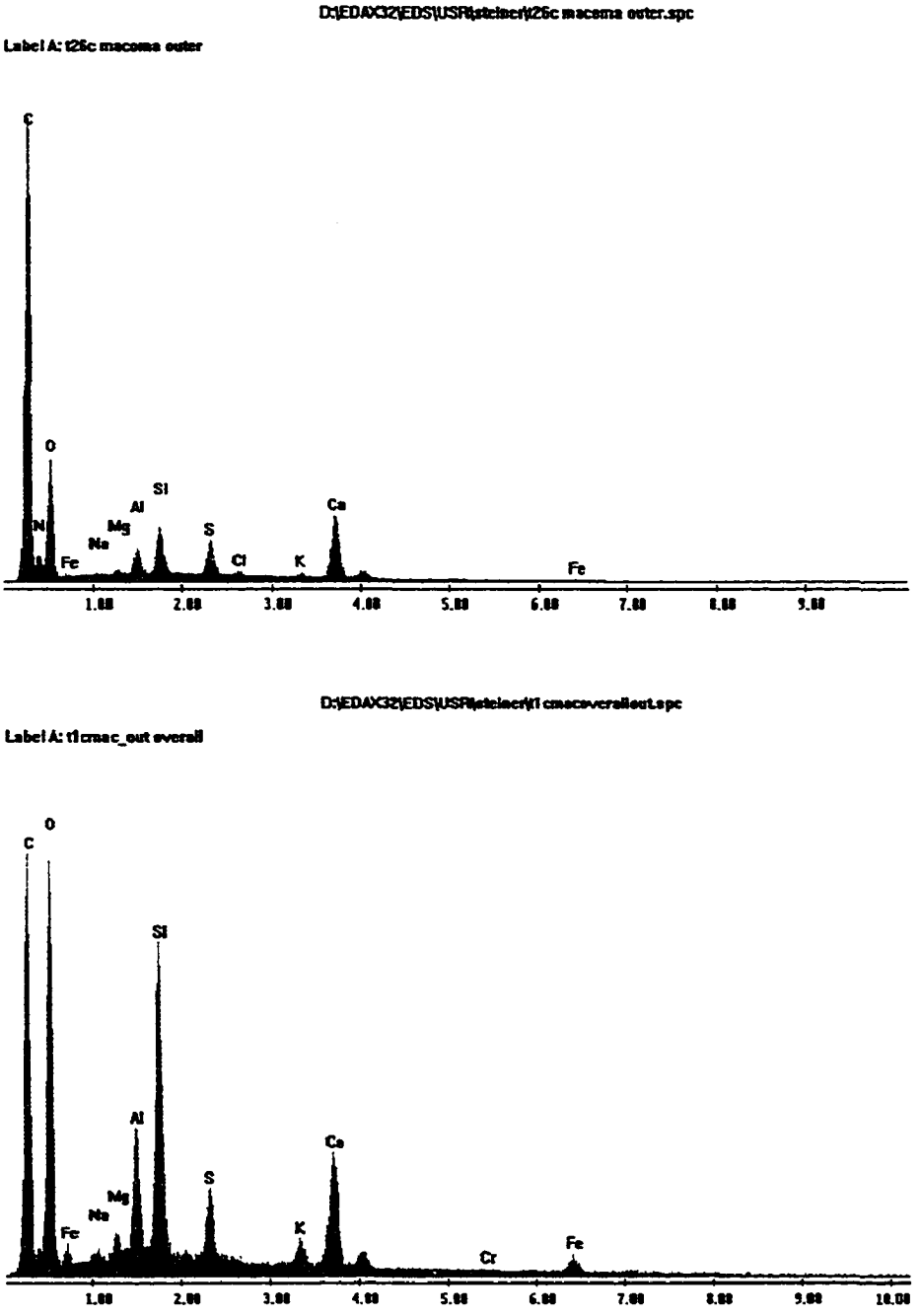

Figure 50b-c. *The outer shell Macoma balthica T1C,(top) (darker in backscatter) has similar chemistry but much reduced non-carbonate elements. The lower scan shows general chemistry of bulk shell.*

Macoma balthica shell chemistry is shown to be more complex than simple aragonite with metals in substitution for calcium. Figure 50 shows that bulk shell material contains significant silicon, aluminum, magnesium, potassium, sulfur, iron, and chlorine along with the elements that form aragonite. The isolated bright spots identified in backscatter imaging show that there is very less carbonate (primarily Ca) in those areas. Compounds containing metals of higher atomic weight instead replace Ca CO3. The darker areas constitute regions of low metal content and are primarily aragonite.

E. XRD and Unit Cell Refinement

X-ray diffraction spectra of mollusc shells are generally consistent with the aragonite structure (see Figure 49). In the present study we attempt to find small departures from the ideal structure that may be due to the impurities in shells discussed in the earlier sections. In this effort we calculate the fundamental unit cell for the aragonite structure to see if the cell edges depart from the ideal in a manner consistent with the major elements that are most abundant in the shell material. For example, if iron is the major cation in shells, is the unit cell displaced in a manner consistent with a siderite (iron carbonate) component, and is the cell symmetry retained with substitution. Aragonite is orthorhombic, and substantial distortion of the shell might degrade the symmetry to monoclinic.

A sample diffractogram for mollusc shell, T9aMb (Figure 51), shows sets of sharply defined diffraction maxima indicating relatively coarse grain size (20 micron), and an apparent absence of structural distortion (line broadening). Comparison of shells to the aragonite structure and to the results obtained through cell refinements shows that the majority of shells are dominantly aragonite, but that a subset of the spectra belongs to an as yet unidentified set of phases (See spectra in Appendix 1). In this study we emphasize the degree to which the shell structures agree with the classical aragonite structure. The carbonate spectra for Hudson molluscs agree with the aragonite structure, as discussed below, however, changes in the metal content have affected the relative intensity of various peaks. What is normally the 100-intensity peak (111) is consistently lower than the 60-intensity peak (012) in the present study. Peak intensity variation can occur due to preferential orientation of crystals in the sample, particularly in cases where

the mineral has a strong preferred cleavage direction. Techniques that minimize preferential

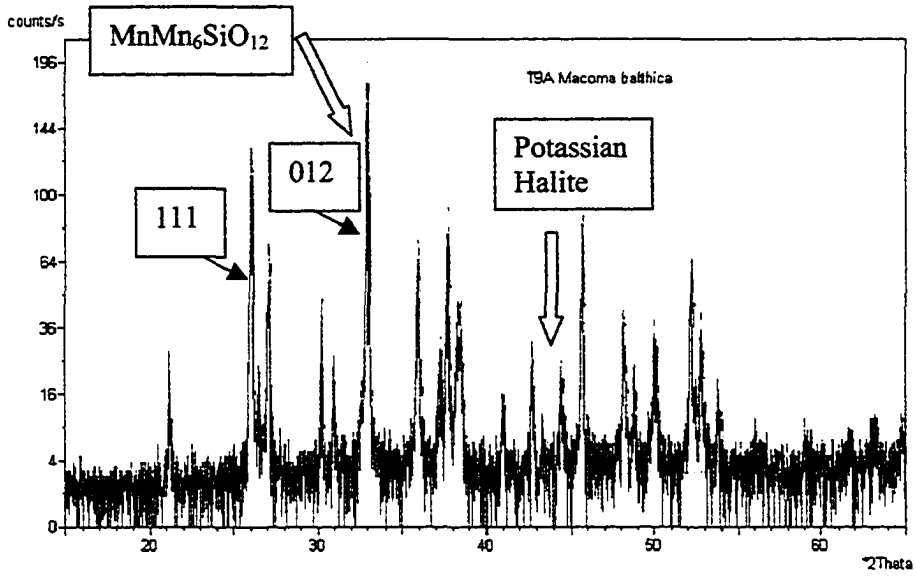

Figure 51. *Diffraction spectrum for mollusc shell showing non-Aragonite peaks as well as peaks showing deviations in expected Intensity*

alignment were all undertaken in this examination, the most important of which is ultra-fine grinding in a non-polar medium. Peak intensity is a function of the number of electrons in the electron cloud of elements in the aragonite structure. Heavy-metal substitution for Ca may thus alter expected peak heights. Another alternative that may cause peak intensity aberrations is peak overlap by the presence of additional minerals. One possible match ($MnMn_6SiO_{12}$) is indicated in Figure 51. The relationship between metal substitution and diffraction maximum will be pursued in a later study but can be introduced here with a look at the unit cell parameters for other orthorhombic, triclinic and cubic carbonates (See Figure 52).

Speer, 1983 establishes that for organic aragonite the prominent substitutions for calcium occur most commonly by strontium Sr, and to a lesser extent, sodium Na and magnesium Mg. A second subset of shells is consistent with structures that have been elastically strained by such substitutions (see Figure 51). The ratio

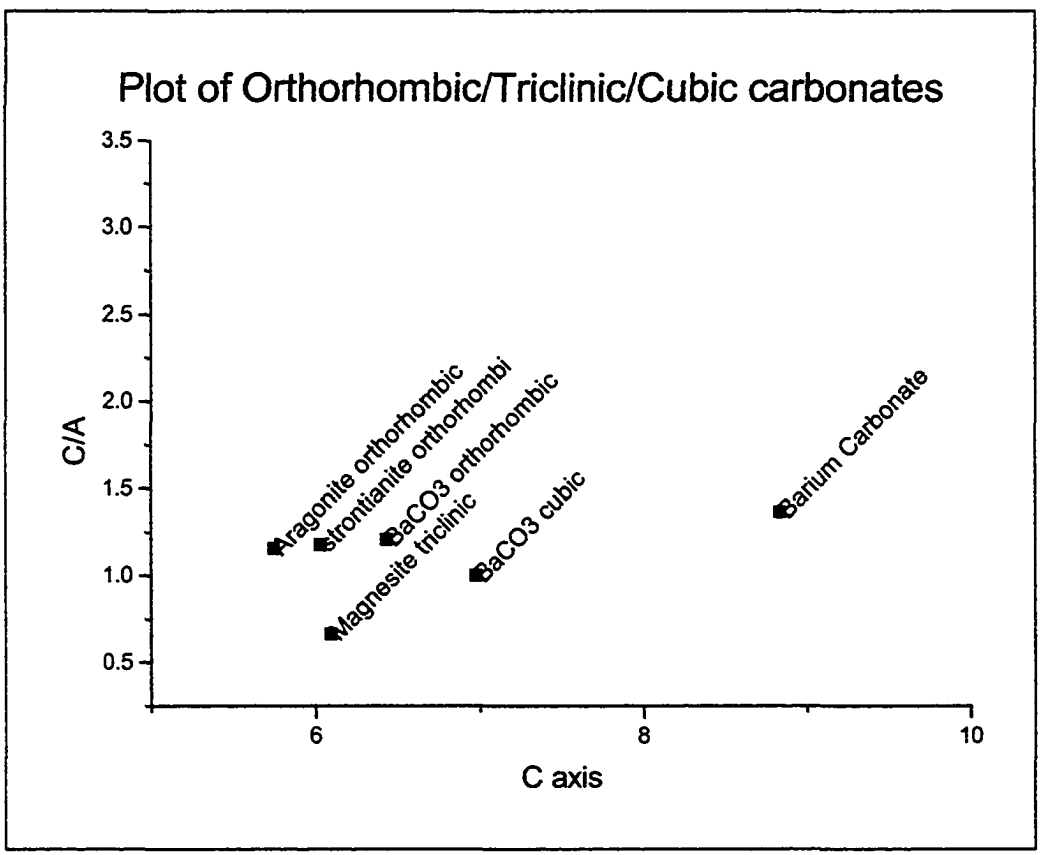

Figure 52. *Carbonates plotted by unit cell dimensions. Data from ASTM file for various carbonates. C/A is standard for calcite. There are no studies examining orthorhombic carbonate unit cell refinement for organic aragonite, therefore by convention this research conforms to this type of expression.*

C/A has been chosen as a reference since the structural change is reflected in the c-axis relative to, for example, the a or b-axis and this representation is standard for evaluation of other carbonates (Speer, 1983). The outlier *Macoma balthica* shell from T3C has a

c-axis length consistent with aragonite, but a reduced c/a outside the error range (Figure 53 (lower square). This ratio is consistent with a modification in the shell aragonite by the substitution of magnesium for calcium (See Figure 52).

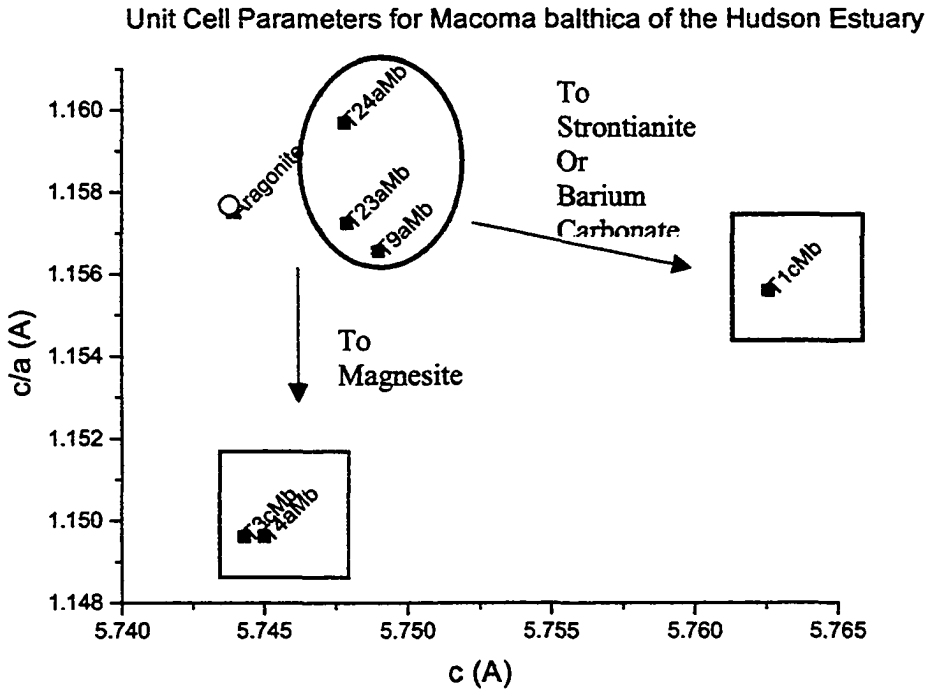

Figure 53. *Comparison of Macoma balthica specimens based on unit cell dimensions. Red and blue boxes indicate distorted shells within statistical error. Black circle marks shells with error values that fall within the range of aragonite*

The XRF data supports this finding as this sample has 10 times more magnesium than all other shells. The T1C outlier has a similar c/a ratio but a c-axis length departure from aragonite that suggests the replacement of calcium by strontium, barium or magnesium (Figure 53 right square). XRF data also supports this assertion since this sample exhibits a Sr concentration that is 100 times greater than all other specimens.

F. Neutron Activation

Neutron activation analysis to measure select transition metals, metalloids, REE concentrations in select molluscs was undertaken at Oregon State University Radiation Laboratory. This technique provides reliable element information and is used for a variety of applications ranging from environmental studies to forensics. We had the fortunate opportunity to utilize this technique for a small subset of the mollusk collection. For this reason we focused on elements that are below detection levels for our in-house analytical techniques.

1. Rare Earth elements (REE)

A standard set of REE elements was examined and as expected not all were present at detectable levels. The REE under investigation are: La, Ce, Nd, Sm, Eu, Tb, Yb, Lu and Th. Of the group only La, Ce, Sm and Eu are present in significant concentrations. La and Ce are presented together since values are comparable (Figure 54). Both elements vary randomly throughout the sample region showing spikes in concentration at T4A (8 ppm Ce, 4.8ppm La), T7C (6ppm Ce, 3.5ppm La), and T2C (5 ppm Ce, 2.9ppm La). The remaining REE are found in trace amounts and presented in Figure 55. Again, trace REE concentration is not a function of salinity or temperature that vary inversely towards the right of the plot. The elements continue to show a scattered variability that must be attributed to local REE availability most likely as a dissolved component.

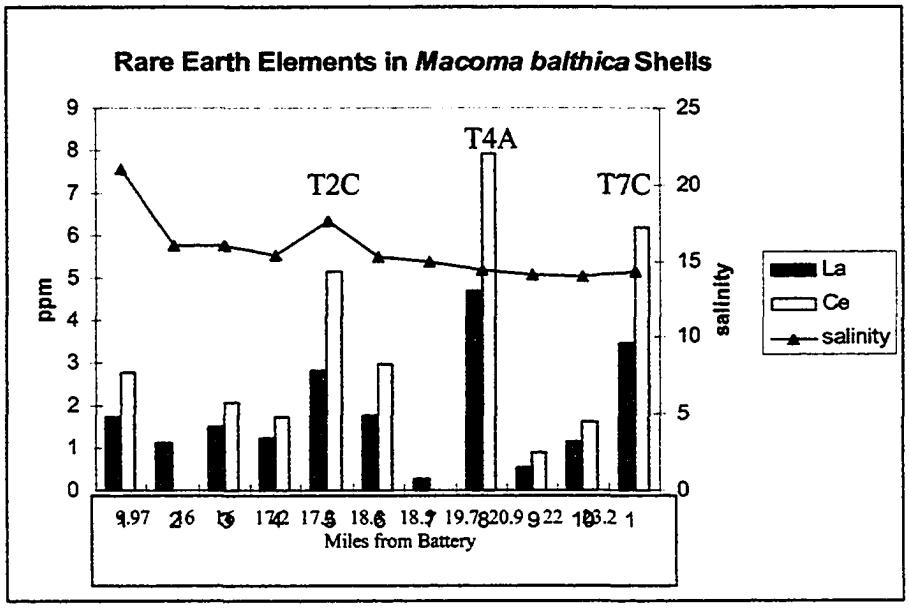

Figure 54. *REE La and Ce in Macoma balthica. Variability showing no relevance to salinity or temperature, but random site-specific spikes at T4A, and T7C, and perhaps T2C. Average error on La +/-.1ppm, Ce +/-.4ppm*

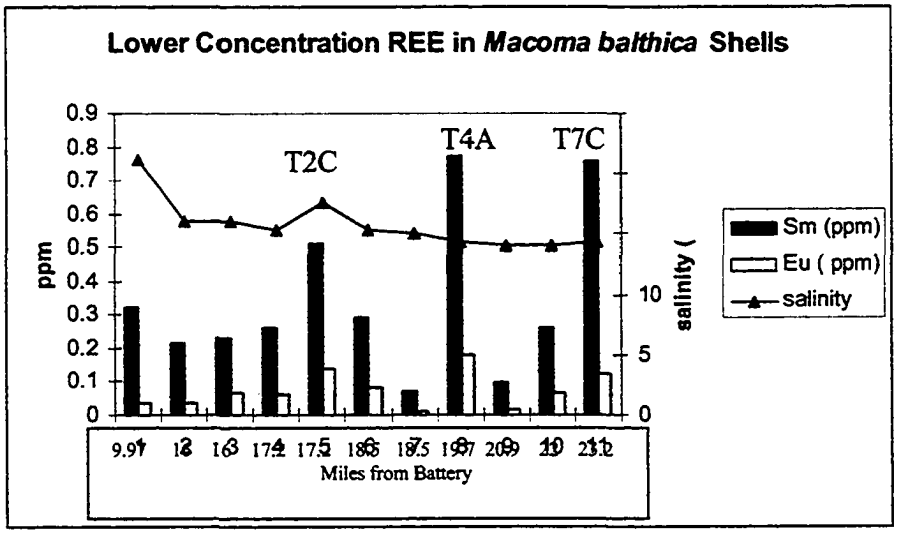

Figure 55. *Sm and Eu Macoma balthica showing lack of correlation with water parameters (temperature increases and salinity decreases to the right—north) Sm error av +/- 0.01 ppm, Eu error < +/-.01.*

2. Transition metals

Macoma balthica shells contain transition metals in the low part per million range Figure 56). Cobalt is by far the most prevalent of this group at a high of 2.3 in T4A *Macoma balthica* though all elements except Ta and Au are also relatively high. There seems to be no apparent pattern in element variation from the standpoint of location within the study area suggesting that concentrations of these metals, though thought to be salinity controlled by some researchers are probably controlled in the Hudson by site-specific dissolved metal availability. In the case of the transition metal variation illustrated in Figure 56, values are extremely low, so that pattern determination is suspect. One common thread thus far is that almost all of the examined elements are more greatly concentrated in *Macoma* shells from T4A.

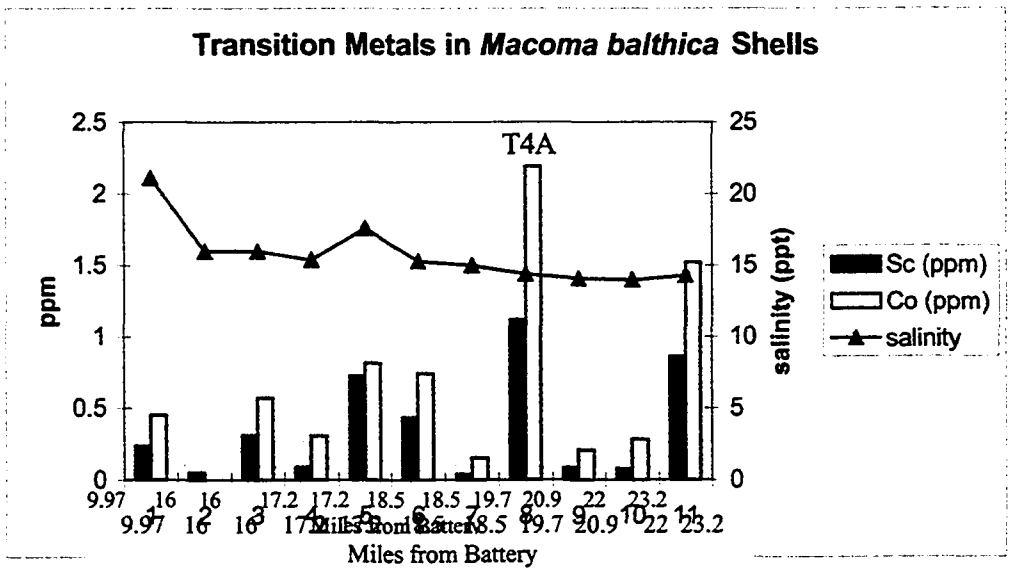

Figure 56. *Transition Metal concentration in Macoma balthica shells. Sc and Co are compared because of similar concentrations. Sc error +/-.003-.01 ppm, Co +/- 0.02-0.05ppm.*

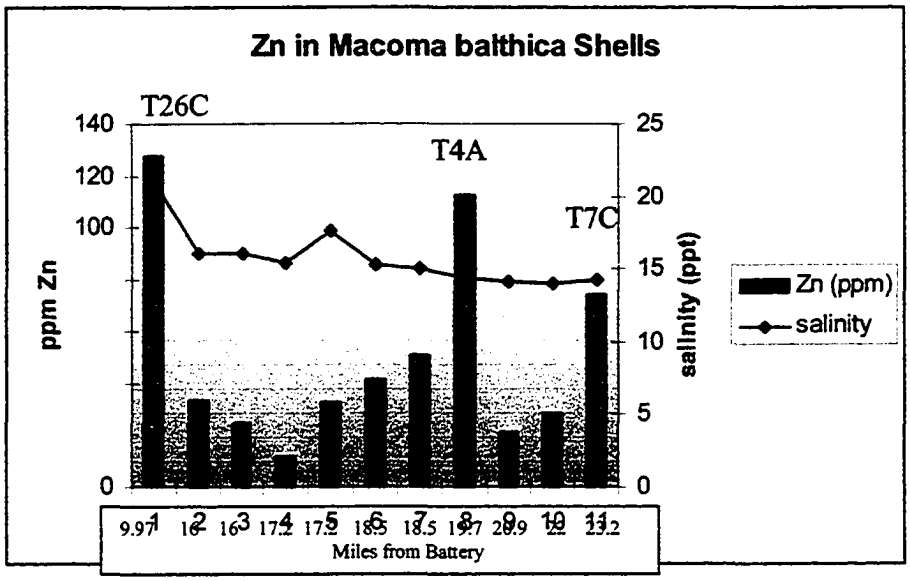

Figure 57. *Transition metal Zn in Macoma baltica. Spikes at T26A, T4A, and T7C. Error < 2-10ppm*

Zinc is plotted alone as the concentrations range from 10 to 120 ppm (Figure 57). Evidence suggests that Zn uptake though more substantial, is also not salinity or temperature driven. Three spikes, T26A, T4A, T7C exist. These locations are fairly well distributed within the range of *Macoma balthica* again suggesting a local source. The most interesting outcome of the Neutron activation results is that trace element concentrations, however minute, are detectable by this method.

G. Electron Microprobe

One of the first examinations conducted on shells in this study was limited electron microscopy to establish whether trace metals concentrate in shell aragonite. Microprobe analysis requires preparation of polished thin sections that are subsequently rendered conductive with carbon coating. Since shell material is extremely fragile, especially the shells of the estuarine species, *Rangea cuneata*, because of its robust shell, was chosen. Another deciding circumstantial reason for the choice of *Rangea* is its newly recognized addition to the Hudson benthic fauna. Prior to 1997, *Rangea* was not a recognized Hudson resident.

Figure 58 shows a light microscope image of the polished section of *Rangea cuneata* used in the examination. This organism was sampled live from site T13D approximately 4 miles south of Croton-on-Hudson on the eastern margin of the Hudson.

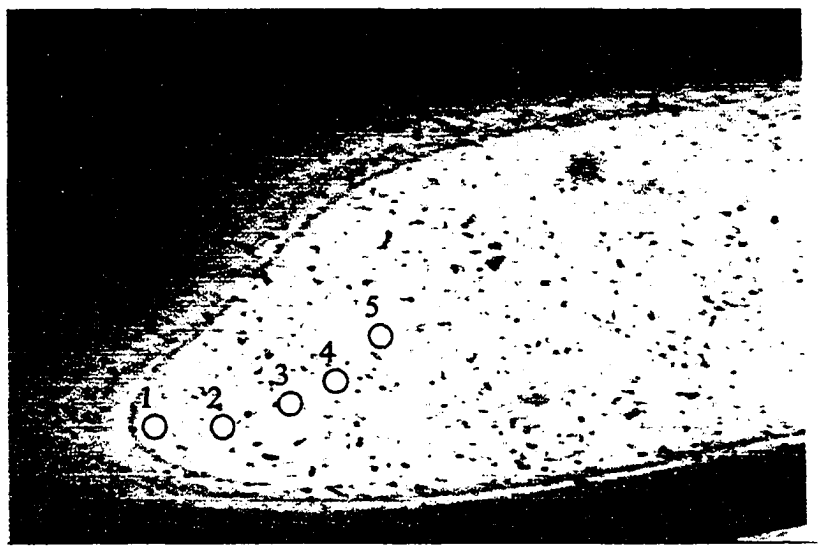

Figure 58. *Magnification of tip of Rangea cuneata, lower margin represents outer surface. Circles indicate locations of microprobe map analyses.*

From initial light microscope imaging, a fine scale pattern of sub-parallel growth lines oriented at an angle of about 90 degrees to the larger scale growth bands was

detected. This fine scale pattern is described by Jones 1985 regarding *Spisula solidissima*. The sample map was determined based on this fine-scale pattern. The series of circles on figure 58 approximates the location across several of these bands and perhaps reflects a bi-weekly (daily?) stepping back in time. The analyses are presented in Appendix 3. As expected, calcium from site to site is

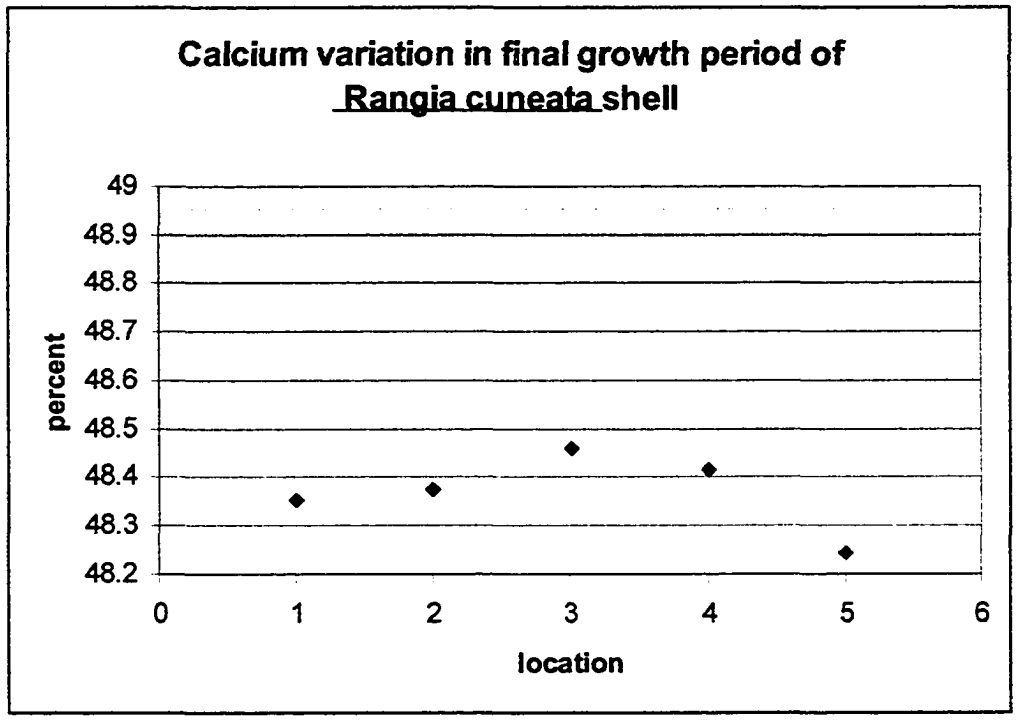

Figure 59. *Calcium variation in fine scale layers of Rangea cuneata showing statistically constant values.*

not dramatically variable as would be expected since relative to all other elements calcium is dominant. Sodium and Phosphorus vary slightly in different growth bands and show a moderate direct relationship. Both elements increase and

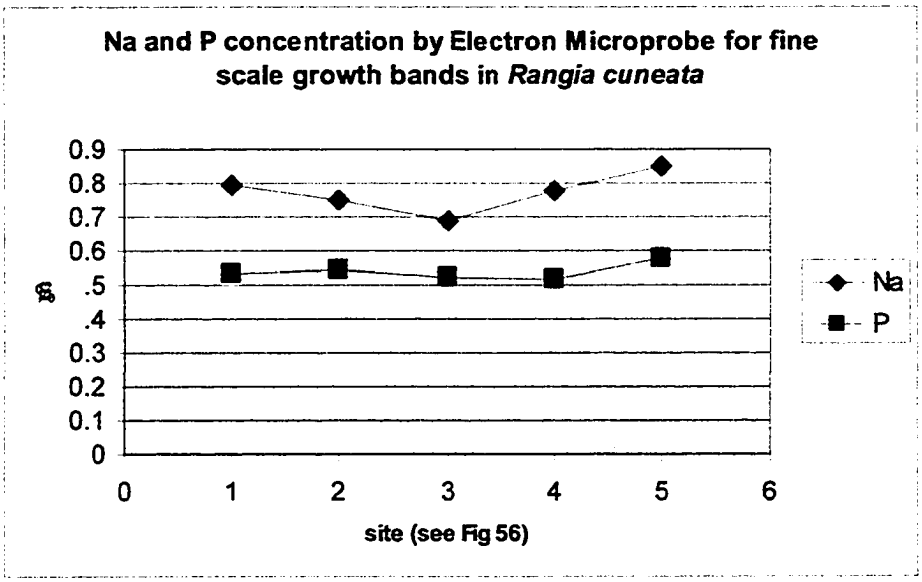

Figure 60. *Na (diamonds) and P (squares) by electron microprobe.*

decrease together with Na concentrations always higher. Values range from 0.7 to 0.85% for Na and slightly lower values for P. Na and P also vary inversely with Ca (Figure 60). The comparison of mineral forming elements in the alkali and alkaline and transition groups also demonstrate variability in trace metal component in shell growth layers, but element relationships are absent.

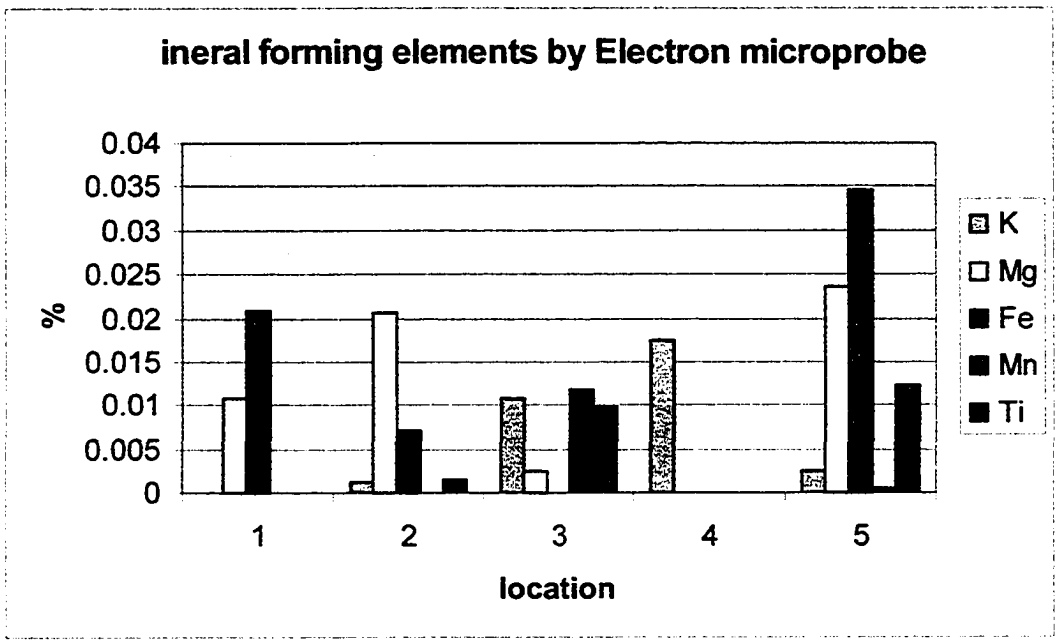

Figure 61. *Variation in mineral forming metals illustrating extreme variability in deposition throughout the shell*

Metal partitioning in shell layers is a function of metal availability at the time of shell generation. Interestingly, Fe varies from 0.035% to 0% over the examined growth interval. Mn and Ti are only present at 2 and 3 locations respectively (Figure 61). Select REE examination also shows extreme variation from 0 to almost .03% (Figure 62). Again, element concentrations fluctuate independently probably based on site-specific dissolved metal content. As previously noted, rare earth elements are not exactly rare to mollusc shells.

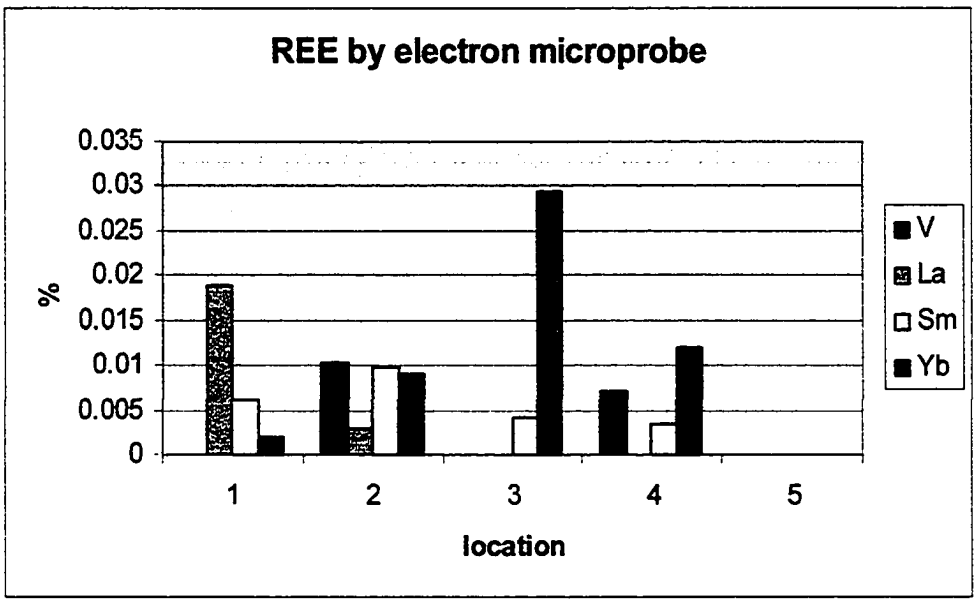

Figure 62. *REE variation in minor growth bands of Rangea cuneata*

Elements capable of substituting for Ca in aragonite were also examined (Figure 61). Once again extreme variability is illustrated.

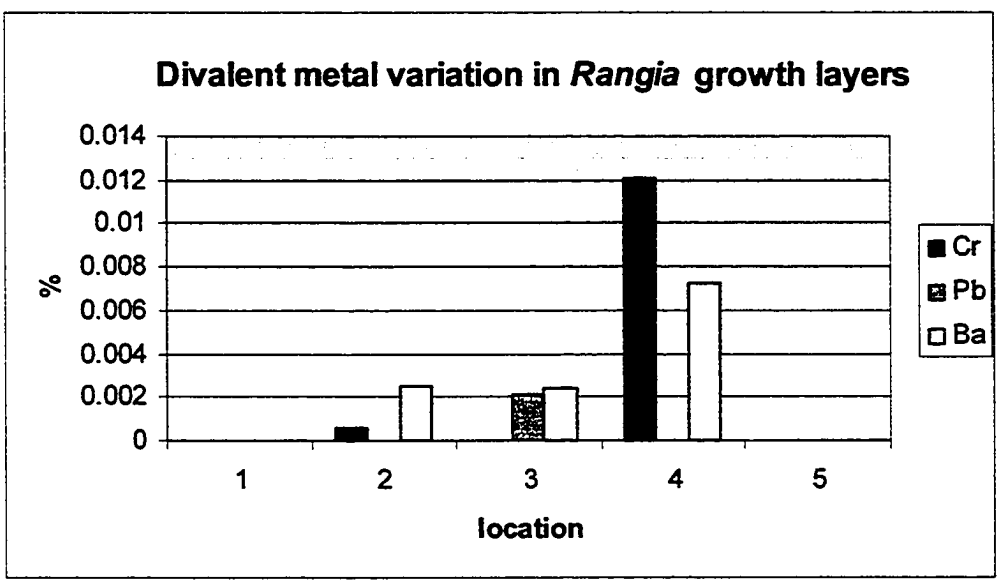

Figure 63. *Variation in minor growth bands for Divalent metals Cr, Pb and Ba in Rangia cuneata shell.*

This preliminary electron microprobe research demonstrates that precipitation of calcium carbonate is definitely not uniform in terms of trace metal concentration; even REE become incorporated in shells and vary in concentration over time. A future investigation exclusively focusing on *Rangea cuneata* may prove worthwhile for establishing trace metal uptake by filter feeders.

CHAPTER 5: DISCUSSION AND CONCLUSION

A. Distribution

Mollusc assemblage has changed dramatically since the investigations of the 1970s. The most notable differences lie in the absence of live specimens of the low brackish estuarine organism, *Mytilopsis leucophaeata* and a drastic reduction in population numbers of the high brackish *Mulinia lateralis* and *Mya arenaria.* The absence of *Mytilopsis* does not necessarily indicate a total absence. The 1997 sampling grabs were much more successful in muddy substrates, environments not suitable to byssally attached forms such as *Mytilopsis.* In 1999, sampling was almost exclusively carried out in locations containing mud bottoms. Therefore, *Mytilopsis* may have been in part overlooked. Disarticulated valves of *Mytilopsis* were recovered suggesting that they exist in nearby harder substrates. In 1997 and 1999, *Mulinia lateralis* occurrence is limited to the Battery region. In the previous sampling surveys *Mulinia* was more widespread though numbers of organisms north of the Battery were also low (<5 individuals). *Mulinia* is especially sensitive to contaminants; in fact, it is often used as a pollution indicator (Shaw, 1975). The most remarkable modification to the initial investigations of the 1970s is the northward relocation of the *Macoma balthica* distribution range and the increase in live individuals. Live *Macoma* specimens were recovered from most mud substrate locations in the estuary north of the Bronx within the mesohaline salinity zone. Also notable is the establishment of *Rangea cuneata,* previously un-reported in the Hudson. *Rangea cuneata* replaces *Macoma* in the region spanning from the Tappan Zee Bridge to Croton-on-Hudson. Crandall (1977) performed a rigorous investigation of the invertebrates of Croton Bay and reported only *Congeria*

leucophaeata (Mytilopsis) and *Balanus improvisus* coexisting. Today, there is substantial evidence that *Rangea cuneata* inhabits Croton Bay in great numbers. In the northern reaches of the Poloyhaline salinity zone, there appears to be a 'species free' zone that corresponds with the entire length of Manhattan. This is a dramatic divergence from the findings of the 1970s when *Macoma balthica* and *Mulinia lateralis* and even *Mya arenaria* inhabited this region in fairly large numbers. The new absence may reflect a drastic reduction in nutrient input resulting from the transformation of the once raw sewage outlet to the North River Water Treatment Plant at 140th street and The Hudson River. Based on mollusc findings, the Hudson benthic environment is thriving, though not much overlap in species exists so diversity remains low. This does not reveal a dramatic difference from the results of the 1970s.

B. Geochemistry-Trace Metals and Aragonite Structure

XRF, SEM, Neutron activation, Electron microprobe results demonstrate that substantial trace element variation exists in the shell material of *Macoma balthica*. *Macoma balthica*, a deposit- and filter-feeding mollusc is a reasonable choice for metal determinations since metals are often bound to the sediment and to a much lesser degree dissolved in water. Through XRF studies substantiated by SEM, it has been determined that mineral forming elements enter the shell matrix either as particles embedded in the aragonite or as part of the organic matrix component. Concentrations of elements such as Sr, Na, Fe, Al, K and Mg all vary based on salinity. Most metals have demonstrated a direct relationship with salinity, but only Na shows a first order relationship. Other researchers have demonstrated that in shells, Mg concentration is inversely related to salinity, but this research indicates that Mg has a bimodal distribution at least over the

distribution range for live *Macoma balthica* and shows no evidence for increase up estuary. One reasonable explanation for the inconsistency with other published research is that *Macoma balthica* does not occur far enough up estuary to find the expected increase in shell magnesium. Another might be that magnesium uptake by bivalves is a species specific process that behaves differently in *Macoma balthica.* XRD studies support the presence of non-calcium ions by the distortion of the aragonite unit cell and the alteration of relative intensity values for the peaks corresponding to the aragonite lattice. However, at the current resolution, XRD spectra do not show peaks belonging to other orthorhombic carbonates. The only solution is to conduct high intensity Synchrotron diffraction analyses that may be able to detect trace carbonates, if present. *UNIT CELL* plots of XRD data seem to indicate some degree of substitution for calcium with alterations in the aragonite structure towards barium carbonate and magnesite. REE and transition metals are present in varying amounts in *Macoma balthica* shells. These elements do not correlate with salinity temperature or any other measured parameter but vary site to site and most probably reflect normal dissolved component variations. REE and metals are present within shell aragonite on or within the aragonite lattice, organic matrix, or protein interlayers. Electron microprobe and neutron activation techniques are capable of identifying micro-scale variations in metal concentrations in shell material. These results can show periodic shifts on a very small scale in water and/or sediment chemistry conditions. Overall, dissolved or sediment bound metals in the local environment do not seem to not adversely affect *Macoma balthica* though the dual feeding style of processing deposits and filtering water would suggest that this species might be preferentially impacted by contaminants. Many elements show a spike at sites

T4A and T1C north of the Westchester/Bronx border. Tributaries enter the Hudson in these general vicinities, one originating in Northern NJ and the other entering the Hudson near Yonkers. These streams may be transporting groundwater contaminants and may partially explain some of the metal concentration increases.

It is evident through this research that standard geologic analyses (XRF, XRD, SEM, neutron activtion, and electron microprobe) on materials (shell and other organic hard parts) that have otherwise eluded these types of examinations can provide valuable baseline chemical data that can be linked to environmental conditions. Future research planned for the summer 2004 will provide a more rigorous, multifaceted analysis of the Hudson benthic environment, correlating sediment, water, shell and soft tissue data. These data will more completely characterize the Hudson benthic environment and can be used to formulate future decisions concerning the estuary and its watershed.

Appendix 1: X-ray Diffractograms for aragonite of *Macoma balthica* shells

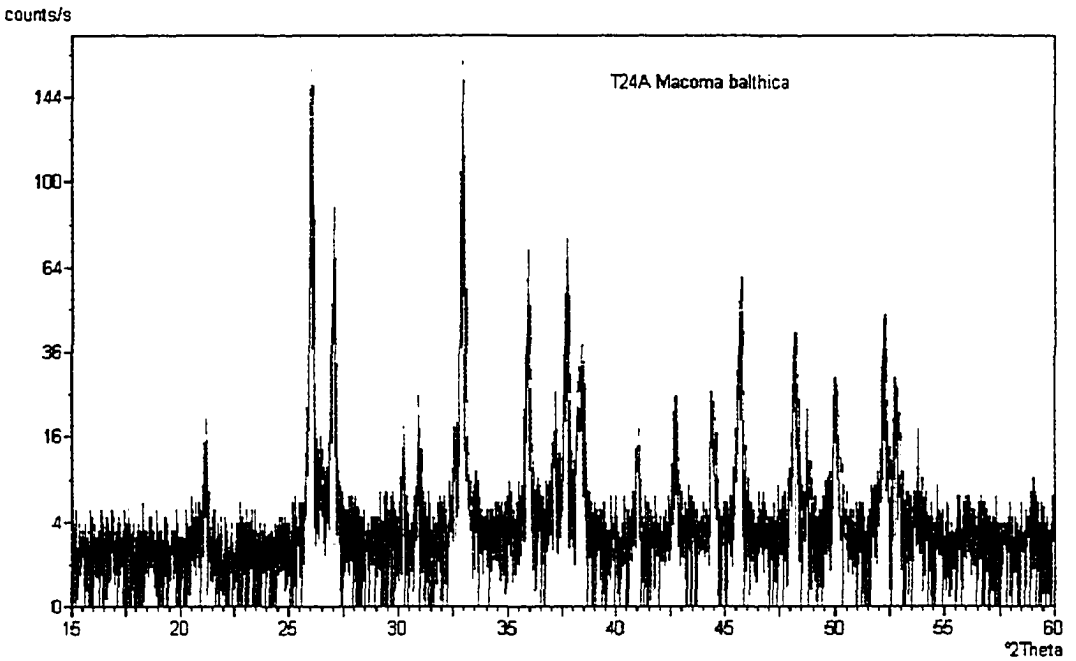

		2-Theta	Intensity	2-Theta	Intensity
SampleIdent T24A *Macoma balthica*					
Exported by X-Pert Software		17.5992	1	38.4002	25
Generated by Liz Rudolph: Project Shells		18.5773	1	41.0102	7
DiffrType,PW3710		21.1981	9	42.697	10
Anode,Cu	GeneratorVoltage: 40 Kv	26.0373	97	44.4163	13
LabdaAlpha1: 1.54056	TubeCurrent: 40 ma	27.0339	40	45.6879	33
LabdaAlpha2: 1.54439	FileDateTime: 4-Jul-01; 19:04	30.271	8	48.1963	19
RatioAlpha21: 0.50000	DataAngleRange: 5.01 to 74.99	30.9387	12	48.7455	8
DivergenceSlit,Automatic,12	ScanStepSize: 0.02	32.5876	9	50.1092	14
ReceivingSlit: 0.20	ScanType,STEP	32.937	100	52.1923	23
Monochromator Used	ScanStepTime: 1.50	35.8998	30	52.7719	15
	ConvertedTo,AUTO	37.1859	10	53.7867	4
		37.7016	50		

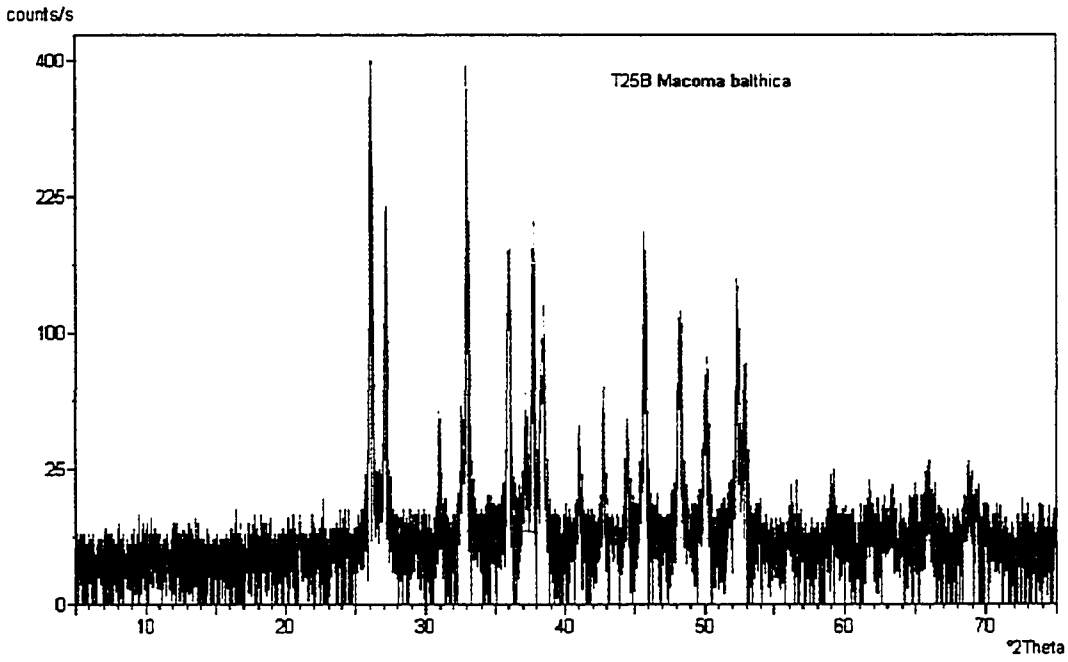

SampleIdent T25B *Macoma balthica*		2-Theta	Intensity	2-Theta	Intensity
Exported by X-Pert Software		9.5156	0	44.4872	12
Generated by Liz Rudolph: Project Shells		12.674	1	45.6951	36
DiffrType,PW3710		21.0289	1	45.8562	29
Anode,Cu	GeneratorVoltage: 40 Kv	26.1422	100	48.2912	27
LabdaAlpha1: 1.54056	TubeCurrent: 40 ma	27.1509	54	50.1136	19
LabdaAlpha2: 1.54439	FileDateTime: 4-Jul-01; 18:11	30.9752	12	52.2657	32
RatioAlpha21: 0.50000	DataAngleRange: 5.01 to 74.99	32.6592	10	52.8336	19
DivergenceSlit,Automatic,12	ScanStepSize: 0.02	32.9875	89	56.1814	2
ReceivingSlit: 0.20	ScanType,CONTINUOUS	36.0664	41	59.1147	3
Monochromator Used	ScanStepTime: 1.00	37.1918	14	61.7172	2
	ConvertedTo,AUTO	37.7677	45	63.3438	2
		38.5211	24	64.8207	2
		41.0419	8	65.9338	4
		42.7536	11	68.9038	4

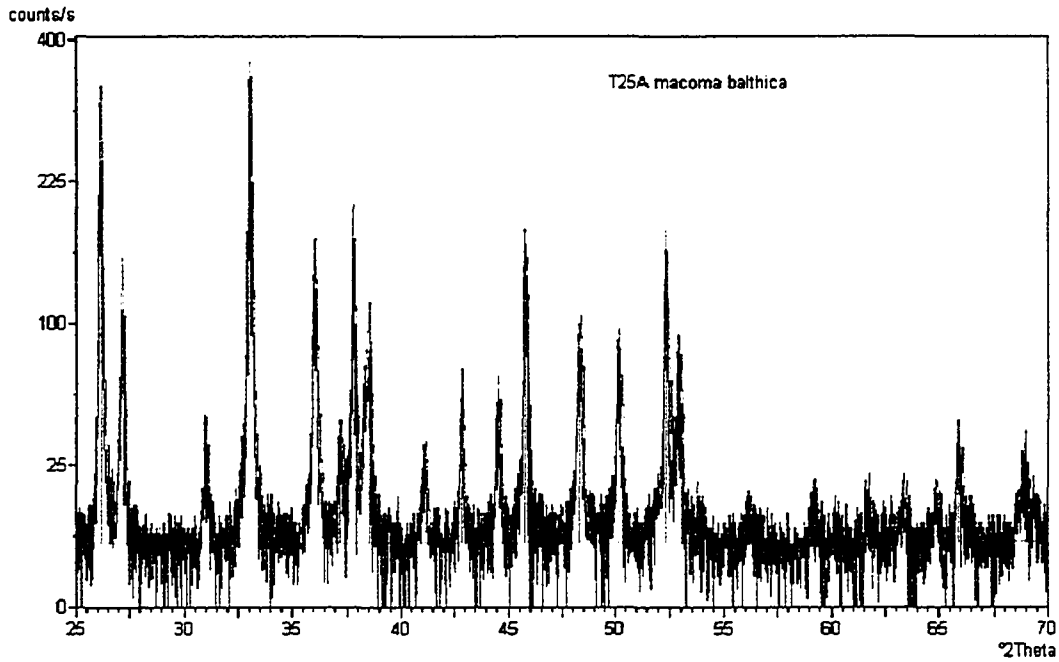

SampleIdent T25A *Macoma balthica*		2-Theta	Intensity	2-Theta	Intensity
Exported by X-Pert Software		26.1905	96	48.3249	27
Generated by Liz Rudolph: Project Shells		27.2371	39	50.1608	25
DiffrType,PW3710		30.9978	9	52.3487	53
		33.0521	100	52.9057	24
Anode,Cu	GeneratorVoltage: 40 Kv	36.051	49	56.2614	2
LabdaAlpha1: 1.54056	TubeCurrent: 40 ma	37.2373	10	59.2233	3
LabdaAlpha2: 1.54439	FileDateTime: 4-Jul-01; 16:38	37.8062	59	60.2057	1
RatioAlpha21: 0.50000	DataAngleRange: 25.01 to 69.99	38.5688	32	61.7179	3
DivergenceSlit,Automatic,12	ScanStepSize: 0.02	41.1484	8	63.3986	3
ReceivingSlit: 0.20	ScanType,CONTINUOUS	42.863	18	64.9646	3
Monochromator Used	ScanStepTime: 1.00	44.5046	17	65.9128	7
	ConvertedTo,AUTO	45.7654	51	68.9862	8
		45.9261	36		

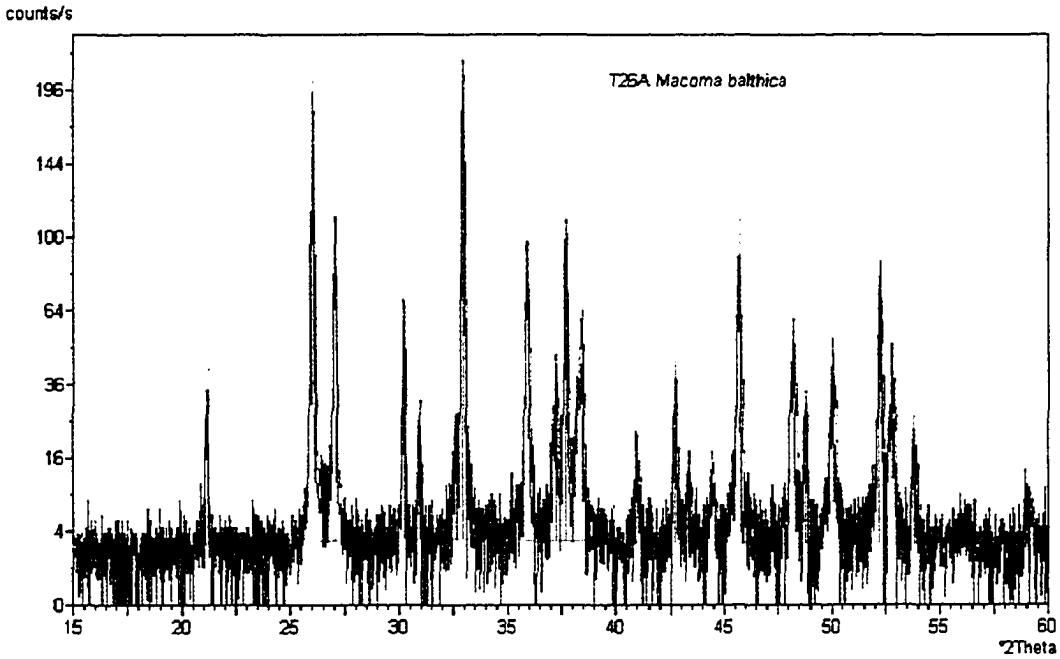

SampleIdent T26A *Macoma balthica*		2-Theta	Intensity	2-Theta	Intensity
Exported by X-Pert Software		21.185	19	40.9609	7
Generated by Liz Rudolph: Project Shells		24.2131	0	42.7198	20
DiffrType,PW3710		26.0308	99	43.3193	5
Anode,Cu	GeneratorVoltage: 40 Kv	27.0577	56	44.4704	6
LabdaAlpha1: 1.54056	TubeCurrent: 40 ma	30.2208	25	45.6871	52
LabdaAlpha2: 1.54439	FileDateTime: 4-Jul-01; 18:11	30.9248	13	48.1797	29
RatioAlpha21: 0.50000	DataAngleRange:15.01 to 60.00	32.5642	11	48.7752	15
DivergenceSlit,Automatic,12	ScanStepSize: 0.02	32.9373	100	50.004	21
ReceivingSlit: 0.20	ScanType,STEP	35.9282	43	52.1954	37
Monochromator Used	ScanStepTime: 1.50	37.0646	10	52.7758	18
	ConvertedTo,AUTO	37.2234	21	53.7985	12
		37.6599	51	56.1844	1
		38.4384	26	59.0288	3
		39.9241	2		

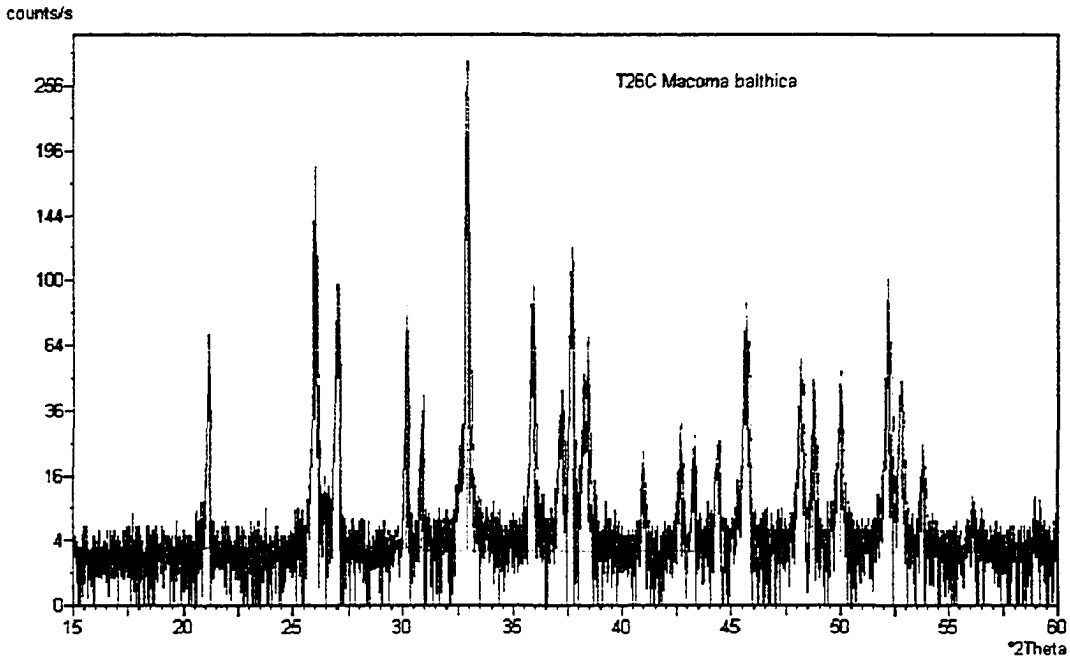

Sample Ident T26C *Macoma balthica*		2-Theta	Intensity	2-Theta	Intensity
Exported by X-Pert Software		15.1268	0	42.6563	10
Generated by Liz Rudolph: Project Shells		21.1694	26	43.3123	9
DiffrType,PW3710		25.9993	68	44.5094	6
Anode,Cu	GeneratorVoltage: 40 Kv	27.056	36	45.6118	31
LabdaAlpha1: 1.54056	TubeCurrent: 40 ma	30.1825	32	48.1528	19
LabdaAlpha2: 1.54439	FileDateTime: 4-Jul-01; 20:23	30.8827	9	48.7357	19
RatioAlpha21: 0.50000	DataAngleRange:15.01 to 60.00	32.9365	100	48.9011	6
DivergenceSlit,Automatic,12	ScanStepSize: 0.02	35.8677	39	50.0076	18
ReceivingSlit: 0.20	ScanType,STEP	37.24	17	52.1794	43
Monochromator Used	ScanStepTime: 1.50	37.686	39	52.7862	19
	ConvertedTo,AUTO	38.202	20	53.7425	9
		38.4237	22	56.1442	2
		38.7671	5	59.0014	2
		40.9977	6		

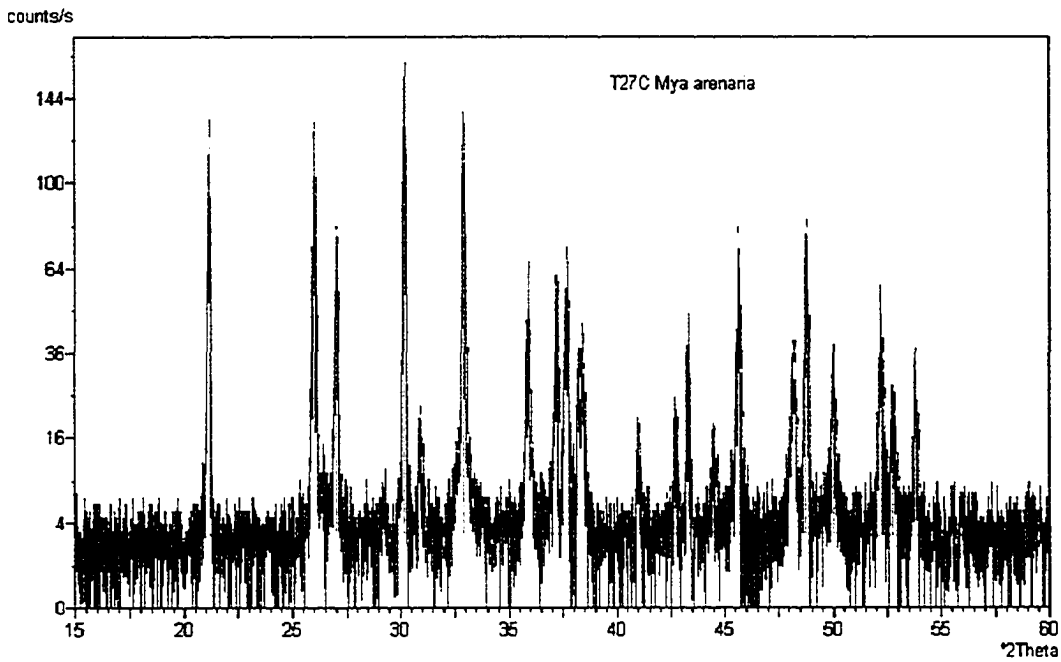

Sample Ident T27C *Mya arenaria*		2-Theta	Intensity	2-theta	Intensity
Exported by X-Pert Software		19.7384	1	42.6945	12
Generated by Liz Rudolph: Project Shells		21.189	76	43.3041	32
DiffrType,PW3710		26.0237	79	43.457	17
Anode,Cu	GeneratorVoltage: 40 Kv	27.0341	51	44.5252	12
LabdaAlpha1: 1.54056	TubeCurrent: 40 ma	29.2695	3	45.632	50
LabdaAlpha2: 1.54439	FileDateTime: 4-Jul-01; 20:38	30.1894	100	48.1765	23
RatioAlpha21: 0.50000	DataAngleRange:15.00 to 60.00	30.923	11	48.7482	45
DivergenceSlit,Automatic,12	ScanStepSize: 0.02	32.9174	89	48.9015	24
ReceivingSlit: 0.20	ScanType,STEP	35.9024	39	50.002	18
Monochromator Used	ScanStepTime: 1.50	37.2564	43	52.188	30
	ConvertedTo,AUTO	37.6809	42	52.7473	14
		38.4747	19	53.7636	23
		41.0278	9	56.2334	1

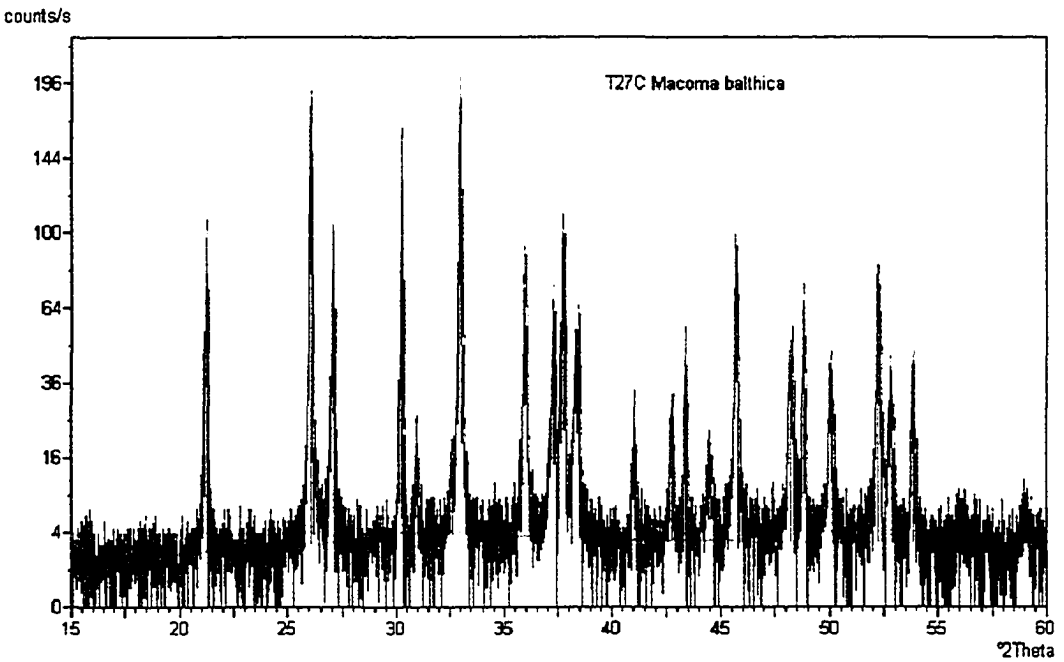

Sample Ident T27C *Macoma balthica*		2-Theta	Intensity	2-Theta	Intensity
Exported by X-Pert Software		15.5595	0	39.004	2
Generated by Liz Rudolph: Project Shells		17.6819	1	41.055	10
DiffrType,PW3710		18.6652	0	42.7968	14
Anode,Cu	GeneratorVoltage: 40 Kv	21.2657	47	43.3669	23
LabdaAlpha1: 1.54056	TubeCurrent: 40 ma	22.8241	1	44.547	7
LabdaAlpha2: 1.54439	FileDateTime: 4-Jul-01; 20:23	24.8041	2	45.6781	40
RatioAlpha21: 0.50000	DataAngleRange:15.00 to 60.00	26.0826	90	48.1991	21
DivergenceSlit,Automatic,12	ScanStepSize: 0.02	27.0792	57	48.8189	31
ReceivingSlit: 0.20	ScanType,STEP	30.2607	71	50.0714	19
Monochromator Used	ScanStepTime: 1.50	30.9612	10	52.2269	37
	ConvertedTo,AUTO	32.585	8	52.4147	20
		32.9713	100	52.8201	19
		35.9339	39	53.8489	21
		37.301	34	53.9926	10
		37.7084	47	56.1451	2
		38.4692	28	59.1196	2

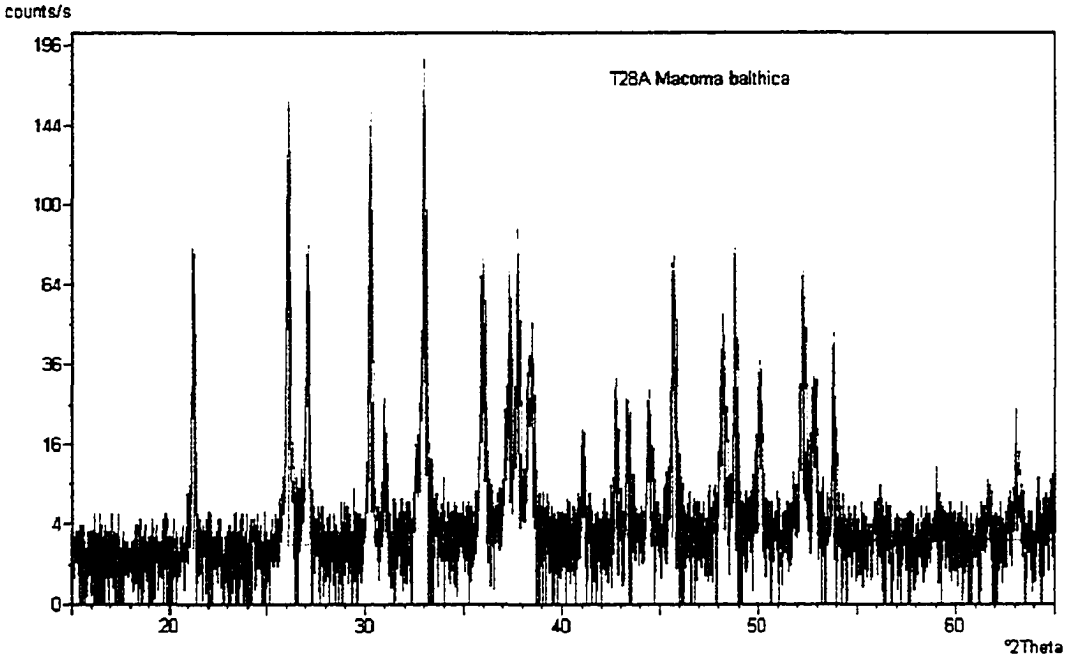

Sample Ident T28A *Macoma balthica*		**2-Theta**	**Intensity**	**2-Theta**	**Intensity**
Exported by X-Pert Software		15.2724	0	43.3646	12
Generated by Liz Rudolph: Project Shells		21.2408	40	44.4487	14
DiffrType,PW3710		23.3993	0	45.6678	39
Anode,Cu	GeneratorVoltage: 40 Kv	26.0852	94	45.8212	27
LabdaAlpha1: 1.54056	TubeCurrent: 40 ma	27.0908	46	48.2138	25
LabdaAlpha2: 1.54439	FileDateTime: 4-Jul-01; 20:44	30.2691	96	48.7896	46
RatioAlpha21: 0.50000	DataAngleRange:15.00 to 65.00	30.9407	12	48.9418	25
DivergenceSlit,Automatic,12	ScanStepSize: 0.02	32.6074	8	50.0475	19
ReceivingSlit: 0.20	ScanType,STEP	32.9468	100	51.0243	1
Monochromator Used	ScanStepTime: 2.0	35.9339	46	52.2558	43
	ConvertedTo,AUTO	37.3135	46	52.7891	19
		37.7059	45	53.828	26
		38.2592	19	56.0021	2
		38.4872	24	56.6577	2
		40.5981	2	59.0577	3
		41.0126	9	61.7052	2
		42.7261	15	63.045	9
				64.1718	2

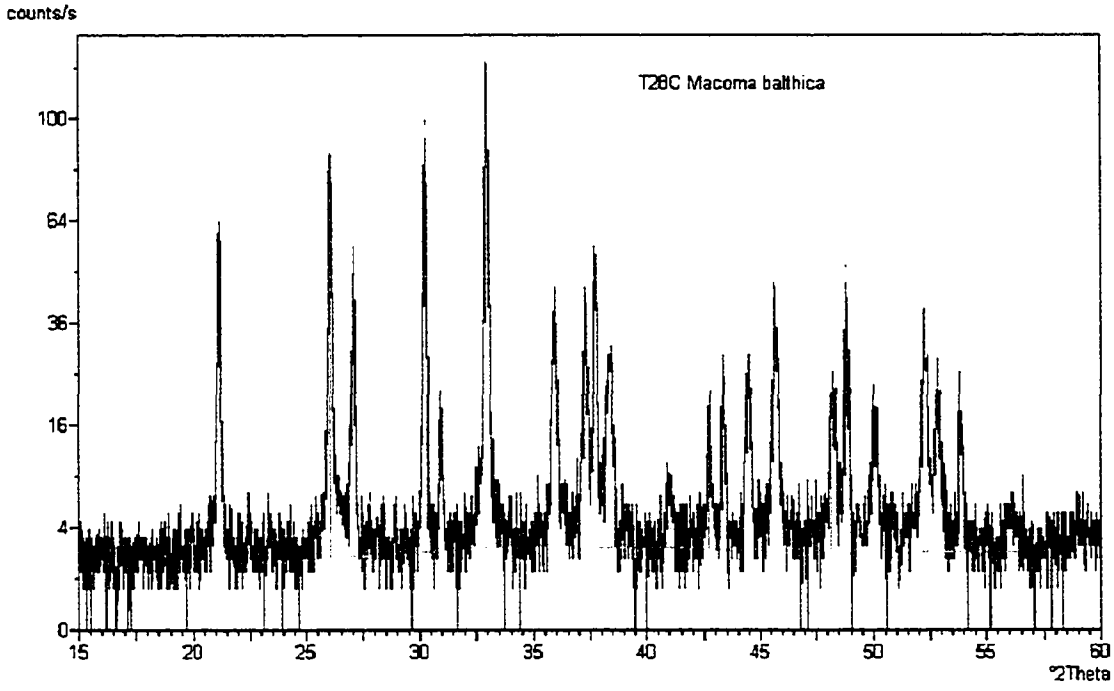

Sample Ident T28C *Macoma balthica*		2-Theta	Intensity	2-Theta	Intensity
Exported by X-Pert Software		15.052	0	42.72	13
Generated by Liz Rudolph: Project Shells		15.6279	0	43.3193	16
DiffrType,PW3710		21.2038	47	44.4698	18
		26.0219	74	45.6364	36
Anode,Cu	GeneratorVoltage: 40 Kv	27.0976	32	47.728	3
LabdaAlpha1: 1.54056	TubeCurrent: 40 ma	27.8492	4	48.1764	15
LabdaAlpha2: 1.54439	FileDateTime: 4-Jul-01; 21:01	30.2346	82	48.7791	41
RatioAlpha21: 0.50000	DataAngleRange:15.00 to 60.00	30.9298	14	50.0211	20
DivergenceSlit,Automatic,12	ScanStepSize: 0.02	32.94	100	52.2205	32
ReceivingSlit: 0.20	ScanType,STEP	35.9521	29	52.3748	26
Monochromator Used	ScanStepTime: 1.50	37.2913	35	52.7652	17
	ConvertedTo,AUTO	37.6751	38	53.7823	15
		38.4086	21	53.9432	10
		41.0112	5	56.0125	2

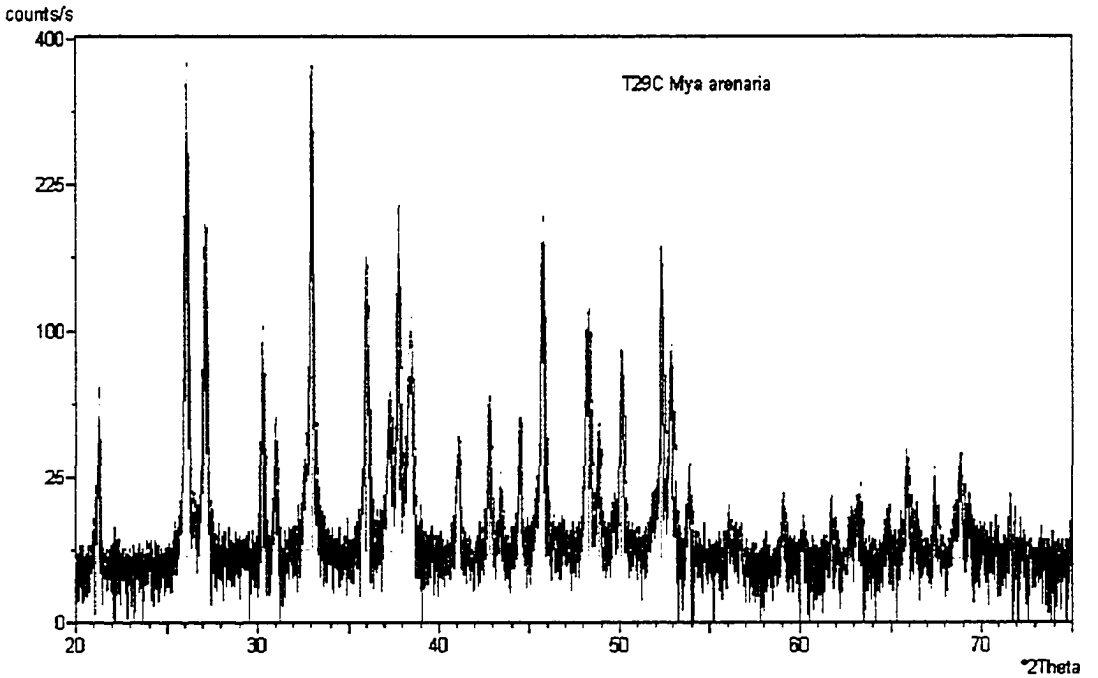

Sample Ident T29C *Mya arenaria*		2-Theta	Intensity	2-Theta	Intensity
Exported by X-Pert Software		21.3036	15	48.99	7
Generated by Liz Rudolph: Project Shells		26.1228	100	50.085	20
DiffrType,PW3710		27.1248	45	52.275	39
Anode,Cu	GeneratorVoltage: 40 Kv	30.297	26	52.89	24
LabdaAlpha1: 1.54056	TubeCurrent: 40 ma	30.9936	11	53.891	8
LabdaAlpha2: 1.54439	FileDateTime: 4-Jul-01; 21:01	32.6409	8	56.037	2
RatioAlpha21: 0.50000	DataAngleRange:20.01 to 74.99	33.0053	97	56.737	1
DivergenceSlit,Automatic,12	ScanStepSize: 0.02	35.9556	39	57.772	1
ReceivingSlit: 0.20	ScanType,CONTINUOUS	36.024	42	59.112	3
Monochromator Used	ScanStepTime: 2.0	37.3584	13	60.209	2
	ConvertedTo,AUTO	37.8022	55	61.695	3
		38.4959	29	62.715	2
		41.1193	9	63.263	3
		42.782	13	64.843	2
		43.4205	6	65.838	7
		44.412	12	67.446	6
		45.7333	51	68.825	8
		48.2439	29	70.132	1
		48.3512	27	71.645	4
		48.8572	11	72.319	1

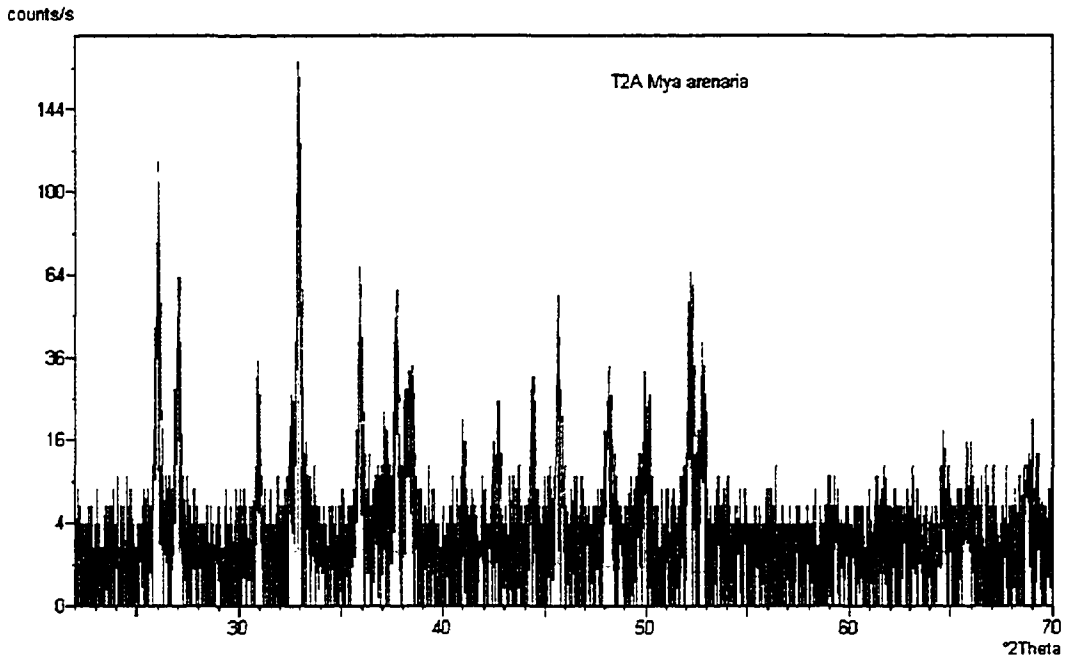

Sample Ident T2A *Mya arenaria*		2-Theta	Intensity	2-Theta	Intensity
Exported by X-Pert Software		26.0642	58	45.6896	27
Generated by Liz Rudolph: Project Shells		27.1214	21	48.2185	17
DiffrType,PW3710		30.929	14	49.756	6
Anode,Cu	GeneratorVoltage: 40 Kv	32.9126	100	49.9613	11
LabdaAlpha1: 1.54056	TubeCurrent: 40 ma	35.929	32	51.0066	2
LabdaAlpha2: 1.54439	FileDateTime: 4-Jul-01; 21:19	37.0984	11	52.2165	27
RatioAlpha21: 0.50000	DataAngleRange:22.00 to 70.00	37.689	28	52.8184	19
DivergenceSlit,Automatic,12	ScanStepSize: 0.02	38.443	18	54.0195	5
ReceivingSlit: 0.20	ScanType,CONTINUOUS	39.4536	1	56.0327	1
Monochromator Used	ScanStepTime: 0.50	41.0784	5	61.5574	2
	ConvertedTo,AUTO	42.7484	10	64.7713	3
		43.7132	3	65.8682	4
		44.4756	14		

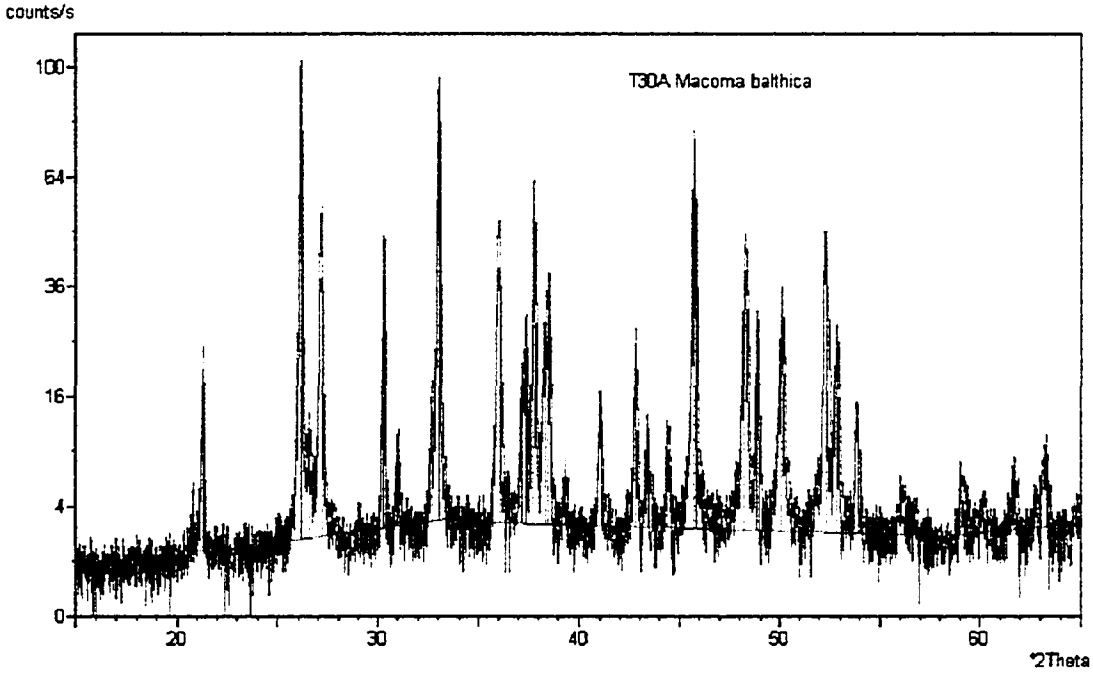

Sample Ident T30A *Macoma balthica*		2-Theta	Intensity	2-Theta	Intensity
Exported by X-Pert Software		20.8034	3	41.079	15
Generated by Liz Rudolph: Project Shells		21.3506	20	42.7895	21
DiffrType,PW3710		23.2225	0	43.423	10
Anode,Cu	GeneratorVoltage: 40 Kv	25.0401	1	44.4044	8
LabdaAlpha1: 1.54056	TubeCurrent: 40 ma	26.1443	100	45.731	75
LabdaAlpha2: 1.54439	FileDateTime: 4-Jul-01; 21:19	26.5635	10	45.8638	44
RatioAlpha21: 0.50000	DataAngleRange:22.00 to 70.00	27.1735	53	48.2224	43
DivergenceSlit,Automatic,12	ScanStepSize: 0.02	28.6243	1	48.8356	28
ReceivingSlit: 0.20	ScanType,CONTINUOUS	29.0462	1	50.0857	33
Monochromator Used	ScanStepTime: 0.50	30.3229	45	52.2948	49
	ConvertedTo,AUTO	30.9882	8	52.8652	26
		32.6928	13	53.8825	12
		33.0202	93	54.0309	7
		36.0657	45	56.031	4
		37.173	15	56.7231	2
		37.3588	27	59.0328	5
		37.7592	59	60.1617	2
		38.38	32	61.6726	6
		38.5011	39	62.699	3
		39.3158	7	63.259	7

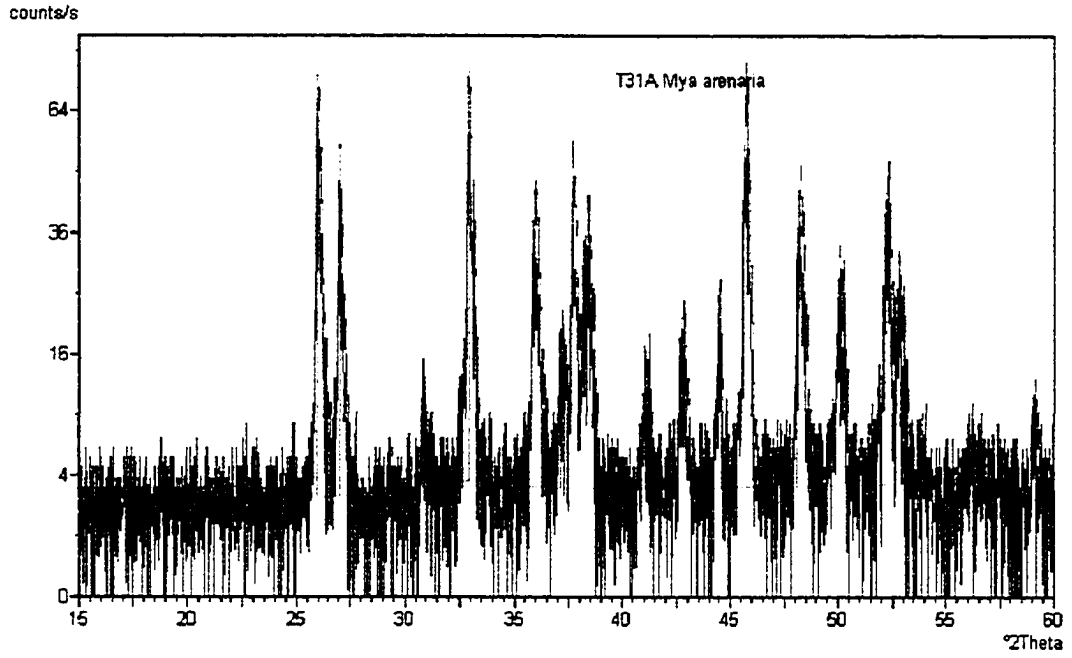

Sample Ident T31A *Mya arenaria*		2-Theta	Intensity	2-Theta	Intensity
Exported by X-Pert Software		24.8433	5	42.6878	27
Generated by Liz Rudolph: Project Shells		25.9785	98	44.488	29
DiffrType,PW3710		27.0151	72	45.6791	78
Anode,Cu	GeneratorVoltage: 40 Kv	30.8761	10	48.1084	47
LabdaAlpha1: 1.54056	TubeCurrent: 40 ma	32.9106	100	50.0627	32
LabdaAlpha2: 1.54439	FileDateTime: 4-Jul-01; 23:28	35.9403	54	52.1766	48
RatioAlpha21: 0.50000	DataAngleRange:15.00 to 60.00	37.1503	18	52.7965	37
DivergenceSlit,Automatic,12	ScanStepSize: 0.02	37.6651	65	56.1273	5
ReceivingSlit: 0.20	ScanType,STEP	38.4242	48	57.4578	4
Monochromator Used	ScanStepTime: 1.50	41.0658	12	59.0071	12
	ConvertedTo,AUTO				

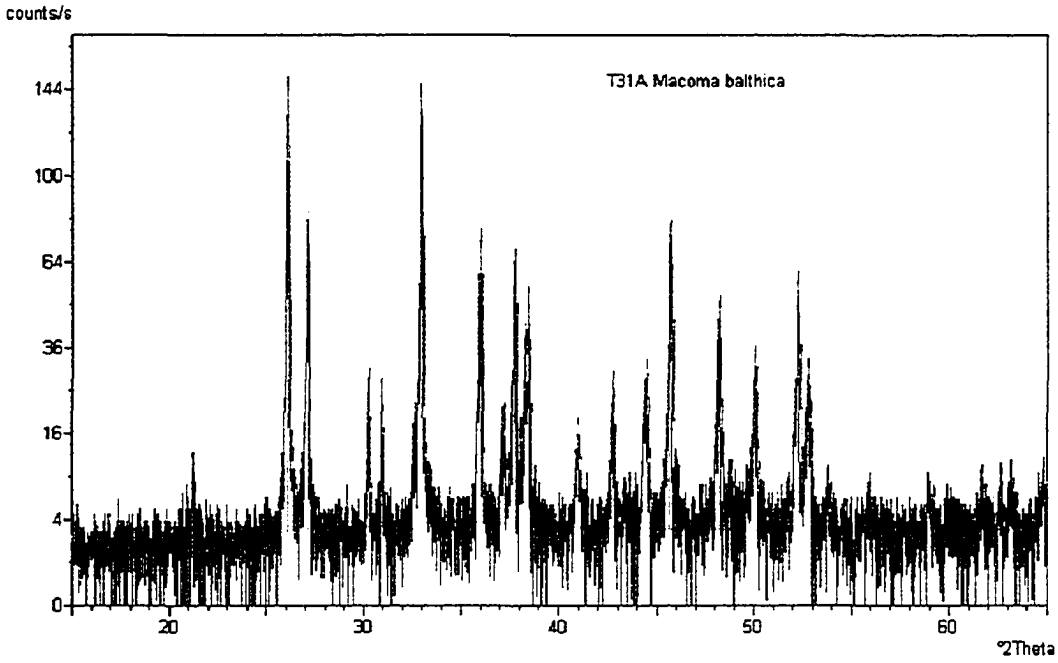

Sample Ident T31A *Macoma balthica*		2-Theta	Intensity	2-Theta	Intensity
Exported by X-Pert Software		21.2407	6	44.4923	17
Generated by Liz Rudolph: Project Shells		26.0801	86	45.6726	48
DiffrType,PW3710		27.101	55	47.2946	2
Anode,Cu	GeneratorVoltage: 40 Kv	30.2459	15	48.1629	24
LabdaAlpha1: 1.54056	TubeCurrent: 40 ma	30.9647	11	48.8383	4
LabdaAlpha2: 1.54439	FileDateTime: 5-Jul-01; 9:31	32.6244	11	50.013	18
RatioAlpha21: 0.50000	DataAngleRange:15.00 to 65.00	32.9608	100	52.2243	33
DivergenceSlit,Automatic,12	ScanStepSize: 0.02	35.9659	43	52.7742	18
ReceivingSlit: 0.20	ScanType,STEP	37.2064	10	53.846	3
Monochromator Used	ScanStepTime: 2.0	37.7329	45	56.2413	1
	ConvertedTo,AUTO	38.2574	22	59.0798	2
		38.489	22	61.6903	3
		41.015	8	63.2032	3
		41.7804	1		
		42.765	12		

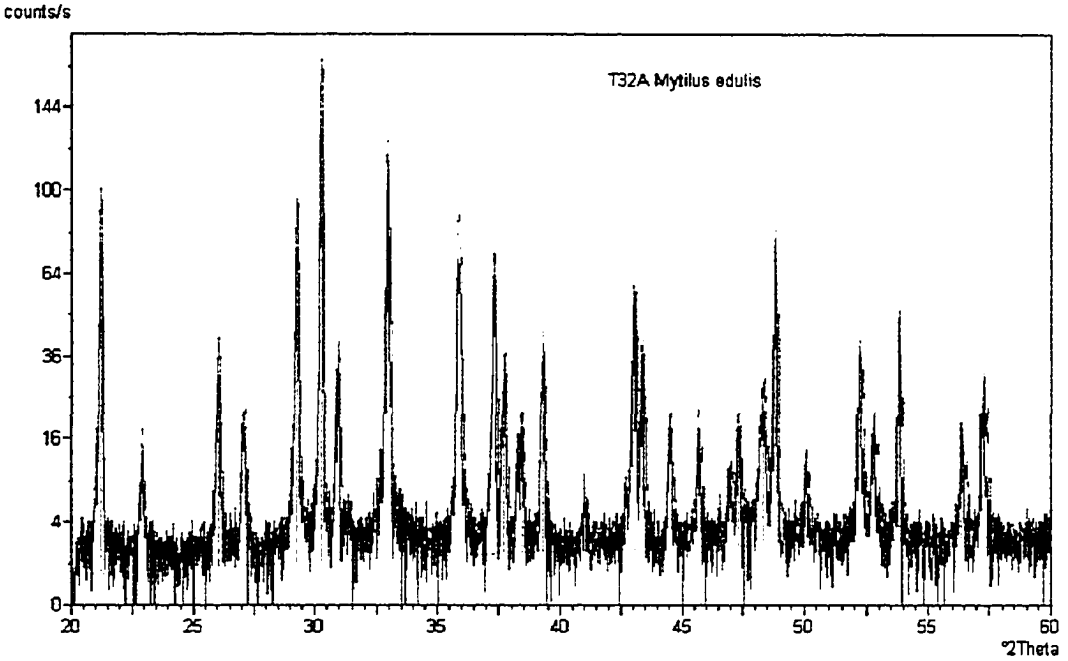

Sample Ident T32A *Mytilus edulis*					
Exported by X-Pert Software		**2-Theta**	**Intensity**	**2-Theta**	**Intensity**
Generated by Liz Rudolph: Project Shells		20.3632	1	43.3646	21
DiffrType,PW3710		21.2319	55	44.474	11
		22.9182	9	45.7005	11
Anode,Cu	GeneratorVoltage: 40 Kv	25.3291	1	46.9894	6
LabdaAlpha1: 1.54056	TubeCurrent: 40 ma	26.064	23	47.3651	9
LabdaAlpha2: 1.54439	FileDateTime: 5-Jul-01; 9:31	27.0988	11	48.3524	16
RatioAlpha21: 0.50000	DataAngleRange:20.01 to 59.99	29.2842	54	48.8063	44
DivergenceSlit,Automatic,12	ScanStepSize: 0.02	30.262	100	48.9614	23
ReceivingSlit: 0.20	ScanType,CONTINUOUS	30.9351	23	50.0325	7
Monochromator Used	ScanStepTime: 4.0	31.0058	19	52.2011	20
	ConvertedTo,AUTO	32.944	72	52.4122	11
		34.9701	1	52.8297	13
		35.8159	40	52.9904	8
		37.2798	36	53.814	27
		37.7033	20	54.0016	12
		38.4619	10	54.6901	1
		39.2947	25	56.3997	9
		41.028	3	57.2556	16
		43.0298	37		

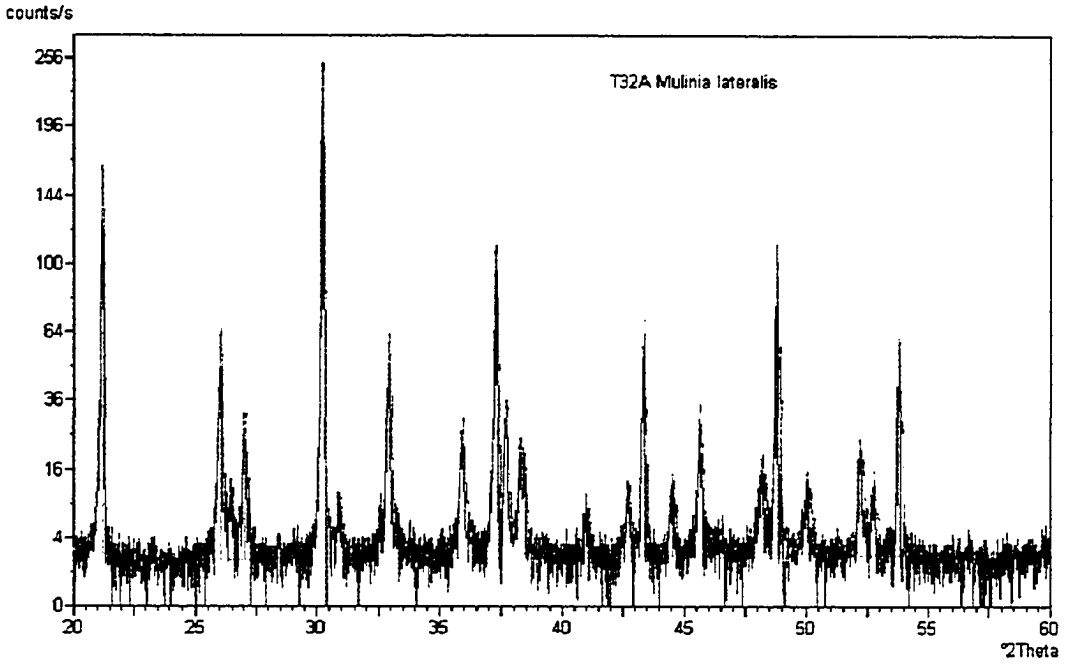

Sample Ident T32A *Mulinia lateralis*		2-Theta	Intensity	2-Theta	Intensity
Exported by X-Pert Software		20.3632	1	43.03	37
Generated by Liz Rudolph: Project Shells		21.2319	55	43.365	21
DiffrType,PW3710		22.9182	9	44.474	11
Anode,Cu	GeneratorVoltage: 40 Kv	25.3291	1	45.701	11
LabdaAlpha1: 1.54056	TubeCurrent: 40 ma	26.064	23	46.989	6
LabdaAlpha2: 1.54439	FileDateTime: 5-Jul-01; 9:31	27.0988	11	47.365	9
RatioAlpha21: 0.50000	DataAngleRange:20.01 to 59.99	29.2842	54	48.352	16
DivergenceSlit,Automatic,12	ScanStepSize: 0.02	30.262	100	48.806	44
ReceivingSlit: 0.20	ScanType,CONTINUOUS	30.9351	23	48.961	23
Monochromator Used	ScanStepTime: 4.0	31.0058	19	50.033	7
	ConvertedTo,AUTO	32.944	72	52.201	20
		34.9701	1	52.412	11
		35.8159	40	52.83	13
		37.2798	36	52.99	8
		37.7033	20	53.814	27
		38.4619	10	54.002	12
		39.2947	25	54.69	1
		41.028	3	56.4	9
				57.256	16

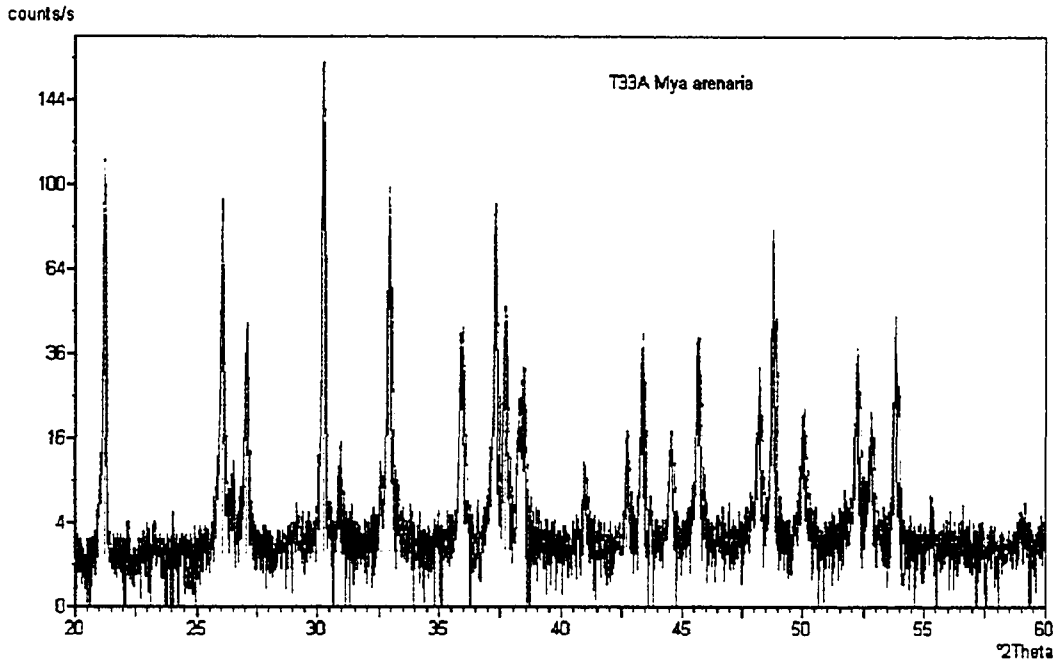

Sample Ident T33A *Mya arenaria*		2-Theta	Intensity	2-Theta	Intensity
Exported by X-Pert Software		21.2327	68	41.0057	5
Generated by Liz Rudolph: Project Shells		22.2039	1	42.7291	8
DiffrType,PW3710		23.2575	1	43.3466	23
Anode,Cu	GeneratorVoltage: 40 Kv	24.5745	1	43.4859	11
LabdaAlpha1: 1.54056	TubeCurrent: 40 ma	26.0447	47	44.5675	10
LabdaAlpha2: 1.54439	FileDateTime: 5-Jul-01; 10:16	26.5469	6	45.6864	26
RatioAlpha21: 0.50000	DataAngleRange:20.01 to 59.99	27.0758	28	48.2446	13
DivergenceSlit,Automatic,12	ScanStepSize: 0.02	29.201	2	48.8005	50
ReceivingSlit: 0.20	ScanType,CONTINUOUS	30.2384	100	48.9338	23
Monochromator Used	ScanStepTime: 4.0	30.9407	6	50.049	11
	ConvertedTo,AUTO	32.2028	1	52.2531	20
		32.9325	55	52.8254	12
		34.9548	2	53.8413	24
		35.9254	26	54.0022	13
		37.2757	52	55.2836	4
		37.6742	27	59.0658	1
		38.4255	19		

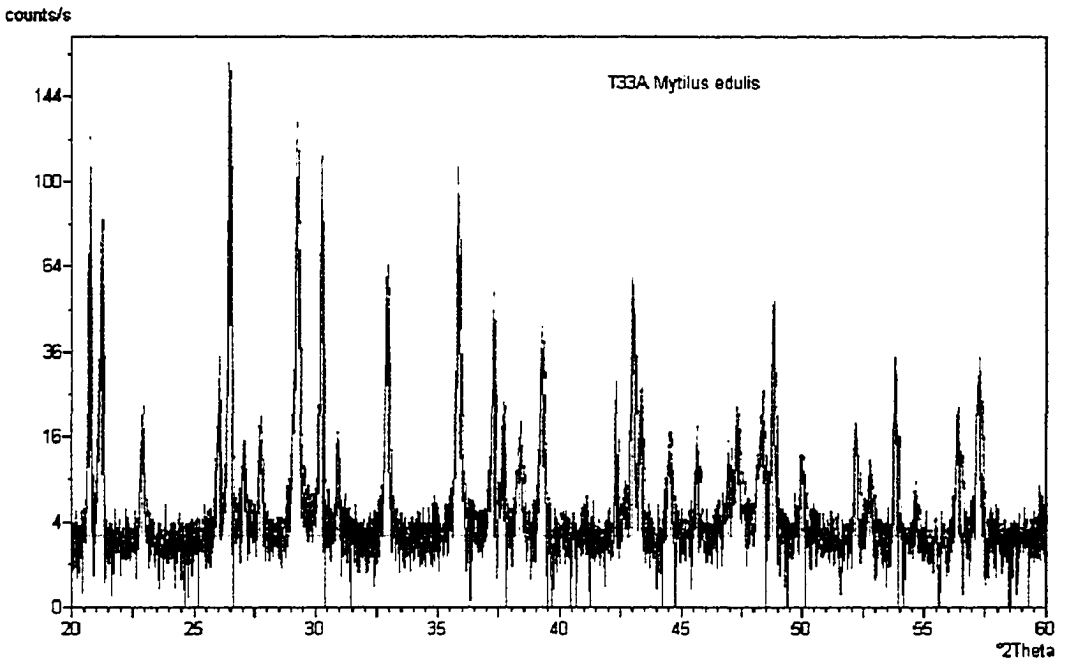

Sample Ident T33A *Mytilus edulis*					
Exported by X-Pert Software					
Generated by Liz Rudolph: Project Shells		20.7375	76	43.0081	37
DiffrType,PW3710		21.2337	52	43.3495	15
		22.8913	10	44.5714	8
Anode,Cu	GeneratorVoltage: 40 Kv	26.0722	16	45.6806	9
LabdaAlpha1: 1.54056	TubeCurrent: 40 ma	26.4655	100	46.9465	8
LabdaAlpha2: 1.54439	FileDateTime: 5-Jul-01; 10:23	27.0656	10	47.3287	12
RatioAlpha21: 0.50000	DataAngleRange:20.01 to 59.99	27.7471	9	48.369	14
DivergenceSlit,Automatic,12	ScanStepSize: 0.02	29.231	69	48.7797	29
ReceivingSlit: 0.20	ScanType,CONTINUOUS	30.2308	69	48.9307	19
Monochromator Used	ScanStepTime: 4.0	30.9126	9	50.0088	6
	ConvertedTo,AUTO	32.9376	37	52.1974	10
		35.8182	59	52.8083	5
		37.3055	32	53.8093	21
		37.6949	12	53.9714	11
		38.3843	8	54.6638	3
		39.2553	25	56.412	12
		40.2095	1	57.2529	22
		41.1483	2	57.4112	13
		42.3099	17		

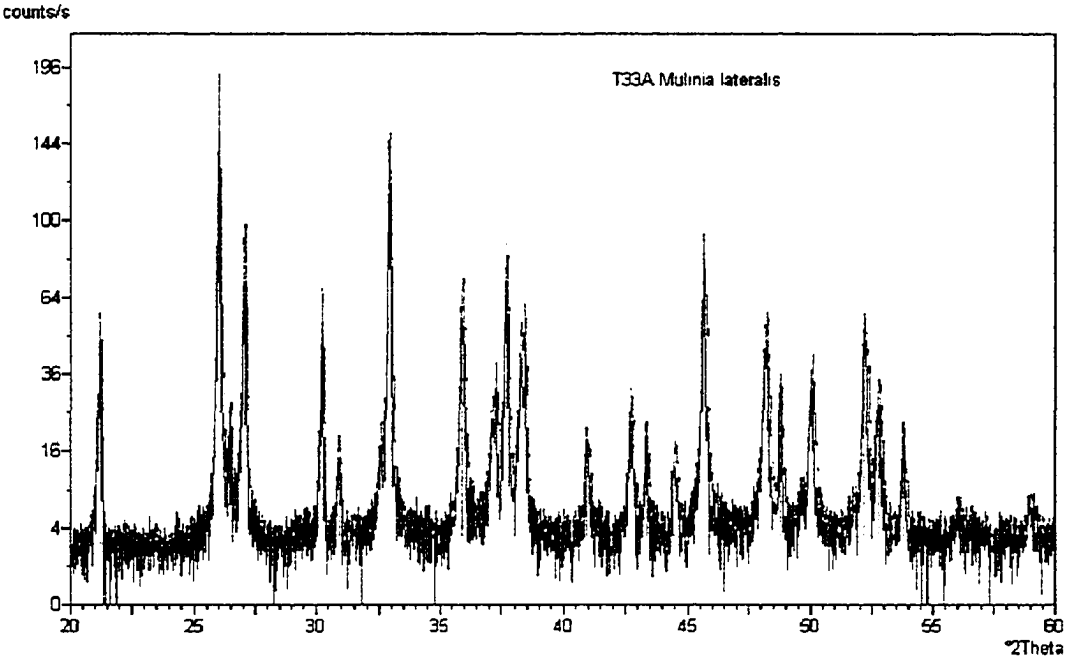

Sample Ident T33A *Mulinia lateralis*		2-Theta	Intensity	2-Theta	Intensity
Exported by X-Pert Software		21.1974	28	40.943	8
Generated by Liz Rudolph: Project Shells		26.0343	100	42.708	14
DiffrType,PW3710		26.4698	11	43.349	8
Anode,Cu	GeneratorVoltage: 40 Kv	27.0745	46	44.469	6
LabdaAlpha1: 1.54056	TubeCurrent: 40 ma	30.2232	32	45.665	46
LabdaAlpha2: 1.54439	FileDateTime: 5-Jul-01; 10:52	30.8966	6	48.23	23
RatioAlpha21: 0.50000	DataAngleRange:20.01 to 59.99	32.6041	10	48.767	15
DivergenceSlit,Automatic,12	ScanStepSize: 0.02	32.9372	72	50.048	18
ReceivingSlit: 0.20	ScanType,CONTINUOUS	35.8822	32	52.187	27
Monochromator Used	ScanStepTime: 4.0	35.9508	35	52.771	14
	ConvertedTo,AUTO	37.2868	18	52.976	8
		37.6857	43	53.798	8
		38.2526	22	56.059	2
		38.418	26	58.999	2

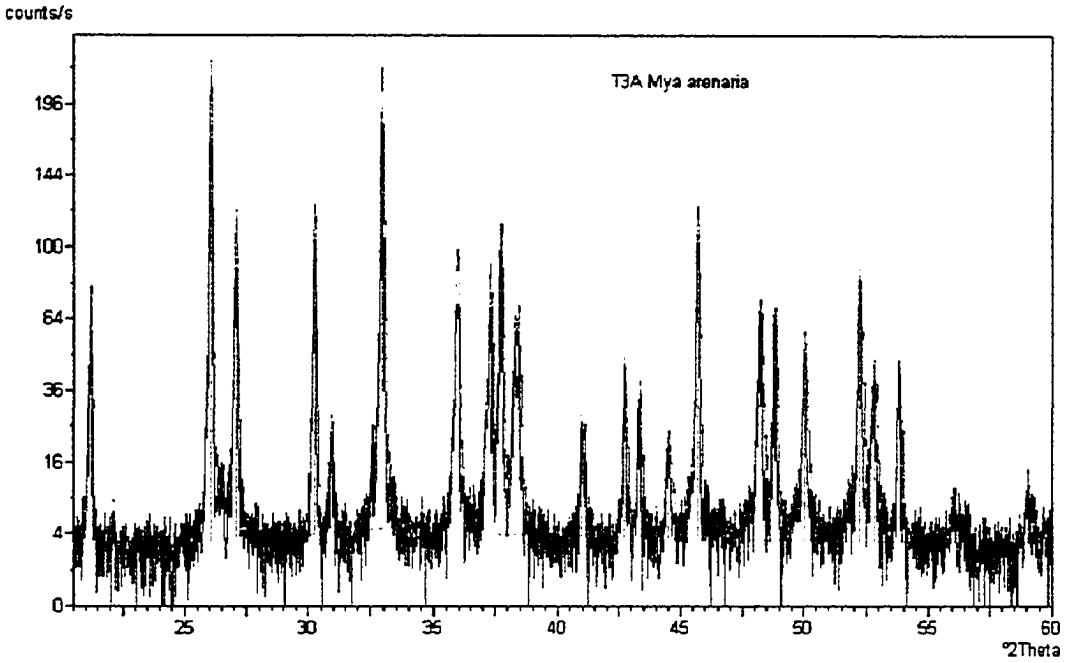

Sample Ident T3A *Mya arenaria*		2-Theta	Intensity	2-Theta	Intensity
Exported by X-Pert Software	**Peak fit**				
Generated by Liz Rudolph: Project Shells		21.2157	38	44.5551	8
DiffrType,PW3710		26.0668	100	45.7165	52
		27.0859	52	48.2055	27
Anode,Cu	GeneratorVoltage: 40 Kv	30.2561	58	48.3289	14
LabdaAlpha1: 1.54056	TubeCurrent: 40 ma	30.9619	11	48.8034	30
LabdaAlpha2: 1.54439	FileDateTime: 5-Jul-01; 10:59	32.5959	7	48.9409	15
RatioAlpha21: 0.50000	DataAngleRange:15.00 to 80.00	32.9742	93	50.0494	22
DivergenceSlit,Automatic,12	ScanStepSize: 0.02	35.9692	43	50.1925	10
ReceivingSlit: 0.20	ScanType,STEP	37.3014	35	51.814	3
Monochromator Used	ScanStepTime: 10.0	37.7376	49	52.2353	34
	ConvertedTo,AUTO	38.2904	18	52.372	17
		38.4542	24	52.828	18
		40.9926	9	53.833	18
		41.1166	8	53.99	8
		42.7628	17	59.0639	3
		43.3745	14		

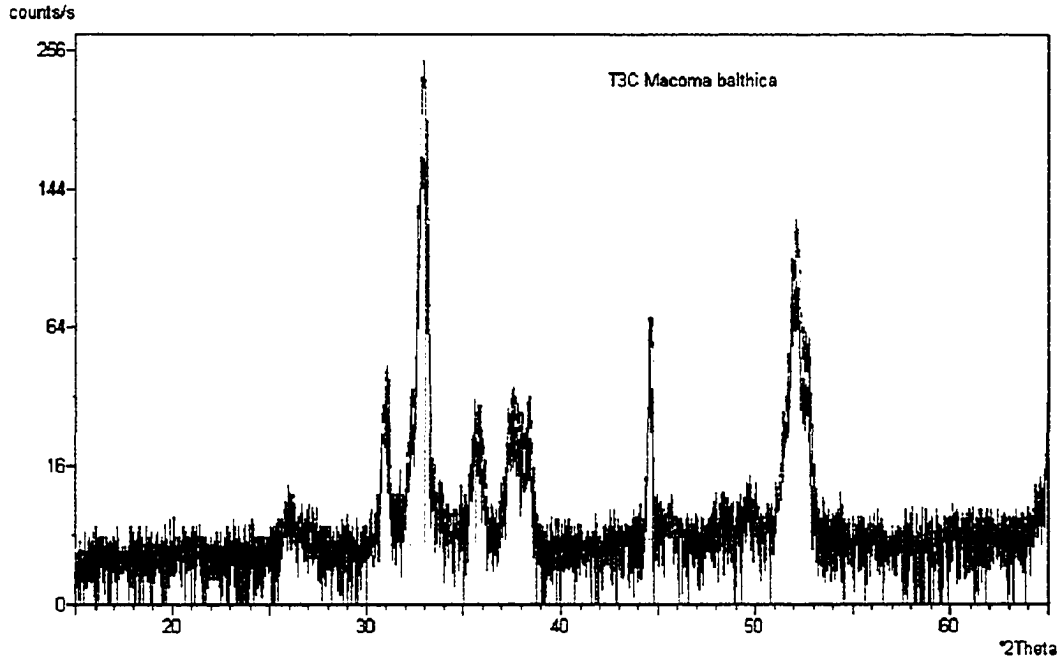

Sample Ident T3C *Macoma balthica*		2-Theta	Intensity	2-Theta	Intensity
Exported by X-Pert Software	**Peak fit**				
Generated by Liz Rudolph: Project Shells		21.2157	38	44.5551	8
DiffrType,PW3710		26.0668	100	45.7165	52
		27.0859	52	48.2055	27
Anode,Cu	GeneratorVoltage: 40 Kv	30.2561	58	48.3289	14
LabdaAlpha1: 1.54056	TubeCurrent: 40 ma	30.9619	11	48.8034	30
LabdaAlpha2: 1.54439	FileDateTime: 27-Jul-01; 16:23	32.5959	7	48.9409	15
RatioAlpha21: 0.50000	DataAngleRange:15.00 to 65.00	32.9742	93	50.0494	22
DivergenceSlit,Automatic,12	ScanStepSize: 0.02	35.9692	43	50.1925	10
ReceivingSlit: 0.20	ScanType,STEP	37.3014	35	51.814	3
Monochromator Used	ScanStepTime: 10.0	37.7376	49	52.2353	34
	ConvertedTo,AUTO	38.2904	18	52.372	17
		38.4542	24	52.828	18
		40.9926	9	53.833	18
		41.1166	8	53.99	8
		42.7628	17	59.0639	3
		43.3745	14		

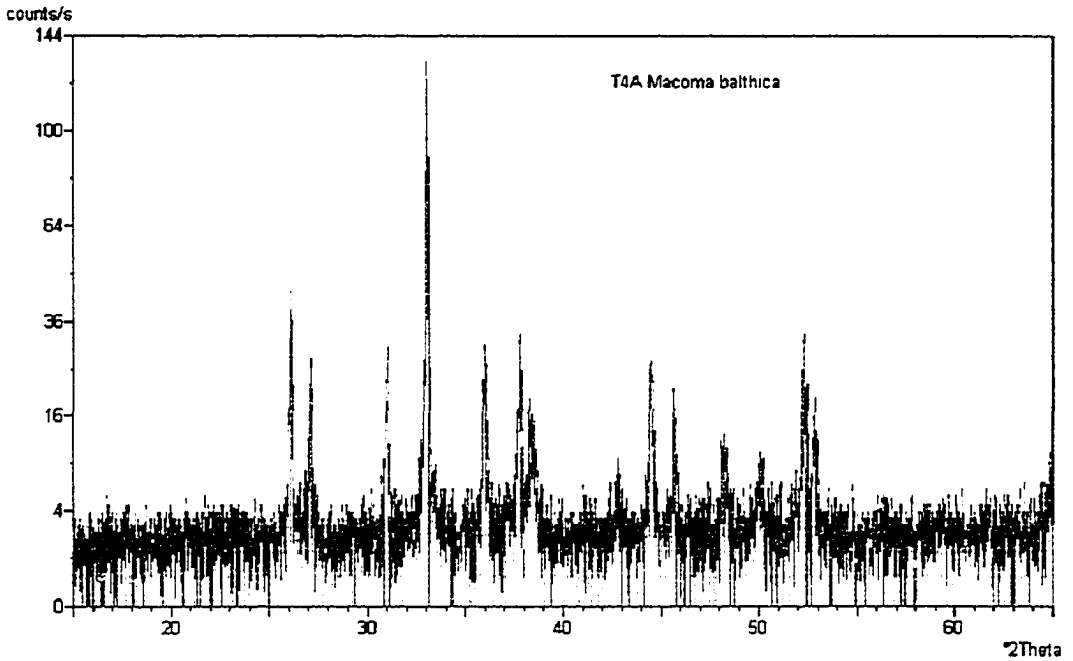

Sample Ident T4A *Macoma balthica*		2-Theta	Intensity	2-Theta	Intensity
Exported by X-Pert Software					
Generated by Liz Rudolph: Project Shells		18.1658	3	45.6978	9
DiffrType,PW3710		23.2546	3	48.1719	6
		26.0985	35	50.1049	6
Anode,Cu	GeneratorVoltage: 40 Kv	27.1074	16	52.2447	24
LabdaAlpha1: 1.54056	TubeCurrent: 40 ma	31.0401	20	52.8494	10
LabdaAlpha2: 1.54439	FileDateTime: 31, Augl-01; 16:23	32.9898	100	55.0057	4
RatioAlpha21: 0.50000	DataAngleRange:15.00 to 65.00	35.9823	25	56.291	1
DivergenceSlit,Automatic,12	ScanStepSize: 0.02	37.768	23	57.7985	2
ReceivingSlit: 0.20	ScanType,STEP	38.2649	11		
Monochromator Used	ScanStepTime: 10.0	38.4999	9		
	ConvertedTo,AUTO	41.1041	2		
		42.8068	4		
		44.4413	20		

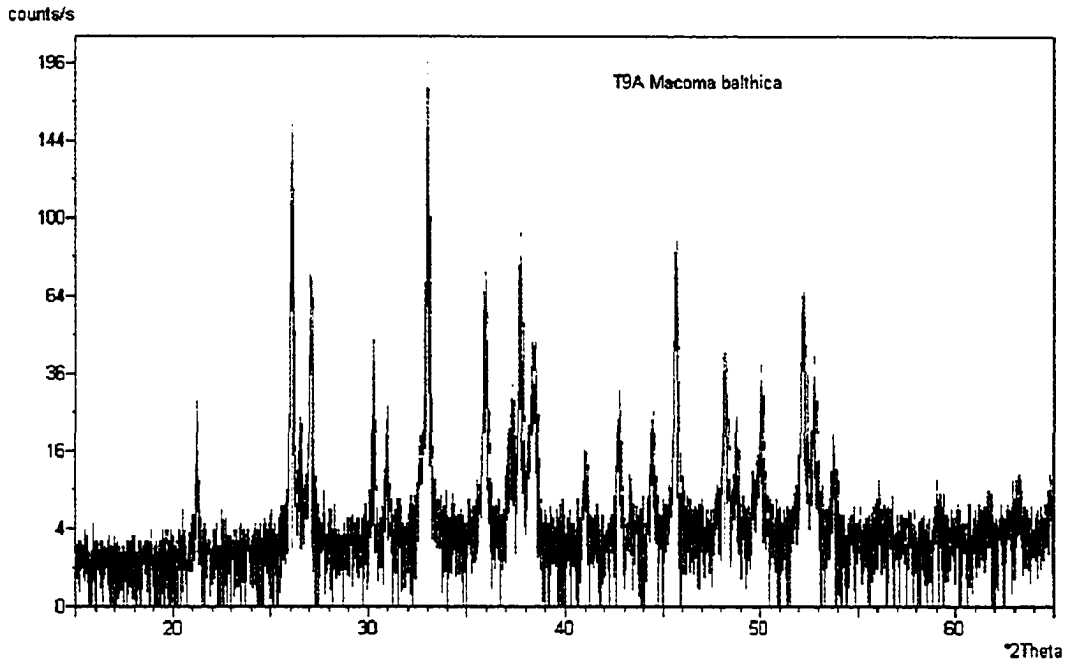

Sample Ident T9A *Macoma balthica*		2-Theta	Intensity	2-Theta	Intensity
Exported by X-Pert Software		21.2245	11	42.7326	11
Generated by Liz Rudolph: Project Shells		26.0927	78	43.3597	3
DiffrType,PW3710		26.5246	8	44.4483	10
		27.1373	36	45.6856	42
Anode,Cu	GeneratorVoltage: 40 Kv	27.7294	2	48.1617	20
LabdaAlpha1: 1.54056	TubeCurrent: 40 ma	30.2398	21	48.7757	10
LabdaAlpha2: 1.54439	FileDateTime: 31, Augl-12; 16:23	30.9843	7	50.0486	17
RatioAlpha21: 0.50000	DataAngleRange:15.00 to 65.00	32.9771	100	52.2449	37
DivergenceSlit,Automatic,12	ScanStepSize: 0.02	35.9083	33	52.8055	18
ReceivingSlit: 0.20	ScanType,STEP	37.3316	13	53.823	6
Monochromator Used	ScanStepTime: 10.0	37.709	43	56.1159	2
	ConvertedTo,AUTO	38.4847	20	59.0733	1
		41.1019	6	61.7192	2
		41.6502	1	63.2001	3

Appendix 2: Colorimetric Data Calibration for Lead

```
========== METROHM 757 VA COMPUTRACE (5.757.0010) ==========
Determ.     :  06131114_T34A_1.dth
Date        :  2000-06-13            Time:  11:14:08
Modified    :  ---                   User:              Cell volume: 11.000 ml
--------------------------------------------------------------------------------
 Ident                                                            Sample volume
 T34A_1                                                              10.000 ml
--------------------------------------------------------------------------------
Method  :  Det of Pb in sample with CalCrv.mth
Title   :  Pb determination with calibration curve
Remark1 :  10ml calibration solution + 1 ml acetate buffer pH 4.6 (1mol/l)
Remark2 :
--------------------------------------------------------------------------------
 Substance : Pb                                                  Comments
 Mass conc.:    9.178  ug/l                                      ----------
 MC.dev.   :    1.092  ug/l       (   11.90%)
 Mass      :  100.955  ng
 Add.mass  :  100.000  ng

            VR     V     nA      i.mean  Std.Dev. i.delta   Comments
            ----  -----  ------  ------  -------  -------   ----------
            1-1   -0.386  0.978  1.085   0.151
            1-2   -0.386  1.192
            2-1   -0.386  1.974  1.990   0.050    0.905
            2-2   -0.386  2.006
            3-1   -0.386  3.122  2.971   0.214    0.981
            3-2   -0.386  2.820
            4-1   -0.386  4.114  4.028   0.122    1.056
            4-2   -0.386  3.942
            5-1   -0.386  4.931  4.792   0.196    0.764
            5-2   -0.386  4.654


Substance    Calibr.    Y.reg/offset   Slope        Nonlin.      Mean deviat.
---------    --------   ------------   ----------   ----------   ------------
     Pb      std.add.     1.009e-009   1.106e-004                 7.411e-011

Solutions
--------------------------------------------------------------------------------

 No. Content                                          Vol. (ml) Predose (ml)
 --- ------------------------------------------------ --------- -------------


Final results                        +/- Res. dev.   %     Comments
-------------------------------      -------------------   ----------
       Pb =      10.096 ug/l         1.201       11.896
```

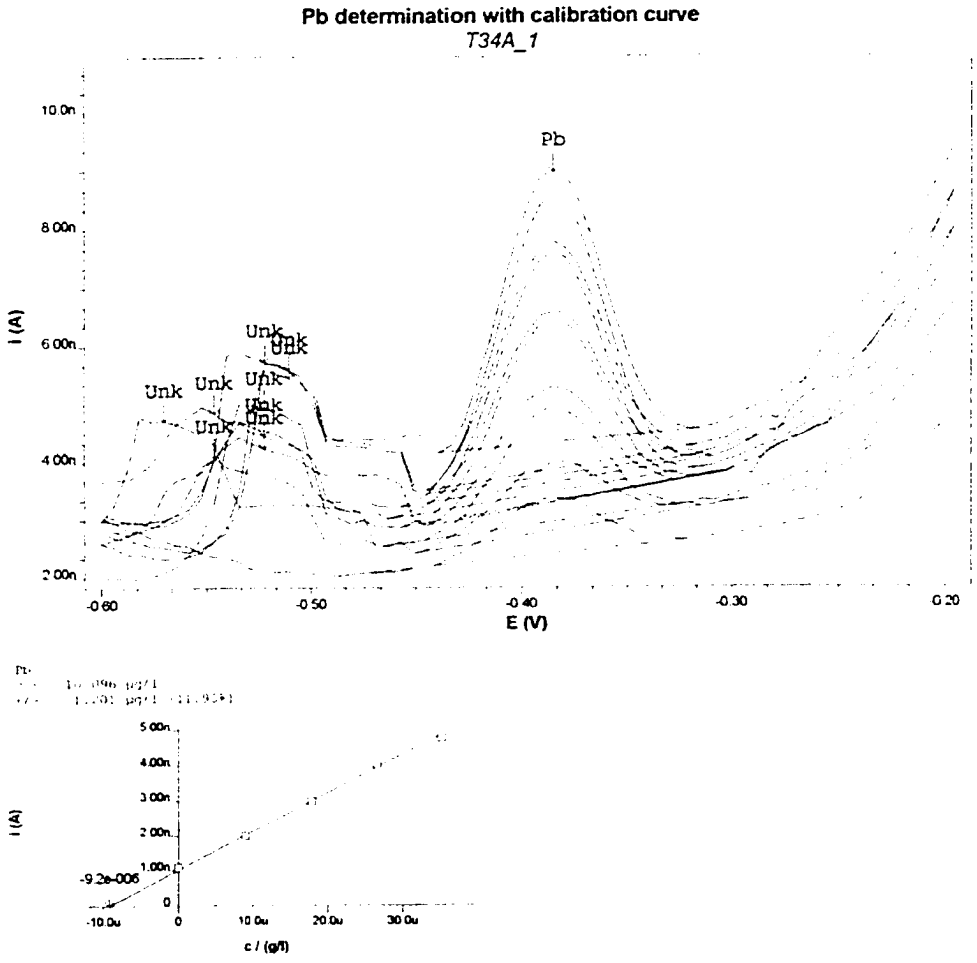

```
==================== METROHM 757 VA COMPUTRACE (5.757.0010) ====================
Determ.     :  06131212_T33A_1.dth
Date        :  2000-06-13          Time:  12:12:43
Modified    :  ---                 User:              Cell volume: 11.000 ml
--------------------------------------------------------------------------------
 Ident                                                              Sample volume
 T33A_1                                                                10.000 ml
--------------------------------------------------------------------------------
Method  :  Det of Pb in sample with CalCrv.mth
Title   :  Pb determination with calibration curve
Remark1 :  10ml calibration solution + 1 ml acetate buffer pH 4.6 (1mol/l)
Remark2 :
--------------------------------------------------------------------------------
 Substance : Pb                                                     Comments
 Mass conc.:   14.574  ug/l                                         ----------
 MC.dev.   :    0.855  ug/l       (    5.86%)
 Mass      :  160.319  ng
 Add.mass  :  100.000  ng

            VR     V     nA      i.mean  Std.Dev. i.delta   Comments
            ----  -----  ------  ------  -------  -------   ----------
            1-1   -0.392  1.573  1.549   0.050
            1-2   -0.392  1.525
            2-1   -0.392  2.700  2.463   0.336    0.914
            2-2   -0.386  2.225
            3-1   -0.386  3.421  3.453   0.050    0.990
            3-2   -0.386  3.484
            4-1   -0.386  4.383  4.329   0.076    0.877
            4-2   -0.386  4.276
            5-1   -0.386  5.685  5.512   0.244    1.183
            5-2   -0.386  5.340


Substance    Calibr.    Y.reg/offset   Slope        Nonlin.      Mean deviat.
---------    --------   ------------   ----------   ----------   ------------
      Pb     std.add.     1.547e-009   1.063e-004                 4.819e-011

Solutions
--------------------------------------------------------------------------------

 No. Content                                          Vol. (ml) Predose (ml)
 --- ------------------------------------------------ --------- -------------


Final results                        +/- Res. dev.   %     Comments
-------------------------------      ------------------    ----------
       Pb =      16.032 µg/l         0.940         5.864
```

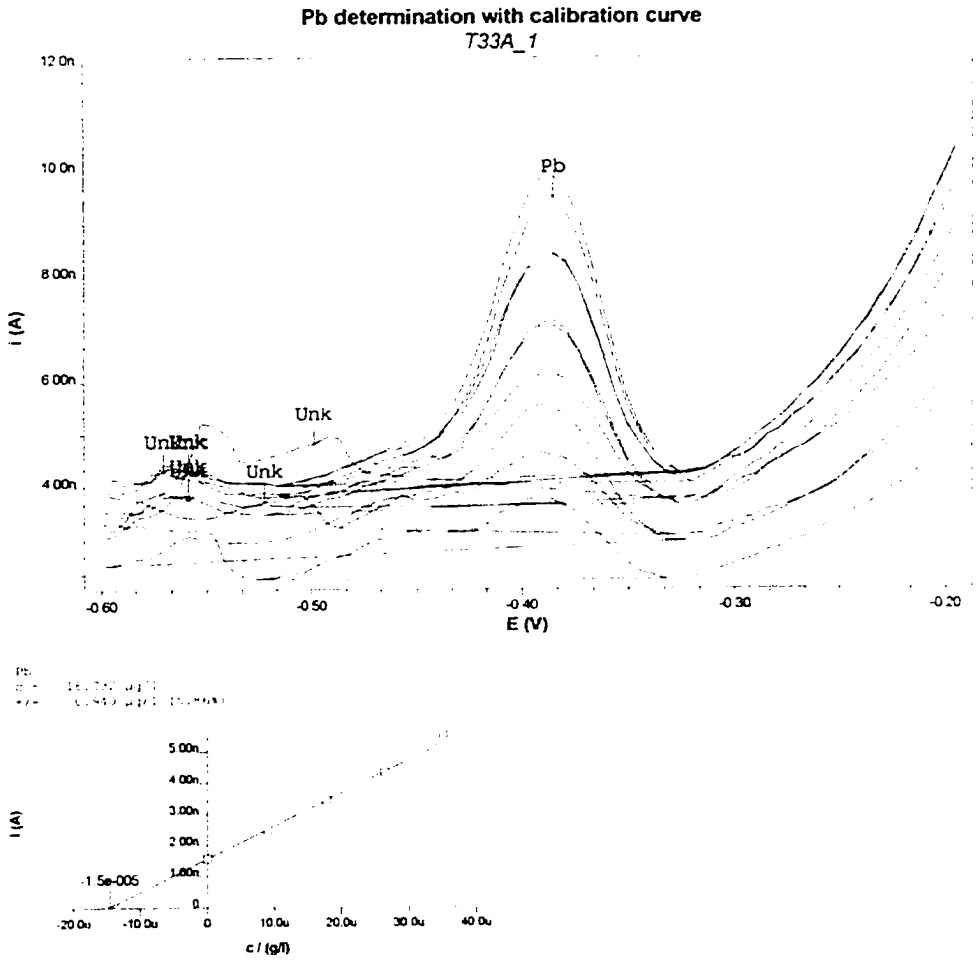

```
---------- METROHM 757 VA COMPUTRACE (5.757.0010) ----------
Determ.     : 06131141_T2C_1.dth
Date        : 2000-06-13          Time:  11:41:17
Modified    : ---                 User:              Cell volume: 11.000 ml
-------------------------------------------------------------------------------
 Ident                                                          Sample volume
 T2C_1                                                             10.000 ml
-------------------------------------------------------------------------------
Method  :  Det of Pb in sample with CalCrv.mth
Title   :  Pb determination with calibration curve
Remark1 :  10ml calibration solution + 1 ml acetate buffer pH 4.6 (1mol/l)
Remark2 :
-------------------------------------------------------------------------------
 Substance : Pb                                                 Comments
 Mass conc.:   12.216  ug/l                                     ----------
 MC.dev.   :    1.442  ug/l       (   11.80%)
 Mass      :  134.373  ng
 Add.mass  :  100.000  ng

            VP     V     nA      i.mean  Std.Dev.  i.delta   Comments
            ----  -----  ------  ------  -------  -------   ----------
            1-1   -0.392  1.182  1.290   0.153
            1-2   -0.392  1.398
            2-1   -0.392  2.315  2.338   0.050    1.048
            2-2   -0.386  2.361
            3-1   -0.392  3.329  3.303   0.050    0.965
            3-2   -0.392  3.277
            4-1   -0.392  4.181  3.890   0.417    0.587
            4-2   -0.386  3.599
            5-1   -0.392  5.579  5.318   0.369    1.428
            5-2   -0.386  5.057


Substance    Calibr.    Y.reg/offset   Slope        Nonlin.      Mean deviat.
---------    -------    ------------   ----------   ----------   ------------
      Pb     std.add.     1.337e-009   1.101e-004                 8.544e-011

Solutions
-------------------------------------------------------------------------------

 No. Content                                          Vol. (ml) Predose (ml)
 --- ---------------------------------------------- --------- --------------


Final results                      +/- Res. dev.   %     Comments
---------------------------------  --------------  ------  ----------
       Pb =      13.437 ug/l        1.586        11.803
```

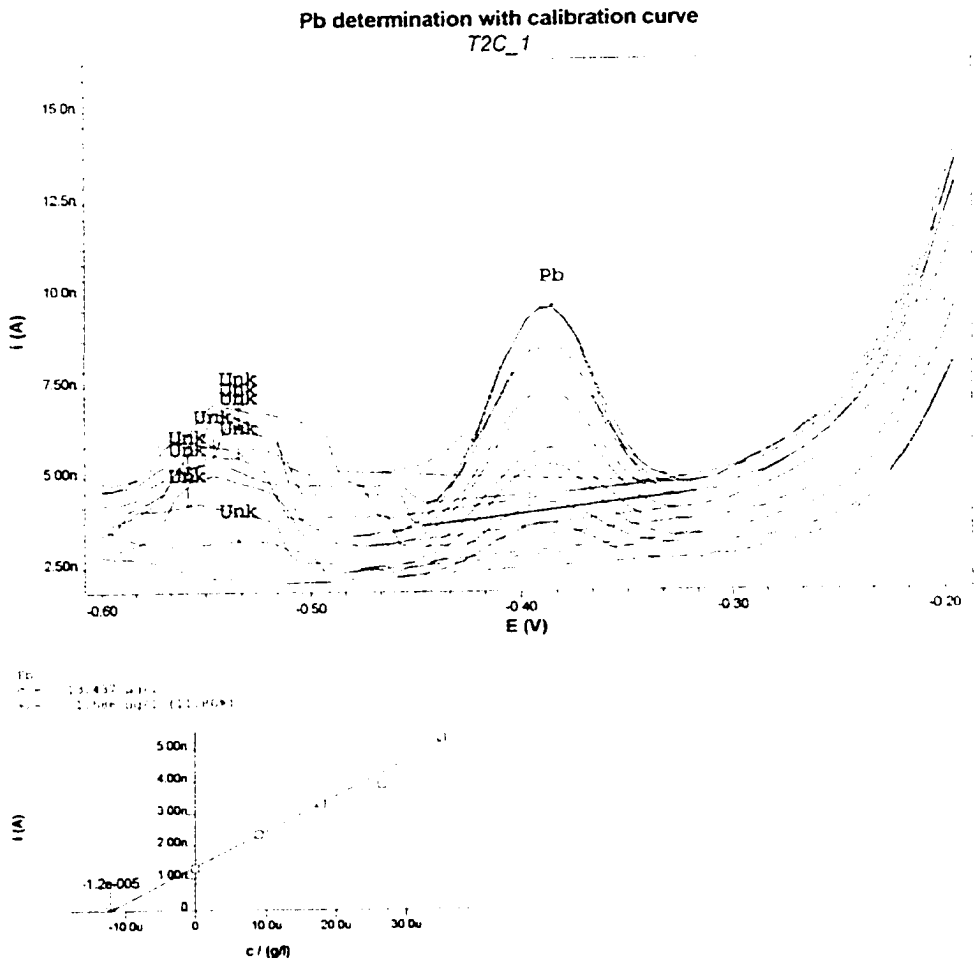

========== METROHM 757 VA COMPUTRACE (5.757.0010) ==========

Determ. : 06131051_T9D_5.dth
Date : 2000-06-13 Time: 10:51:37
Modified : --- User: Cell volume: 11.000 ml

Ident Sample volume
T9D_5 10.000 ml

Method : Det of Pb in sample with CalCrv.mth
Title : Pb determination with calibration curve
Remark1 : 10ml calibration solution + 1 ml acetate buffer pH 4.6 (1mol/l)
Remark2 :

Substance : Pb Comments
Mass conc.: 11.533 ug/l
MC.dev. : 1.019 ug/l (8.84%)
Mass : 126.867 ng
Add.mass : 100.000 ng

VR	V	nA	i.mean	Std.Dev.	i.delta	Comments
1-1	-0.392	1.163	1.202	0.056		
1-2	-0.392	1.242				
2-1	-0.392	2.040	2.002	0.053	0.800	
2-2	-0.392	1.965				
3-1	-0.386	3.072	2.998	0.104	0.996	
3-2	-0.392	2.925				
4-1	-0.392	4.458	4.174	0.402	1.175	
4-2	-0.386	3.890				
5-1	-0.392	4.965	4.806	0.225	0.632	
5-2	-0.392	4.647				

Substance	Calibr.	Y.req/offset	Slope	Nonlin.	Mean deviat.
Pb	std.add.	1.157e-009	1.008e-004		4.883e-011

Solutions

No.	Content	Vol. (ml)	Predose (ml)

Final results		+/- Res. dev.	%	Comments
Pb =	12.687 µg/l	1.121	8.836	

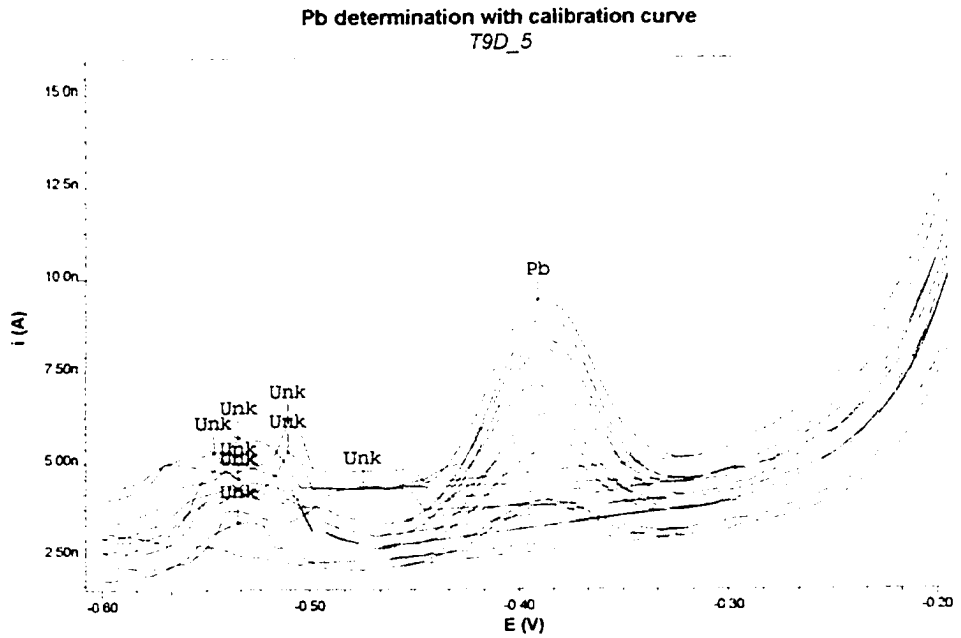

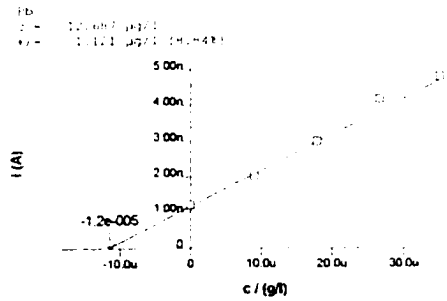

Listing for First SX100 User Tue May 12 21:57:02 1998 Page 1

point n : 7 x= -12378 y= 14854 z= 59
Rc-1 site1

Analysis no. 7 within misc512c

Elt.	Conc. (wt%)	Norm Conc. (wt%)	Norm Conc. (at%)	Compound	Concen. (wt%)
Na	0.4099	0.7037	0.8513	Na2O	0.553
K	0.0021	0.0036	0.0025	K2O	0.002
Si	0.0031	0.0053	0.0052	SiO2	0.007
Al	0.0000	0.0000	0.0000	Al2O3	
Mg	0.0120	0.0206	0.0236	MgO	0.020
Ca	40.4935	69.5226	48.2421	CaO	56.659
Fe	0.0406	0.0696	0.0347	FeO	0.052
Mn	0.0005	0.0009	0.0004	MnO	0.001
Ti	0.0124	0.0212	0.0123	TiO2	0.021
P	0.3745	0.6429	0.5773	P2O5	0.858
V	0.0000	0.0000	0.0000	V2O3	
Cr	0.0000	0.0000	0.0000	Cr2O3	
Ba	0.0000	0.0000	0.0000	BaO	

Camera Quantitative Analysis

point n . 1 x= -12368 y= 14854 z= 59
rel-ltip2

Analysis no 1 within misc512d

Elt.	Conc. (wt%)	Norm Conc. (wt%)	Norm Conc. (at%)	Compound	Concen. (wt%)
Na	0.3947	0.6579	0.7953	Na2O	0.532
K	0.0000	0.0000	0.0000	K2O	
Si	0.0204	0.0340	0.0337	SiO2	0.044
Al	0.0000	0.0000	0.0000	Al2O3	
Mg	0.0056	0.0094	0.0108	MgO	0.009
Ca	41.8363	69.6460	48.3543	CaO	58.537
Fe	0.0252	0.0420	0.0209	FeO	0.032
Mn	0.0000	0.0000	0.0000	MnO	
Ti	0.0000	0.0000	0.0000	TiO2	
P	0.3572	0.5947	0.5242	P2O5	0.819
V	0.0000	0.0000	0.0000	V2O3	
Cr	0.0000	0.0000	0.0000	Cr2O3	
Ba	0.0000	0.0000	0.0000	BaO	
Pb	0.0000	0.0000	0.0000	PbO	
La	0.0567	0.0944	0.0189	La2O3	0.067
Sm	0.0199	0.0332	0.0061	SmO	0.022
Yb	0.0070	0.0116	0.0019	Yb2O3	0.009
O	17.3468	28.8777	50.2259	by stoichiometry	
total	60.0700	100.0000	100.0000		60.070

be careful, strong correction for K (0.00)
be careful, strong correction for Al (0.00)
be careful, strong correction for Mn (0.00)
be careful, strong correction for Ti (0.00)
be careful, strong correction for V (0.00)
be careful, strong correction for Cr (0.00)
be careful, strong correction for Ba (0.00)
be careful, strong correction for Pb (0.00)

miscellaneo. cations on 2 <o,oh> basis

			Wt %	Cations
P2O5	0.8185	P	0.3572	0.0213
SiO2	0.0437	Si	0.0204	0.013
TiO2	0.0000	Ti	0.0000	0.0000
Al2O3	0.0000	Al	0.0000	0.0000
V2O3	0.0000	V	0.0000	0.0000
Cr2O3	0.0000	Cr	0.0000	0.0000
La2O3	0.0665	La	0.0567	0.0008
Yb2O3	0.0079	Yb	0.0070	0.0001
MgO	0.0094	Mg	0.0056	0.0004
CaO	58.5374	Ca	41.8363	1.9255
MnO	0.0000	Mn	0.0000	0.0000
FeO	0.0325	Fe	0.0252	0.0008
BaO	0.0000	Ba	0.0000	0.0000
SmO	0.0221	Sm	0.0199	0.0002
PbO	0.0000	Pb	0.0000	0.0000
Na2O	0.5320	Na	0.3947	0.0317
K2O	0.0000	K	0.0000	0.0000
H2O	19.5323			

point n° 2 x= -12724 y= 15239 z= 45
ref:thiphorth2

Analysis no. 2 within misc512d

Elt.	Conc. (wt%)	Norm Conc. (wt%)	Norm Conc. (at%)	Compound	Concen. (wt%)
Na	0.3635	0.6175	0.7476	Na2O	0.490
K	0.0010	0.0018	0.0013	K2O	0.001
Si	0.0165	0.0280	0.0277	SiO2	0.035
Al	0.0000	0.0000	0.0000	Al2O3	
Mg	0.0106	0.0180	0.0206	MgO	0.018
Ca	41.0163	69.6725	48.3762	CaO	57.390
Fe	0.0085	0.0145	0.0072	FeO	0.011
Mn	0.0000	0.0000	0.0000	MnO	
Ti	0.0015	0.0026	0.0014	TiO2	0.002
P	0.3556	0.6041	0.5428	P2O5	0.815
V	0.0111	0.0188	0.0103	V2O3	0.016
Cr	0.0006	0.0011	0.0006	Cr2O3	0.001
Ba	0.0071	0.0121	0.0025	BaO	0.008
Pb	0.0000	0.0000	0.0000	PbO	
La	0.0087	0.0148	0.0030	La2O3	0.010
Sm	0.0309	0.0525	0.0097	SmO	0.034
Yb	0.0335	0.0568	0.0091	Yb2O3	0.038
O	17.0646	28.8859	53.2402	by stoichiometry	
total :	58.8701	100.0000	100.0000		58.870

be careful, strong correction for Al (0.00)
be careful, strong correction for Mn (0.00)
be careful, strong correction for Pb (0.00)

miscellaneo. cations on 2. <illegible> basis

			wt %	Cations
P2O5	0.8149	P	0.3556	0.0214
SiO2	0.0352	Si	0.0165	0.0011
TiO2	0.0024	Ti	0.0015	0.0001
Al2O3	0.0000	Al	0.0000	0.0000
V2O3	0.0163	V	0.0111	0.0004
Cr2O3	0.0009	Cr	0.0006	0.0000
La2O3	0.0102	La	0.0087	0.0001
Yb2O3	0.0381	Yb	0.0335	0.0004
MgO	0.0175	Mg	0.0106	0.0004
CaO	57.3900	Ca	41.0163	1.9258
MnO	0.0000	Mn	0.0000	0.0000
FeO	0.0110	Fe	0.0085	0.0003
BaO	0.0080	Ba	0.0071	0.0001
SmO	0.0342	Sm	0.0309	0.0004
PbO	0.0000	Pb	0.0000	0.0000
Na2O	0.4900	Na	0.3635	0.0298
K2O	0.0012	K	0.0010	0.0000
H2O	19.1470			

point n : 3 x: -12451 y: 16383 z: 57
rel-1 3north of 2

Analysis no. 3 within misc512d

Elt.	Conc. (wt%)	Norm Conc. (wt%)	Norm Conc. (at%)	Compound	Concen. (wt%)
Na	0.2704	0.5673	0.6876	Na2O	0.364
K	0.0073	0.0152	0.0108	K2O	0.009
Si	0.0082	0.0172	0.0171	SiO2	0.019
Al	0.0000	0.0000	0.0000	Al2O3	
Mg	0.0011	0.0022	0.0025	MgO	0.002
Ca	33.2170	69.6473	48.4582	CaO	46.477
Fe	0.0000	0.0000	0.0000	FeO	
Mn	0.0111	0.0234	0.0118	MnO	0.014
Ti	0.0080	0.0168	0.0098	TiO2	0.013
P	0.2779	0.5831	0.5246	P2O5	0.637
V	0.0000	0.0000	0.0000	V2O3	
Cr	0.0000	0.0000	0.0000	Cr2O3	
Ba	0.0055	0.0116	0.0024	BaO	0.006
Pb	0.0074	0.0156	0.0021	PbO	0.008
La	0.0000	0.0000	0.0000	La2O3	
Sm	0.0106	0.0223	0.0041	SmO	0.012
Yb	0.0868	0.1821	0.0293	Yb2O3	0.099
O	13.7477	28.8459	50.2396	by stoichiometry	
total :	47.6589	100.0000	100.0000		47.659

be careful, strong correction for Al (0.00)
be careful, strong correction for Fe (0.00)
be careful, strong correction for V (0.00)
be careful, strong correction for Cr (0.00)
be careful, strong correction for La (0.00)

miscellaneo. cations on 2. so,obs basis

			Wt.%	Cations
P2O5	0.6368	P	0.2779	0.0209
SiO2	0.0175	Si	0.0082	0.0007
TiO2	0.0134	Ti	0.0080	0.0004
Al2O3	0.0000	Al	0.0000	0.0000
V2O3	0.0000	V	0.0000	0.0000
Cr2O3	0.0000	Cr	0.0000	0.0000
La2O3	0.0000	La	0.0000	0.0000
Yb2O3	0.0988	Yb	0.0868	0.0012
MgO	0.0018	Mg	0.0011	0.0001
CaO	46.4772	Ca	33.2170	1.9291
MnO	0.0144	Mn	0.0111	0.0005
FeO	0.0000	Fe	0.0000	0.0000
BaO	0.0062	Ba	0.0055	0.0001
SmO	0.0118	Sm	0.0106	0.0002
PbO	0.0080	Pb	0.0074	0.0001
Na2O	0.3644	Na	0.2704	0.0274
K2O	0.0087	K	0.0073	0.0004
H2O	15.4797			

point n : 4 x= -17900 y= 22633 z= 79
rel-1 4north of 3

Analysis no. 4 within misc512d

Elt	Conc. (wt%)	Norm Conc. (wt%)	Norm Conc. (at%)	Compound	Concen. (wt%)
Na	0.3783	0.6418	0.7771	Na2O	0.510
K	0.0145	0.0246	0.0175	K2O	0.017
Si	0.0149	0.0253	0.0251	SiO2	0.032
Al	0.0000	0.0000	0.0000	Al2O3	
Mg	0.0000	0.0000	0.0000	MgO	
Ca	41.0861	69.7097	48.4138	CaO	57.488
Fe	0.0000	0.0000	0.0000	FeO	
Mn	0.0000	0.0000	0.0000	MnO	
Ti	0.0000	0.0000	0.0000	TiO2	
P	0.3384	0.5741	0.5160	P2O5	0.775
V	0.0076	0.0129	0.0070	V2O3	0.011
Cr	0.0133	0.0226	0.0121	Cr2O3	0.019
Ba	0.0208	0.0353	0.0072	BaO	0.023
Pb	0.0000	0.0000	0.0000	PbO	
La	0.0000	0.0000	0.0000	La2O3	
Sm	0.0110	0.0186	0.0034	SmO	0.012
Yb	0.0444	0.0753	0.0121	Yb2O3	0.051
O	17.0096	28.8598	50.2067	by stoichiometry	
total :	58.9389	100.0000	100.0000		58.934

be careful, strong correction for Al (0.00)
be careful, strong correction for Mg (0.00)
be careful, strong correction for Fe (0.00)
be careful, strong correction for Mn (0.00)
be careful, strong correction for Ti (0.00)
be careful, strong correction for Pb (0.00)
be careful, strong correction for La (0.00)

miscellaneo. cations on 2. <e,oh> basis

			Wt.%	Cations
P2O5	0.7754	P	0.3384	0.0206
SiO2	0.0319	Si	0.0149	0.0010
TiO2	0.0000	Ti	0.0000	00000
Al2O3	0.0000	Al	0.0000	0.0000
V2O3	0.0112	V	0.0076	0.0003
Cr2O3	0.0195	Cr	0.0133	0.0005
La2O3	0.0000	La	0.0000	0.0000
Yb2O3	0.0505	Yb	0.0444	0.0005
MgO	0.0000	Mg	0.0000	0.0000
CaO	57.4877	Ca	41.0861	1.9285
MnO	0.0000	Mn	0.0000	0.0000
FeO	0.0000	Fe	0.0000	0.0000
BaO	0.0232	Ba	0.0208	0.0003
SmO	0.0121	Sm	0.0110	0.0001
PbO	0.0000	Pb	0.0000	0.0000
Na2O	0.5099	Na	0.3783	0.0310
K2O	0.0175	K	0.0145	0.0007
H2O	19.1526			

Appendix 4: Species Data Sheets

Phylum: Mollucsca
class: Bivalvia
Order: Myoida
Family: Myidae
Genus: Mya
Species: arenaria

Vital Statistics:
* Most important factor in growth and reproduction of soft shells is temperature. Uptake of amino acids increased with increasing temperature
* Salinity is the major environmental factor controlling infaunal species distribution can withstand varying salinities from 10ppt to 25 ppt
* Tolerance of drop in salinity to 4ppt in a few minutes
* Low Salinity and high T fatal
* Sediment of preference high sand to silt ratio with low organic content
* Predators: Urosalpiin unirea, Eupleura caudata, crabs, flatworms, Whelk
* Deep burrowers long siphons
* Feed on detritus and plankton bacteria and microzooplankton

T: 15-21 deg C
DO: 5 mg/l
Substrate: Sand
Environment: Shallow subtidal (10m) estuarine to intertidal, oligohaline to polyhaline
Salinity: 10ppt-25ppt
Spawning: Twice yearly. Spring 10 deg to 20 deg-- mid March to May
Fall to 20 deg C--mid october to November
Morphology: Gray, chalky white, egg shaped shell, 75 - 100 mm, rough surface, dark periostracum, left hinge with spoon shaped chondrophore
Reporduction: dioecious--separate sexes, nonprotandrous--not male development before female. no hermaphrodites--individuals with both m/f organs. Females less than 40mm never graved.
Larvae: fertilized egg develops into trochophore in 12 hrs, veliger in 24-36hr--lasts for 2-6 weeks. juvenile at 200microns--foot replaces velum, bysus secreted
Adults: Maturity 5 yrs 15 cm at 8 yrs. life 10-12 years up to 19 or 28 yrs??

TAXONOMY
NAME - clam, softshell

OTHER COMMON NAMES - softshell clam and soft clam

CATEGORY - Aquatic Molluscs

PHYLUM AND SUBPHYLUM - Mollusca.

CLASS AND SUBCLASS - Bivalvia.

ORDER AND SUBORDER - Myoida.

FAMILY AND SUBFAMILY - Myidae.

GENUS AND SUBGENUS - Mya.

SPECIES AND SSP - arenaria.

SCIENTIFIC NAME - Mya arenaria

AUTHORITY - Linnaeus, 1758

TAXONOMY REFERENCES - 168 and 136

COMMENTS ON TAXONOMY -
Other common names include Steamer (New England), long clam, gaper (Gosner 1978); long-neck clam (Light 1967); manninose (Chesapeake Bay) (Pfitzenmeyer 1972)

STATUS
Coded Status
Commercial
Commercial/consumption
Commercial/industrial
Depleted

REFERENCES FOR STATUS - 52 and 136

COMMENTS ON STATUS -
Overfishing can drastically reduce the value of clam beds. Because of its near-shore habitat, this valuable resource is easily endangered by pollution. Mariculture efforts have been unsuccessful (Ritchie 1976).*52*

Soft clams are prominent members fo the benthic community in Chesapeake Bay and contribute substantially to the economy of the region. Soft clams in the Chesapeake Bay have decreased in abundance in recent years in the Bay. Intense fishing pressure, loss of habitat, and water quality degradation have been blamed for declines in the abundnace of this species *136*.

DISTRIBUTION

HABITAT ASSOCIATIONS
HABITAT - AQUATIC

OTHER COMMON NAMES - blue mussel, bay mussel, edible mussel, black mussel and pile mussel

CATEGORY - Aquatic Molluscs

PHYLUM AND SUBPHYLUM - Mollusca,

CLASS AND SUBCLASS - Bivalvia,

ORDER AND SUBORDER - Mytiloida,

FAMILY AND SUBFAMILY - Mytilidae,

GENUS AND SUBGENUS - Mytilus,

SPECIES AND SSP - edulis,

SCIENTIFIC NAME - Mytilus edulis

AUTHORITY - Linnaeus, 1758

TAXONOMY REFERENCES - 186 and 9

STATUS
Coded Status
Sport Fish
Commercial
Commercial/consumption
Commercial/bait
Game (Consumptive Recreational)
See Comments

REFERENCES FOR STATUS - 168 and 9

COMMENTS ON STATUS -
Blue mussels have been cultured and harvested in western France and Spain for hundreds of years. Although they have substantial commercial potential, blue mussels have not been harvested as extensively in the United States Recently, the demand for mussels as fresh food has increased in the U S *168*
Evidence indicates that mussel populations may be depleted if harvesting continues at present or greater levels (Dow and Wallace 1954; and MARITEC 1978)
The bay mussel, along with the California mussel, supports a small commercial bait fishery and is cultured for food on a small scale in Tomales Bay and just north of San Diego *9*
SPORT FISHERY
A limited sport fishery, where mussels are usually removed from pilings or rocks by hand, now exists during the open season. A daily harvest of 25 pounds is allowed *9*.

DISTRIBUTION
HABITAT ASSOCIATIONS
NATIONAL WETLAND INVENTORY CODES

Rangia cuneata
common rangia, brackish water clam Louisiana road clam
Aquatic mollusc
Bivalvia
Veneroida
Mactridae
Rangia
cuneata
Sowerby, 1831

1) Living Environment
   a) low salinity--nogreater than 18ppt
   b) high turbidity
   c) mud or silt
   d) vegetation
   e) freshwater clam which became adapted to brackish
   f) correlation between size of clam and salinity--larger in less saline
   g) estuarine--important in this environment
   h) transforms large amounts of plant detritus into clam biomass

2) Temperature and Salinity for embryo
   a) 18 to 29 degrees
   b) 6 to 10ppt salinity

3) Oxygen
   a) can withstand anoxic conditions

4) Substrate
   a) soft substrates
   b) prefer high organic content
   c) capable of vertical movement in substrate

5) Food
   a) non-selective filter feeders ingesting detritus and phytoplankton
   b) feeding controlled by gill palp articulations and ciliary currents over gills
   c) pseudofeces extruded from mantle cavity through inhalent siphon when valves are closed

6) Morphology
   a) 2.5 to 6.0 cm in length.
   b) valves obliquely ovate, thick and heavy.
   c) strong smooth light brown to grayish brown or black periostracum
   d) Prominent umbones near anterior end
   e) glossy white interior shell with blue gray tinge
   f) small but distinct pallial sinus

g) Brown rangia--short posterior lateral tooth and nondistinct pallial sinus (southern species)

7) Spawning
   a) spawn from March to May and late summer to November
   b) temperature required 15 deg C
   c) initiated by rapid increase or decrease in salinity
   d) gametes released directly into water
   e) minimum length reached in 2 - 3 years 24mm
   f) settling of larvae--september through March
   g) second settling in mid summer

8) Life Span
   a) 4 to 5 years
   eg--clam 75mm long 10 years
   b) maximum life span 15 years

9) Growth Rate and Size
   a) 0-20mm
   b) difficult to correlate growth rate with salinity--conflicting reports
   c) difficult to correlate growth rate with substrate although sand dwelling species in Va tend to be larger than others.

10) Population
   a) largest in Louisiana

11) Predators and Parasites
   a) Blue catfish
   b) freshwater drum
   c) spot
   d) black drum
   e) river shrimp
   f) blue crab
   g) molluscs
   h) ducks
   I) ctenophores
   j) parasite: fellodistomatid trematodes

12) Competitors none in Hudson???

13) Pollution
   a) concentrate chemical called kepone. concentrations increase during periods of high metabolic rate. Concentrations 2-4 times that of water in which rangia lived. factors of uptake:

      1) temperature

OTHER COMMON NAMES - oyster and eastern oyster

ELEMENT CODE - 09/09/87

CATEGORY - Aquatic Molluscs

PHYLUM AND SUBPHYLUM - Mollusca.

CLASS AND SUBCLASS - Bivalvia.

ORDER AND SUBORDER - Ostreoida.

FAMILY AND SUBFAMILY - Ostreidae.

GENUS AND SUBGENUS - Crassostrea.

SPECIES AND SSP - virginica.

SCIENTIFIC NAME - Crassostrea virginica

AUTHORITY - Gmelin, 1791

TAXONOMY REFERENCES - 186 and 20

COMMENTS ON TAXONOMY -
Other common name is eastern oyster *20*
STATUS
Coded Status
Commercial
Commercial/consumption
Depleted

REFERENCES FOR STATUS - 20 and 136

COMMENTS ON STATUS -
Oysters are valued as a luxury food item *20*
American oysters are prominent members of the benthic community in Chesapeake Bay and contribute substantially to the economy of the region Oysters have recently experienced severe declines in abundance Intense fishing pressure, loss of habitat, and water quality degradation have been blamed for declines in the abundance of this species *136*

DISTRIBUTION

HABITAT ASSOCIATIONS

HABITAT - Aquatic
REFERENCES FOR HABITAT - 142 and 20
LAND USE -
Water
Bays and Estuaries

Appendix 5: Shaw data 1974-1978

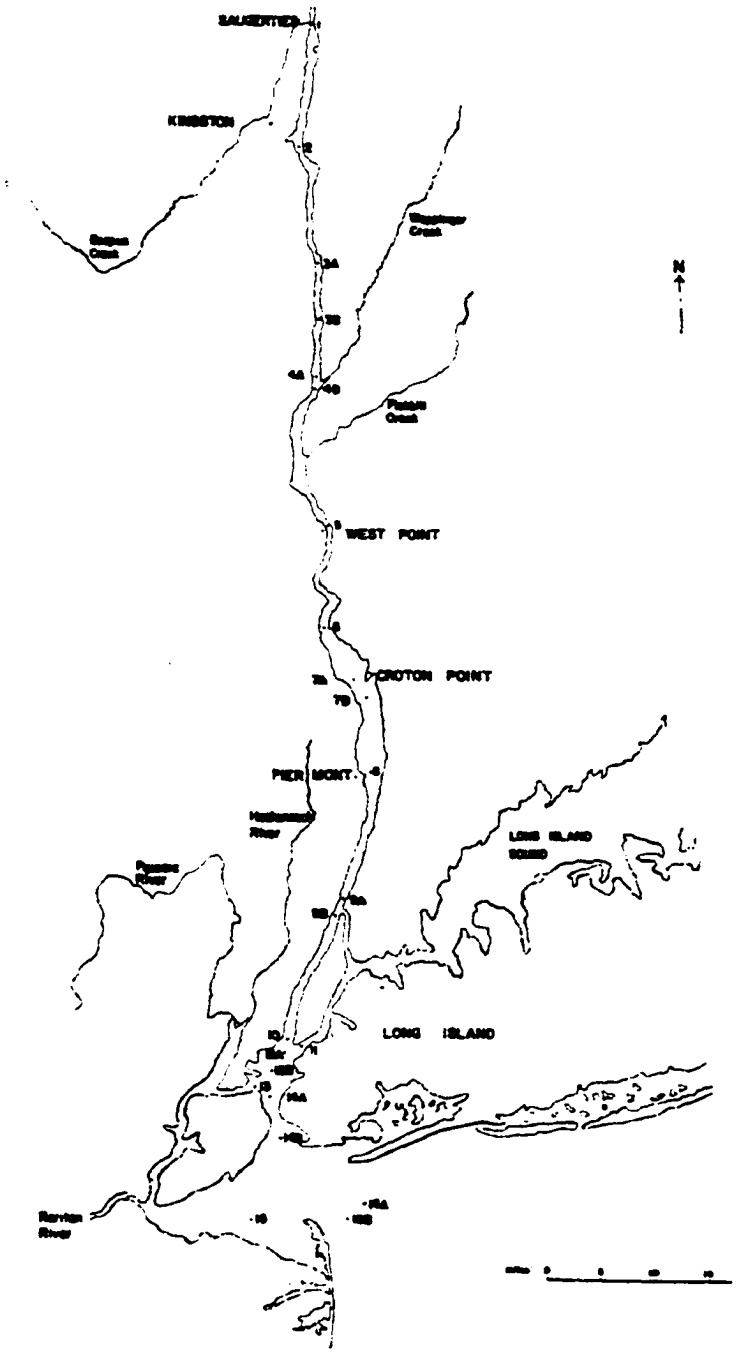

FIGURE 1. MAP OF SAMPLING SITES OF THE HUDSON ESTUARY SURVEY.

Table 1. SECTOR AND STATION LOCATIONS

Sector	Station	Location	Mile Point*
16	16A	N.Y. Bight, 6.0 mi ne of Sandy Hook	-15
	16B	N.Y. Bight, 3.5 mi ne of Sandy Hook	
15	15	Lower Bay, 3 mi nw of Sandy Hook	-12
14	14A	North of The Narrows	- 8
	14B	South of The Narrows	
13	13	Kill Van Kull	- 6
12	12A	North end of Upper Bay	- 2
	12B	South end of Upper Bay	
11	11	East River, near The Battery	0
10	10	Hudson River, near The Battery	0
9	9A	North of Smuyten Duyvil	+ 8
	9B	South of Smuyten Duyvil	
8	8	Piermont, New York	+18
7	7A	North of Croton Point, New York	+25
	7B	South of Croton Point, New York	
6	6	Verplanck, New York	+33
5	5	World's End (West Point, New York)	+50
4	4A	North of Wappinger Creek	+63
	4B	South of Wappinger Creek	
3	3A	North of Poughkeepsie, New York	+71
	3B	South of Poughkeepsie, New York	
2	2	Kingston, New York	+88
1	1	Saugerties, New York	+99

* + north of The Battery; - south of The Battery

DISTRIBUTION OF SHELLED MACROINVERTEBRATE BENTHOS IN THE HUDSON ESTUARY

F.C. SHAW, Department of Geology and Geography, Lehman College of C.U.N.Y., Bronx, New York 10468.

Shelled benthos (primarily molluscs, bryozoans, and barnacles) have been sieved from one liter bottom grab samples. Samples have been taken on a random monthly basis for one year at the 16 stations of the City Institute of Marine and Atmospheric Sciences' Hudson Estuary survey, and are located in or near the main ship channel from the inner New York Bight (station 16) to Saugerties, New York (station 1). The number of live individuals, disarticulated valves, fragments, and preliminary size measurements have been recorded. Three assemblages, characterized by nominate bivalve genera and consisting largely of bivalves are proposed:

1. Elliptio assemblage: an essentially freshwater fauna present from Peekskill to Saugerties
2. Mytilopsis assemblage: occupying the area between Yonkers and northern Haverstraw Bay, showing low species diversity in bottom salinities which may vary as much as 15°/oo in the southern Tappan Zee. Salinities over this entire reach range from 1 to 15°/oo.
3. Mulina - Mya assemblage: essentially marine in generic composition and diversity, present as far north as Riverdale in salinities which may drop as low as 10°/oo.

A typical monthly sample of these assemblages is shown in figure 10 and compared to other proposed estuary classifications in figure 11.

Bottom salinity and temperature appear to be the controlling factors for these assemblages. Dissolved oxygen is judged adequate for molluscs at all stations over the sampling area. Bottom sediments in the study are have not been fully analyzed. There does appear to be little difference in the genera at stations 10, 12, and 13 in spite of major differences in sediment.

A finer grid lateral to the main channel is being sampled at present to fully clarify the local factors controlling the distribution of shelled macroinvertebrate benthos.

Several questions may now be raised on the basis of this new information. First, do local distruptions in this assemblage pattern, such as the very scanty faunas in the south Yonkers - Riverdale area and the demise of the shell fish industry in the Tappan Zee, represent human interference or natural changes in the Estuary? Secondly, can the distribution and individual growth characteristics of bivalves be used as part of a natural monitoring system in the Estuary?

Contribution No. 55 of the City Institute of Marine and Atmospheric Sciences.

over →

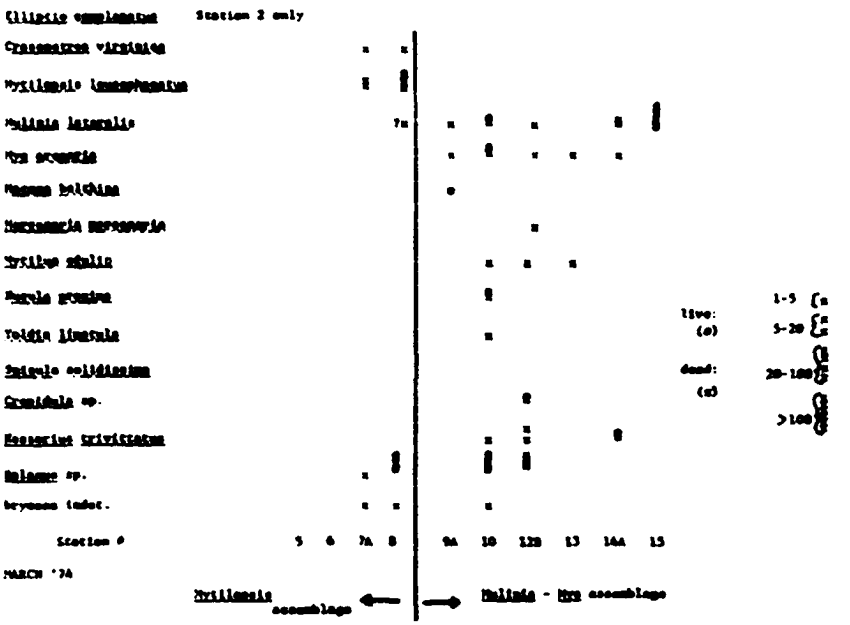

FIGURE 10. SELECTED TALLY OF HUDSON RIVER BENTHIC SPECIES. Numbers refer to survey stations. 5 is to the north.

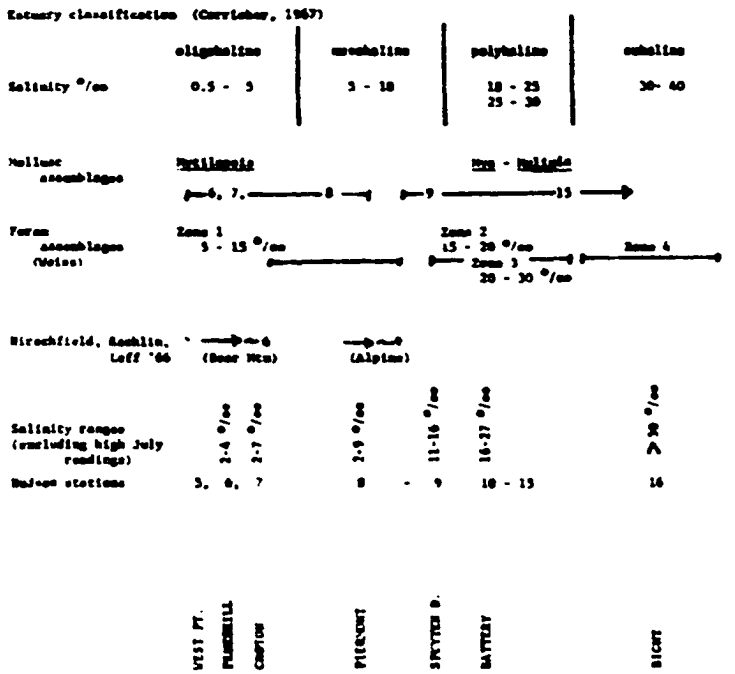

FIGURE 11. COMPARISON OF MOLLUSCAN ASSEMBLAGE DISTRIBUTIONS TO FORAMINIFERAL DISTRIBUTIONS OF WEISS AND STANDARD ESTUARY CLASSIFICATION OF CARRICKER.

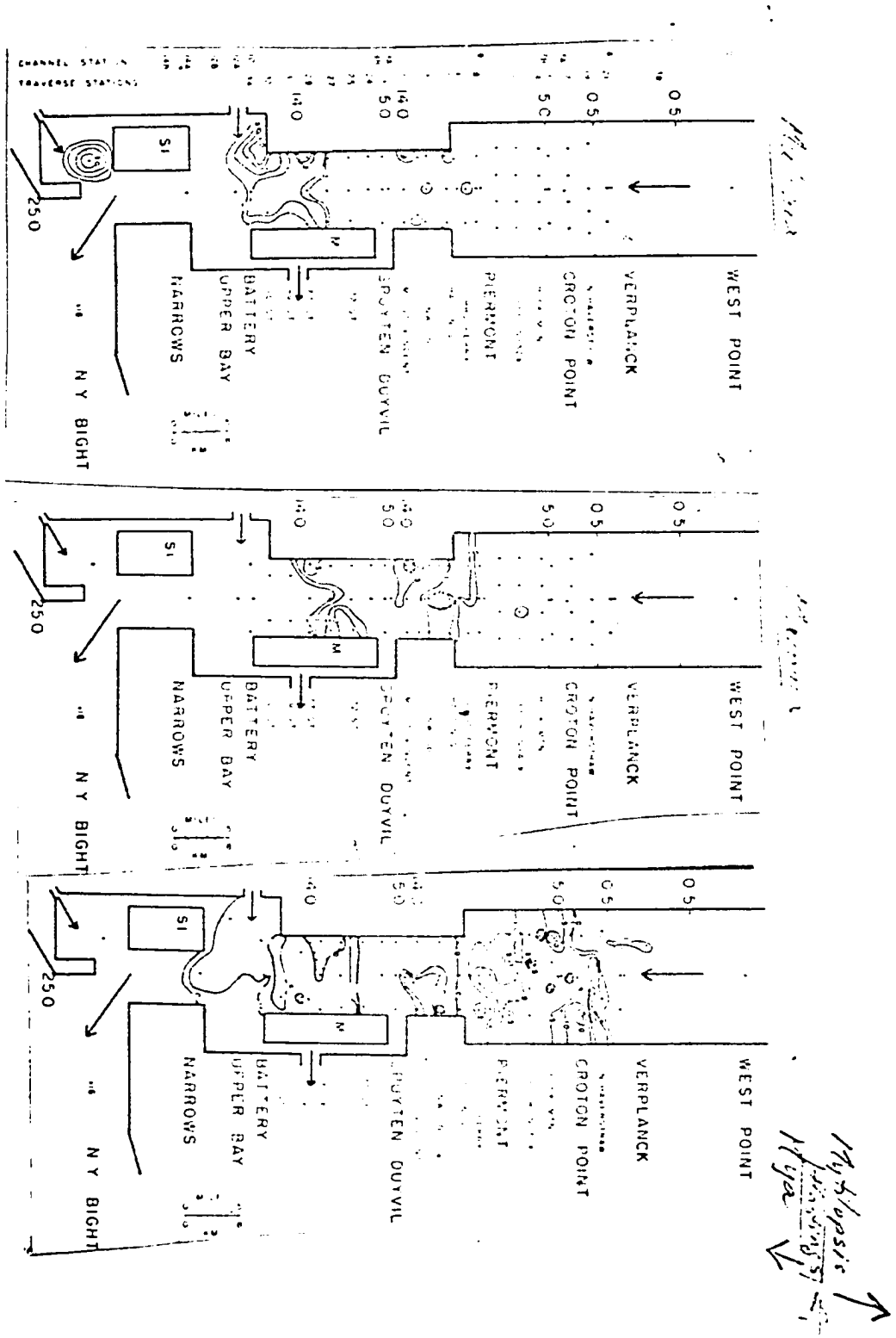

1.

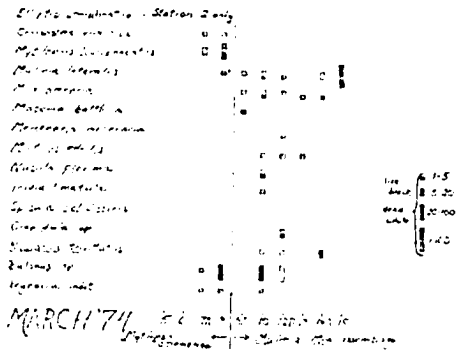

2.

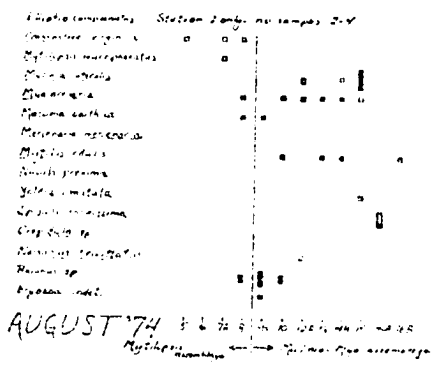

3.

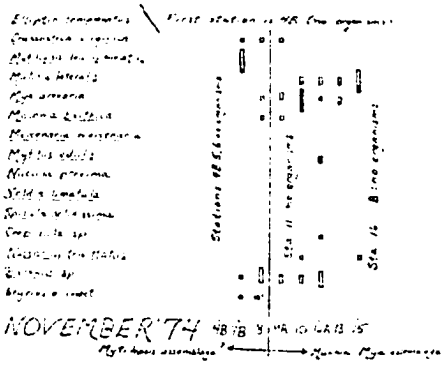

4.

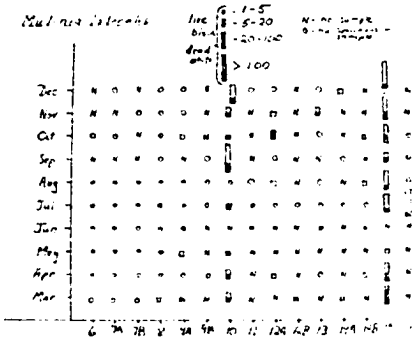

5.

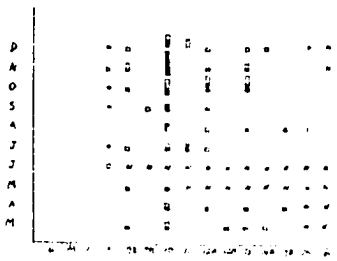

6.

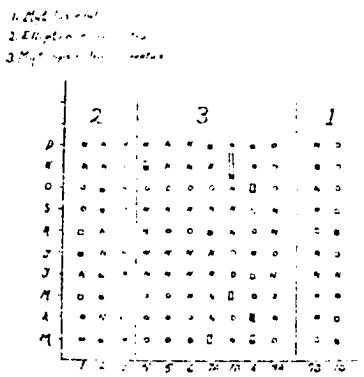

REFERENCES

Adami, G., Aleffi, F., Barbiere, P., Farnetto, A., Predonzani, S., Reisenhofer, E., 1997, Bivalves and heavy metals in polluted sediments: A chemometric approach. *Water Air and Soil Pollution*, v. 99 no. 1/4, pp. 615-622.

Babukutty, Y., Chacko, J., 1992, Trace metals in an estuarine bivalve from the southwest coast of India, *Ambio*, V. 21, No. 4, pp. 292-296

Barlow, M., Kingston, P., 2001, Observations on the effects of barite on the gill tissues of the suspension feeder Cerastoderma edule (Linne) and the deposit feeder Macoma balthica (Linne), *Marine Pollution Bulletin*, V 42, No 1, pp. 71-76.

Baudrimont, M., Lemaire-Gong, S., Ribeyre, F., Metivaud, J., Boudon, A., 1997, Seasonal variations of metallothionein concentrations in Asiatic clam (Corbicula fluminea)- mechanisms of regulation and toxicity at the cellular level. *Comparative Biochemistry and Physiology Part C: Pharmacology, Toxicology and Endocrinology*, v. 18 no.3, pp. 361-367.

Bilos, C., Colombo, J., Rodriguez, P., 1998, Trace metals in suspended particles, sediments and Asiatic Clams (Corbicula fluminea) of Rio de Plata Estuary, Argentina. *Environmental Pollution*, v.99 no. 1, pp. 1-11.

Blackmore, G., 2001, Interspecific variation in heavy metal body concentrations in Hong Kong marine invertebrates. *Environmental Pollution*, v. 114, no. 3, pp. 303-311.

Borbas, J., Wheeler, A., Sikes, S., 1991, Molluscan shell matrix phosphoproteins: correlation of degree of phosphoroylation to shell mineral microstructure and to in-vitro regulation of mineralization. *Journal of Experimental Zoology*, v. 258, pp. 1-13.

Bordin, G., McCourt, J., Raposo, F.C., Rodriguez, A.R., 1997, Metallothionein -like metalloproteins in the Baltic clam Macoma balthica: seasonal variations and induction upon metal exposure. *Marine Biology*, v. 129, pp. 453-463.

Bordin, G., McCourt, J., Rodriguez, A., 1994, Trace metals in marine bivalve Macoma balthica in the Westerschelde Estuary, the Netherlands. Part 2: Intracellular partitioning of copper, cadmium, zinc, and iron—variations of the cytoplasmic metal concentrations in natural and in-vitro contaminated clams. *The Science of the Total Environment*, v. 151, pp. 113-124.

Bottjer, D., Hickman, P., 1985, Mollusks, notes for a short course. *University of Tennessee Department of Geoscience Studies in Geology* 13, 267pp.

Bourgoin, B., Risk, M., Aitken, A., 1991, Factors controlling lead availability to the deposit-feeding bivalve Macoma balthica in sulphate-rich oxic sediments. *Estuarine Coastal and Shelf Science*, v. 32, pp. 625-632.

Carriker, M., 1985, Ecology of estuarine benthic invertebrates: A perspective. In, *Estuaries: Ecology and Populations*, pp. 442-487.

Carriker, M., et al, 1985, Effects of pollutants on benthos, In: *Ecological Stress and the New York Bight*, Mayer, G. ed. Science and Management, pp. 1-21.

Crandall, M., 1977, Epibenthic invertebrates of Croton Bay in the Hudson River. *New York Fish and Game Journal*, v. 24, 2, pp. 178-187.

Davies, T., 1972, Effect of environmental gradients in the Rappahannock River Estuary on the molluscan fauna. *The Geological Society of America, Inc., Memoir 133*, pp. 263-290.

Decho, A., Luoma, S., 1994, Humic and fulvic acids: sink or source in the availability of metals to the marine bivalves Macoma balthica and Potamocorbula amurensis?, *Marine Ecology Progress Series*, v. 108, pp. 133-145.

Dietz, T., Byrne, R., 1990, Potassium and rubidium uptake in freshwater bivalves. *Journal of Experimental Biology*, v. 150, pp. 395-405.

Dodd, R., 1965, Environmental control of strontium and magnesium in Mytilus. *Geochemica et Cosmochimica Acta*, v. 29, pp. 385-398.

Gundacker, C., 2000, Comparison of heavy metal bioaccumulation in freshwater molluscs of urban habitats in Vienna. *Environmental Pollution*, V110, pp. 61-71. *American Zoologist*, v. 24, pp. 45-55.

Kinsman, D., Holland, H., 1969, The co-precipitation of cations with CaCO3-IV, The co-precipitation of Sr 2+ with aragonite between 16 and 96 degrees C. *Geochim. Cosmochim. Acta 33*, 1-17.

Leung, K., Svavarsson, J., Crane, M., Morritt, D., 2002, Influence of static and fluctuating salinity on cadmium uptake and metallothionein expression by the dogwhelk Nucella lapillis. *Journal of Experimental Marine Biology*, v274, pp. 175-189.

Lowenstam, H., 1981, Minerals formed by organisms. Science, v. 211, pp. 1126-1131.

Luoma, S., Fisher, N., Reinfelder, J., Decho, A., 1992, Bioavailability of trace elements associated with particulates. *Canadian Report of Fisheries and Aquatic Science*, 0 (1863): 26

Mallin, M., Burkholder, J., Cahoon, L., Posey, M., 2000, North and South Carolina coasts. *Marine Pollution Bulletin*, v. 49 no. 1 pp. 56-75.

Palacios, R., Orensanz, J., Armstrong, D., 1994, Seasonal and life-long variation of Sr/Ca ratio in shells of Mya arenaria from Grays Harbor (Washington)-an ancillary criterion in demographic studies. *Estuarine, Coastal and Shelf Science*, v. 39, pp. 313-327.

Parker, R., 1969, Benthic invertebrates in tidal estuaries and coastal lagoons. *Lagunas Costeras, Un Simposio*, pp. 563-590.

Pitts, L., Wallace, G., 1994, Lead deposition in the shell of the bivalve Mya arenaria, an indicator of dissolved lead in seawater. *Estuarine, Coastal and Shelf Science*, v. 39, pp. 93-104.

Richards, S., Riley, G., 1967, The benthic epifauna of Long Island Sound. *Bulletin of the Bingham Oceanographic Collection*, v. 19, pp. 89-135.

Ristich, M., Fortier, J., 1977, Benthic and epibenthic macroenvironments of the Hudson River I, distribution, natural history and community structure. *Estuarine and Coastal Marine Science*, v. 5, pp. 255-266.

Roditi, H., Caraco, N., 1996, filtration of Hudson river water by the zebra mussel (Dreissena polymorpha). *Estuaries*, v. 19 (4), pp. 824-832.

Sanders, H., 1960, Benthic studies in Buzzards Bay III. *The structure of the soft-bottom community, Contribution 1033*, Woods Hole Oceanographic Institution, pp. 138-153.

Shaw, F., 1975, Shelled invertebrate benthos of the Hudson Estuary, interim report for 1974, unpublished manuscript

1975, Distribution of shelled macroinvertebrate benthos in the Hudson estuary, *Guidebook for Field Trips in Western Massachusetts, Northern Connecticut and Adjacent Areas of New York, Department of Earth and Planetary Science*, City College of New York. pp 53-54.

Solem, A., 1974, *The Shell makers: Introducing Mollusks*, John Wiley and Sons, New York, 289pp.

Speer, A., 1983, Crystal Chemistry of Orthorhombic Carbonates. In: *Mineralogical Society of America Publication, vol 11*, Carbonates: Mineralogy and Chemistry

Teng, H., Dove, P., Orne, C., Yoreo, J., 1998, Thermodynamics of calcite growth: Baseline for understanding biomineral formation. *Science*, V282, pp.724-727.

Weiss, D., 1974, Late Pleistocene stratigraphy and paleoecology of the lower Hudson River Estuary. *Geological Society of America Bulletin*, v. 85, pp. 1561-1570.

Weiss, D., Geitzenauer, K., Shaw, F., 1978, Foraminifera, diatom and bivalve distribution in recent sediments of the Hudson Estuary. *Estuarine and Coastal Marine Science*, v. 6, pp. 1-8.

Yang, M., Sanudo-Wilhelmy, S., 1998, Cadmium and manganese distributions in the Hudson River estuary: inter-annual and seasonal variability. *Earth and Planetary Science Letters*, v. 160, pp. 403-418.

Zamarreno, I., DePorta, J., Vazquez, A., 1996, The shell microstructure, mineralogy, and isotopic composition of Amussiopecten baransis(pectinidae, bivalvia) from the Miocene of Spain: A valuable paleoenvironmental tool. *Geobios*, v. 29 (6), pp. 707-724.